Spin-orbit technologies: from memory switching to THz generation

Hyunsoo Yang

Department of Electrical and Computer Engineering
National University of Singapore

IEEE MAGNETICS

NUS National University of Singapore

www.ieeemagnetics.org

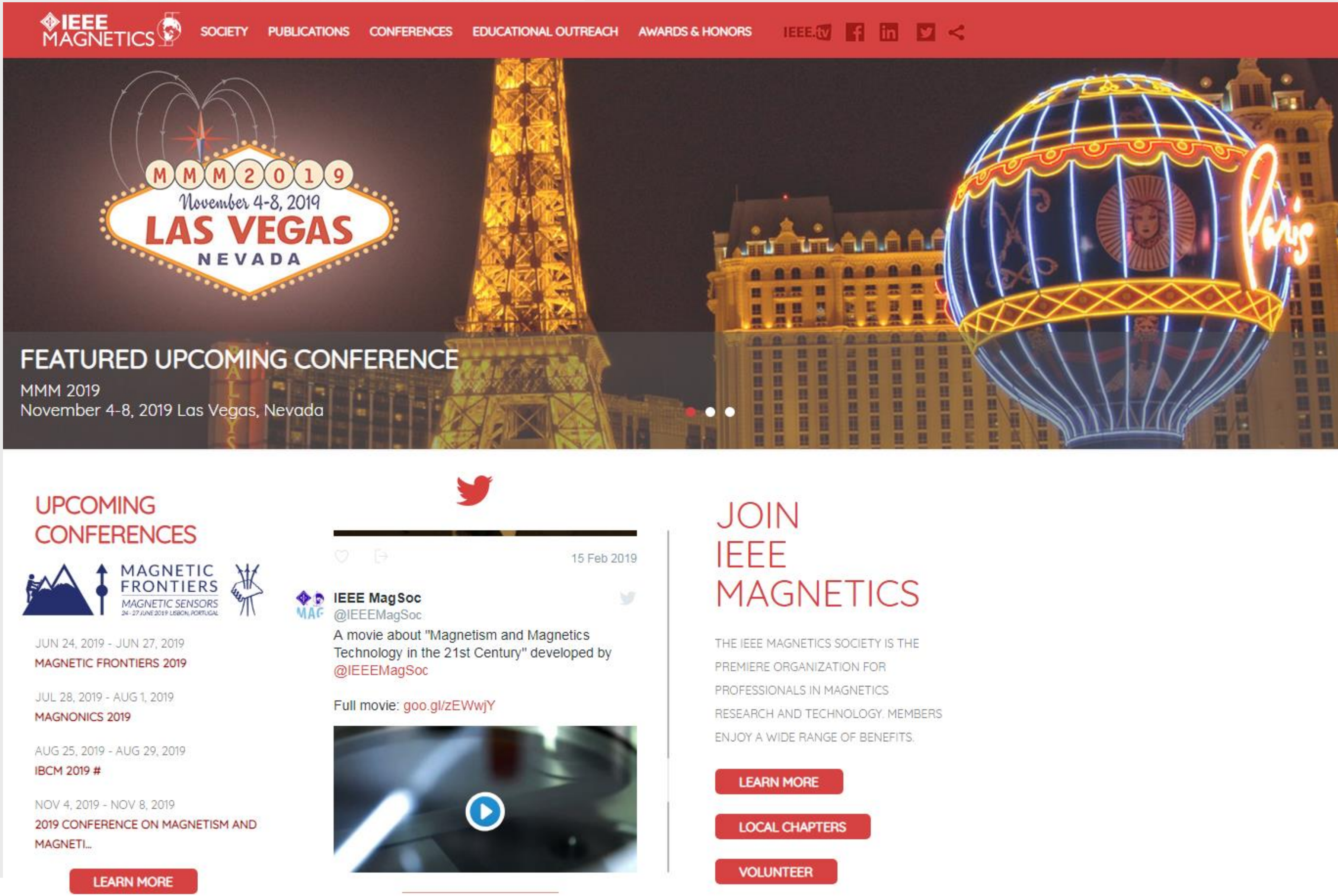

Charge electronics → Spin electronics

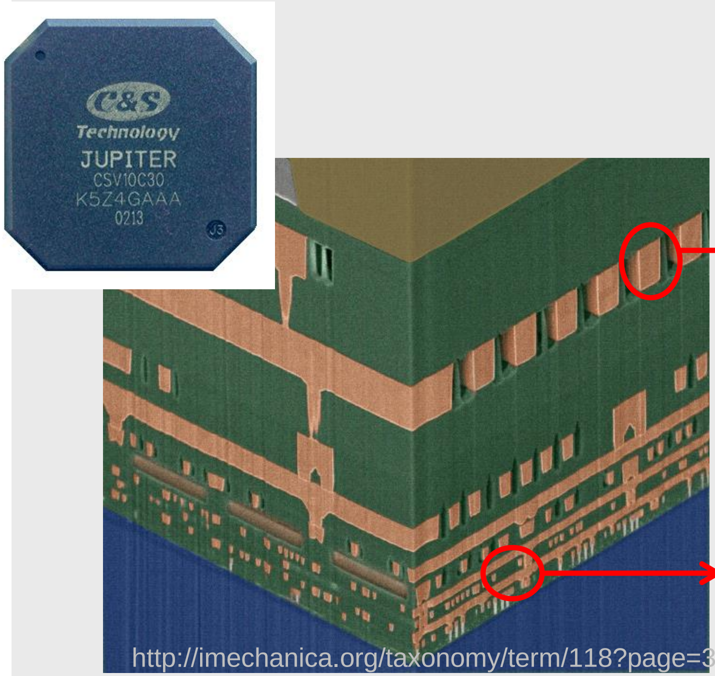

Information transfer
= electron transfer

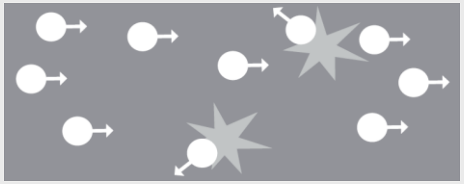

Information processing
= processing electron flow

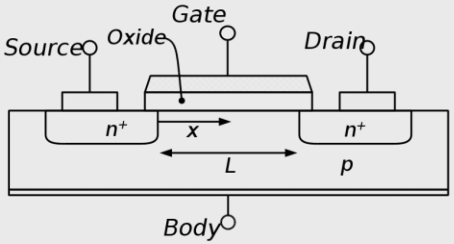

Spin wave

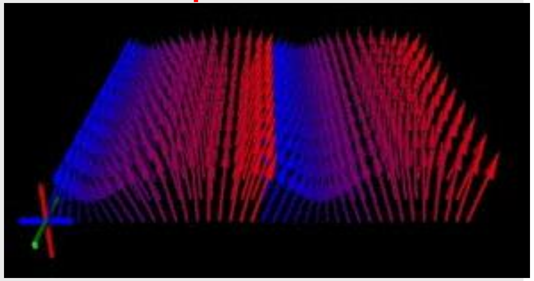

MTJ memory

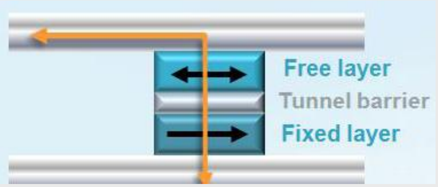

Spin transistor

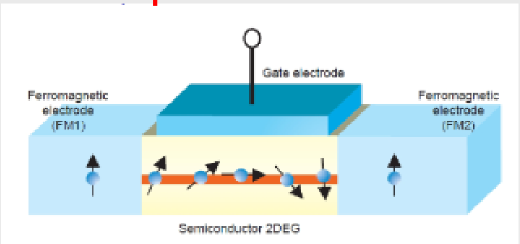

Charge transfer and processing energy loss is huge
→ All spin electronics

NUS National University of Singapore

Spin switches/filters for spin logic devices

Mechanical switch

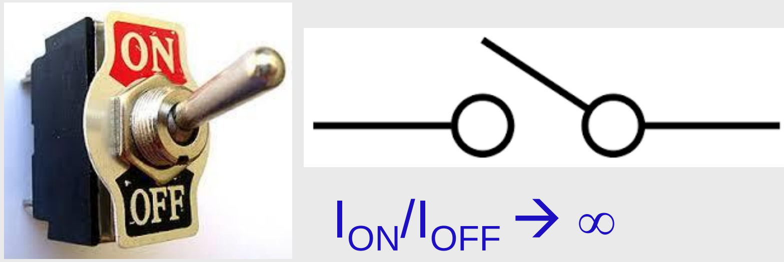

$I_{ON}/I_{OFF} \rightarrow \infty$

Transistor

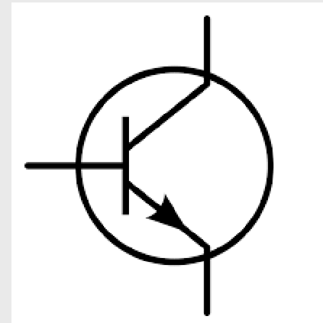

$I_{ON}/I_{OFF} \sim 10^6$

Optical filter

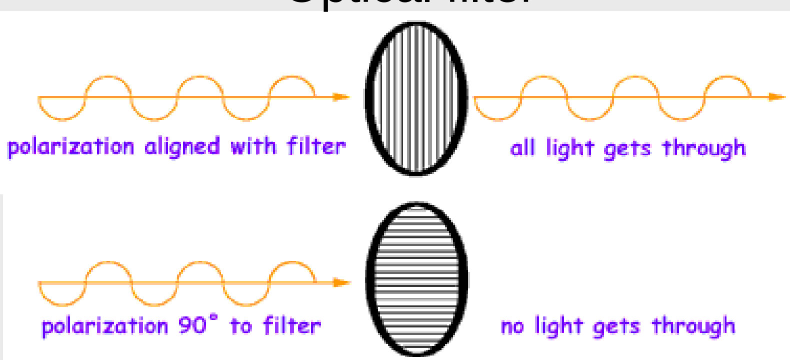

$I_{ON}/I_{OFF} \rightarrow \infty$

Microwave

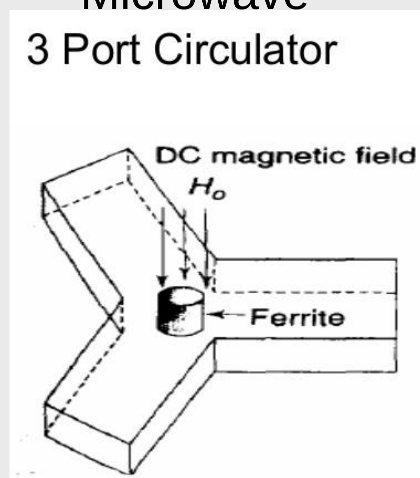

$I_{ON}/I_{OFF} \sim 1000$

Crystalline MgO barrier

Coherent Tunneling

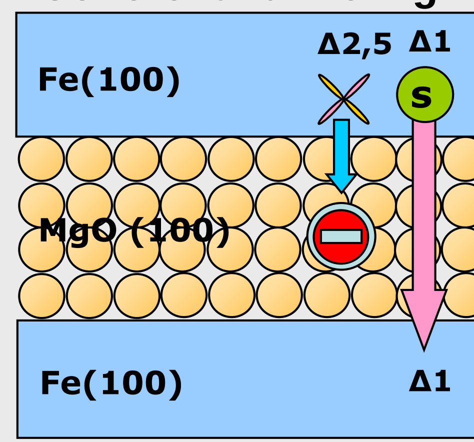

$I_{ON}/I_{OFF} << 10$

Is there any better component in spintronics?

Spin wave nonreciprocity

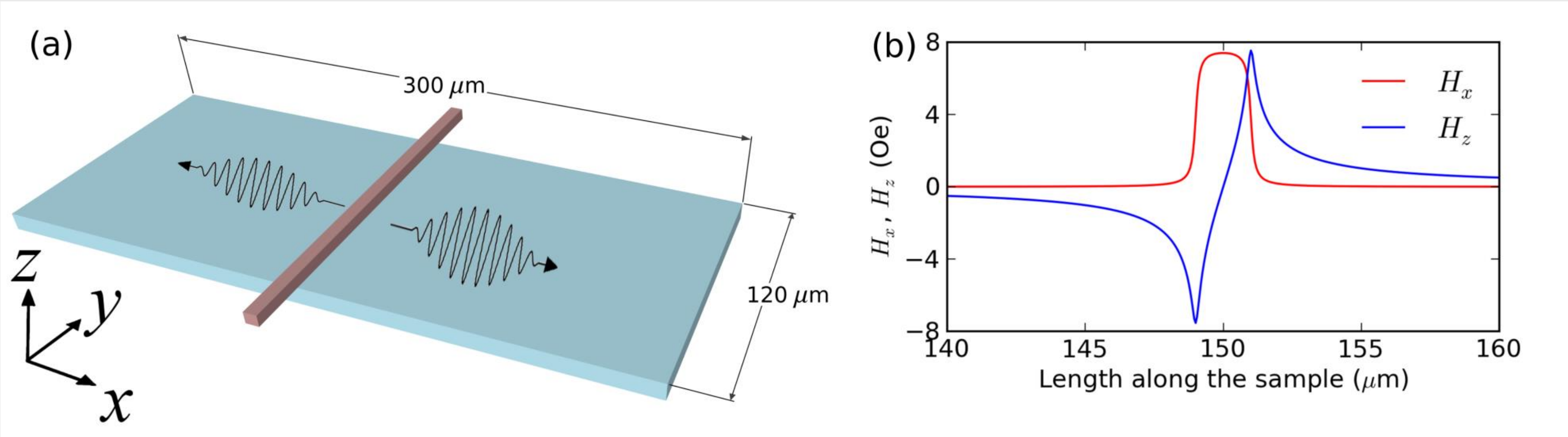

Well known phenomenon [e.g. PRB 77, 214411 (2008), APL 95, 112509 (2009), APL 97, 022508 (2010)]

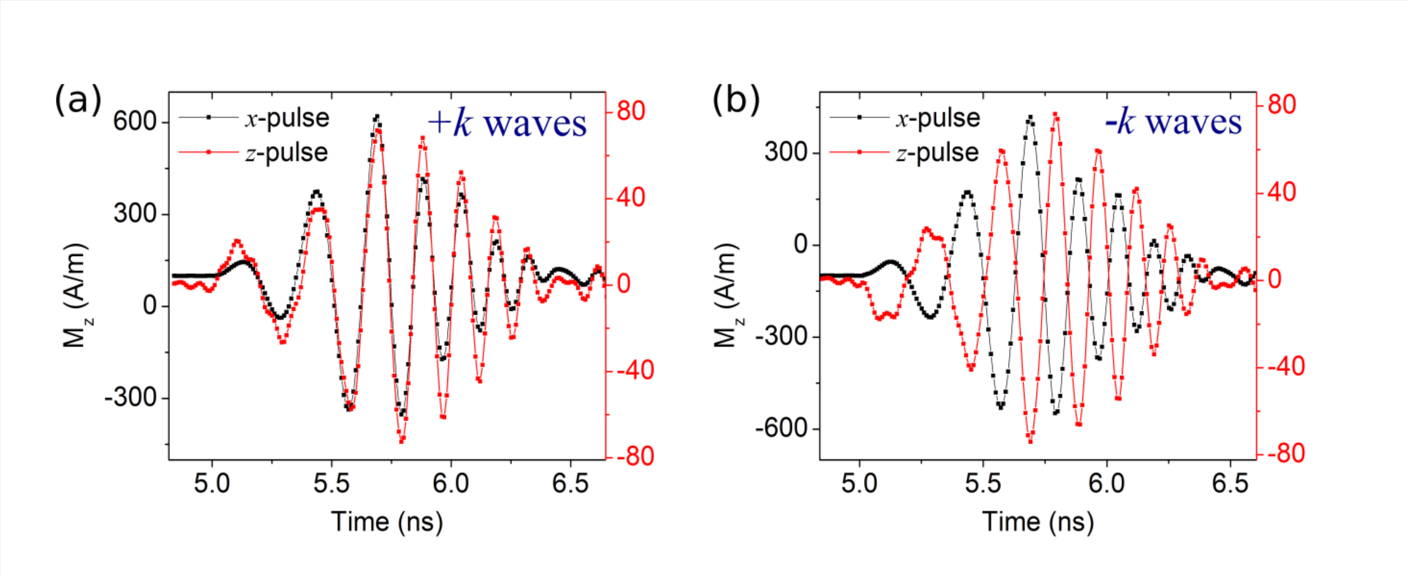

J. Phys. D: Appl. Phys. **47**, 385002 (2014), Curr. Appl. Phys. **14**, S129 (2014)

Surface mode nonreciprocity in Py

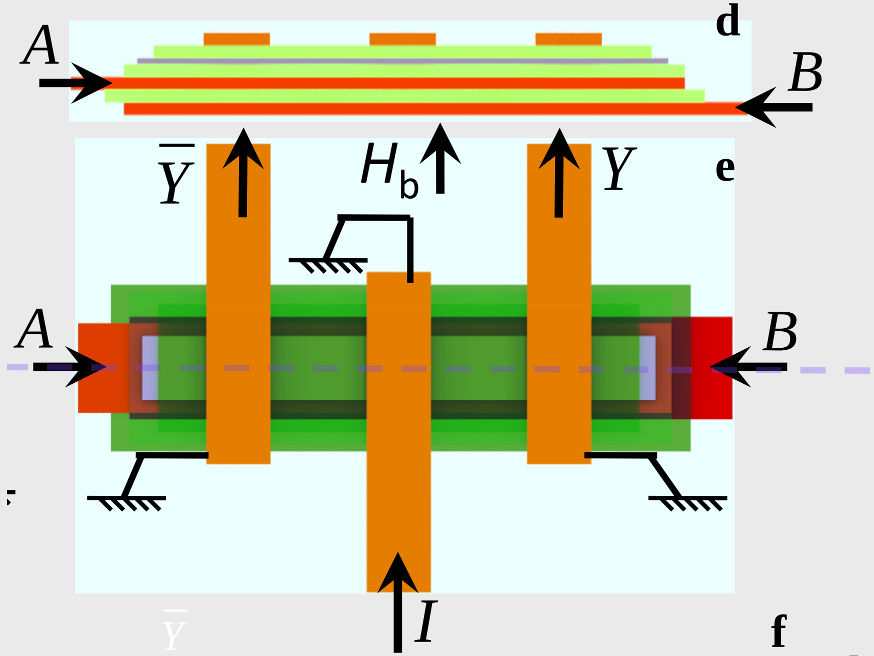

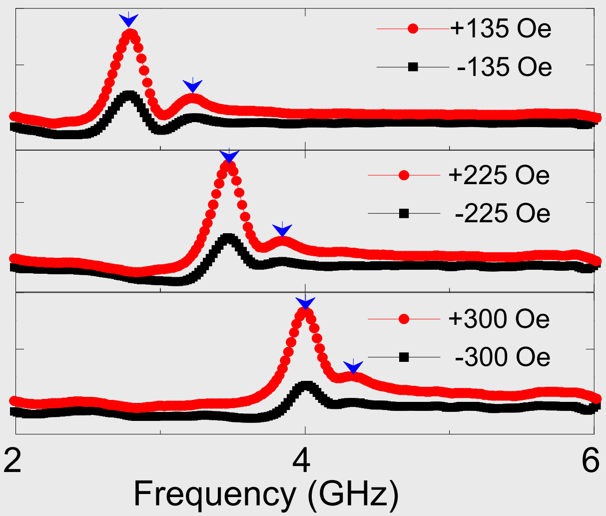

f

A	B	$\overline{Y}$	Y
0	0	0	1
1	0	1	0
0	1	0	1
1	1	0	1

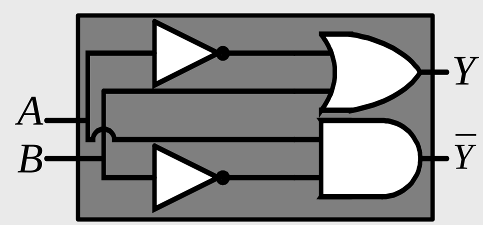

$$Y = \overline{A} + B$$

$$\overline{Y} = A\overline{B}$$

Sci. Rep. **3**, 3160 (2013), APL **107**, 022401 (2015)

Spin wave nonreciprocity in bilayer (Ta/Py)

bias field (H_z)

z ⊗

-z ⊙

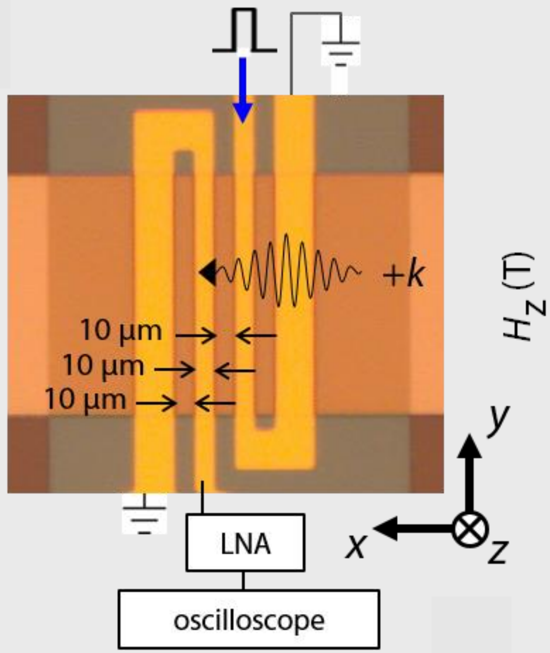

< stack of layers >

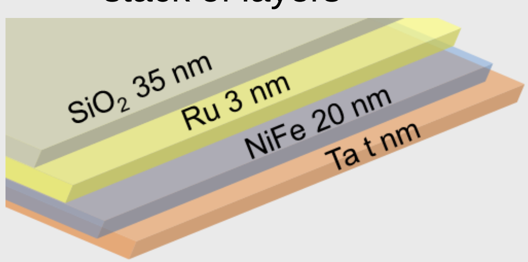

t_{Ta} (Ta thickness) ranges from 0 to 10 nm

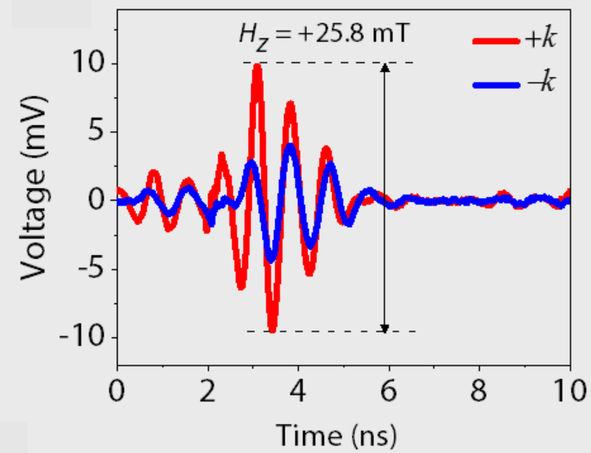

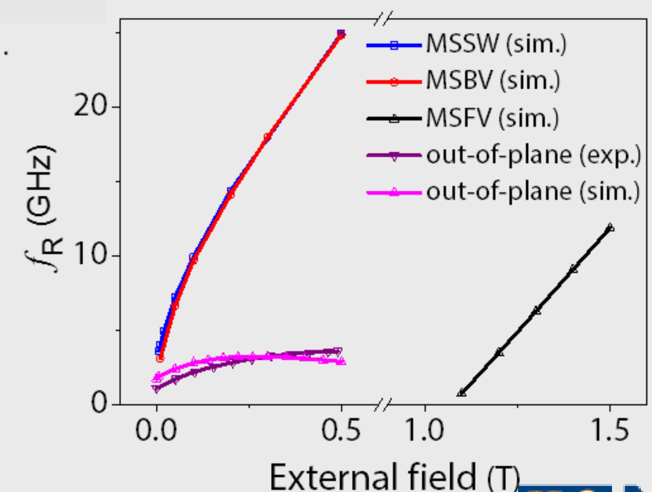

Sci. Adv. **2**, e1501892 (2016)

Giant nonreciprocal emission of spin wave in Ta (*t* nm)/Py

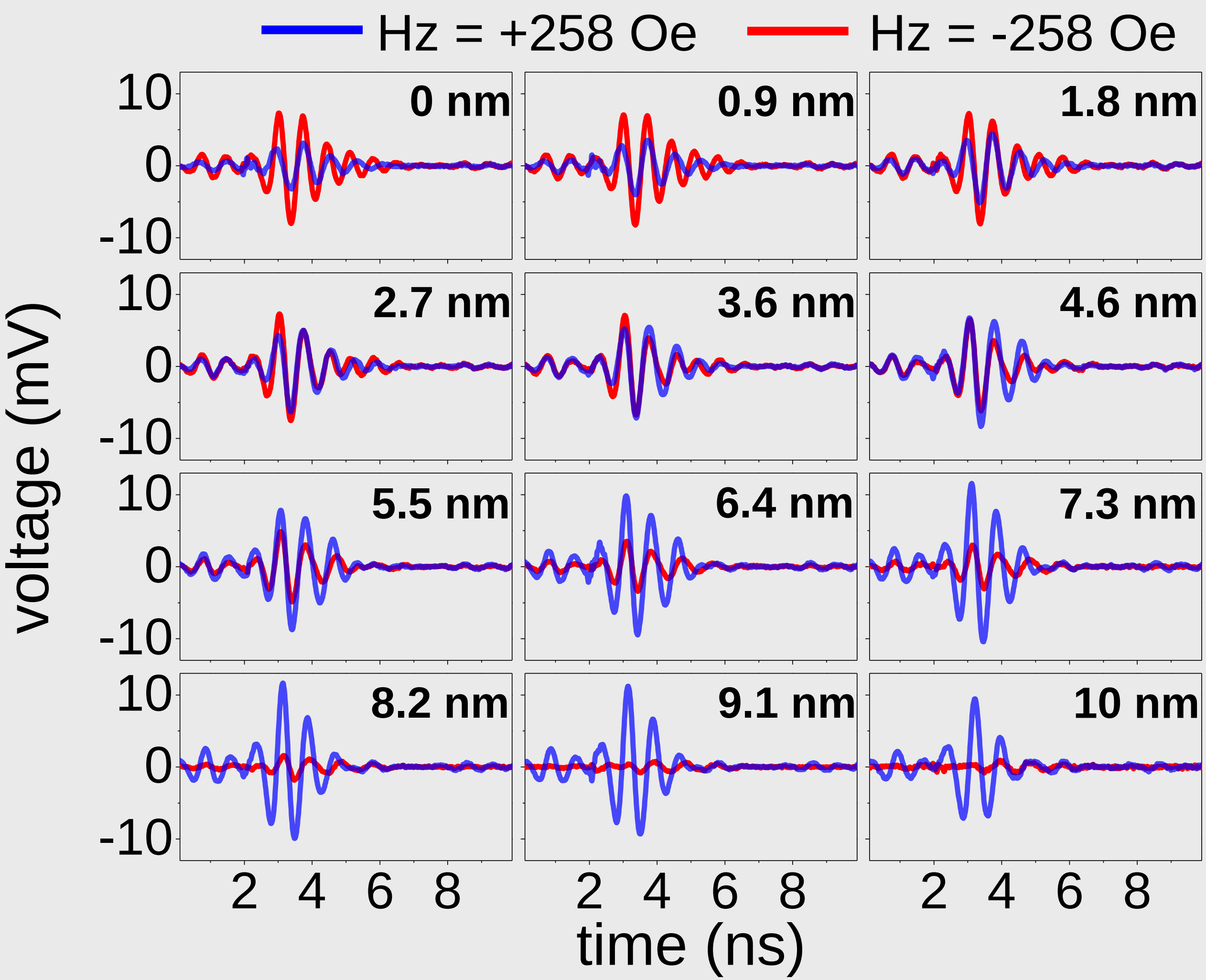

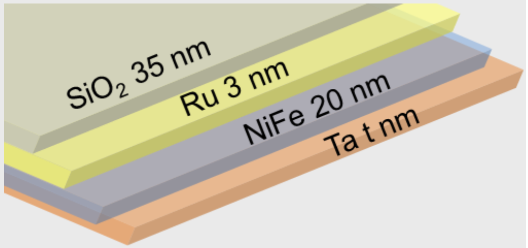

ON/OFF ratio of 60

- The amplitude at -258 Oe is higher than that at +258 Oe in the device for $0 < t_{Ta} < 2.7$ nm.
- However, the amplitude at +258 Oe is higher than that at -258 Oe for $4.6 \text{ nm} < t_{Ta} < 10$ nm

Sci. Adv. **2**, e1501892 (2016)

k-dependent enhanced damping

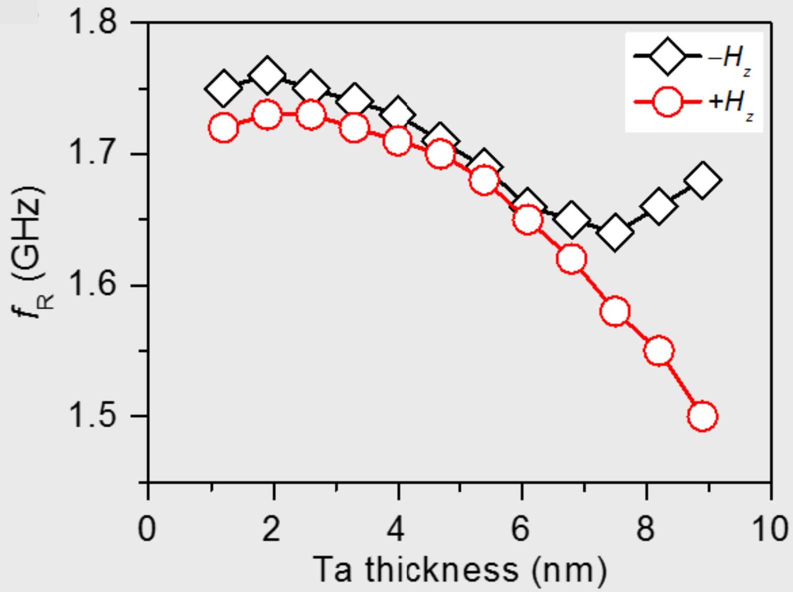

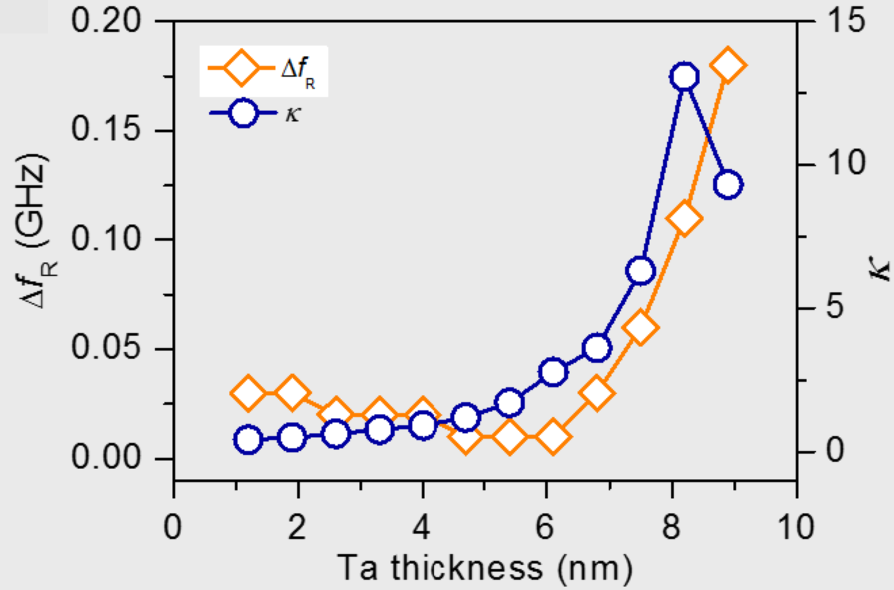

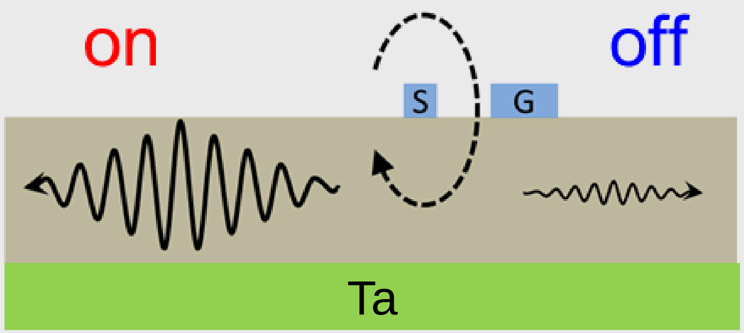

PRL **92**, 026602 (2004), PRB **73**, 014408 (2006)

$$\Delta\alpha(k) \propto \mathrm{Re}[g_{\uparrow\downarrow}]\sigma k^2 l_{sf}^2 \left[l_{sf} \coth\left(t_{\mathrm{Ta}} / l_{sf}\right) - t_{\mathrm{Ta}} \sinh\left(t_{\mathrm{Ta}} / l_{sf}\right)^{-2} \right]$$

Sci. Adv. **2**, e1501892 (2016)

NUS National University of Singapore

Future applications of magnetic tunnel junctions

- Replace eFlash in smart cards.
- Replace SRAM in wearable chips.
- Apply to bio-compatible chips

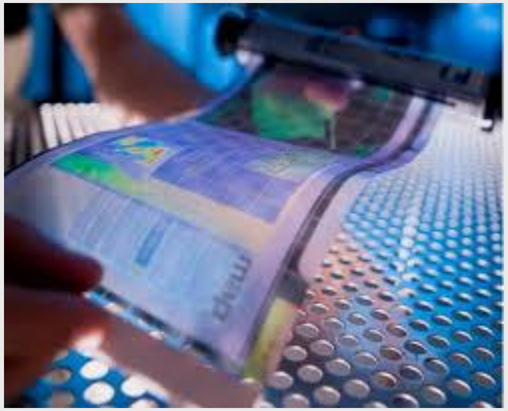

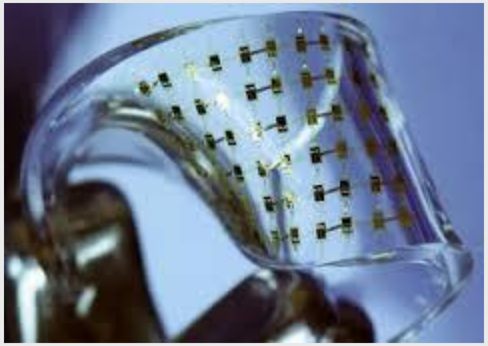

from google images

Understanding of strain effect in MTJs is important!

NUS National University of Singapore

Flexible MTJs transfer process

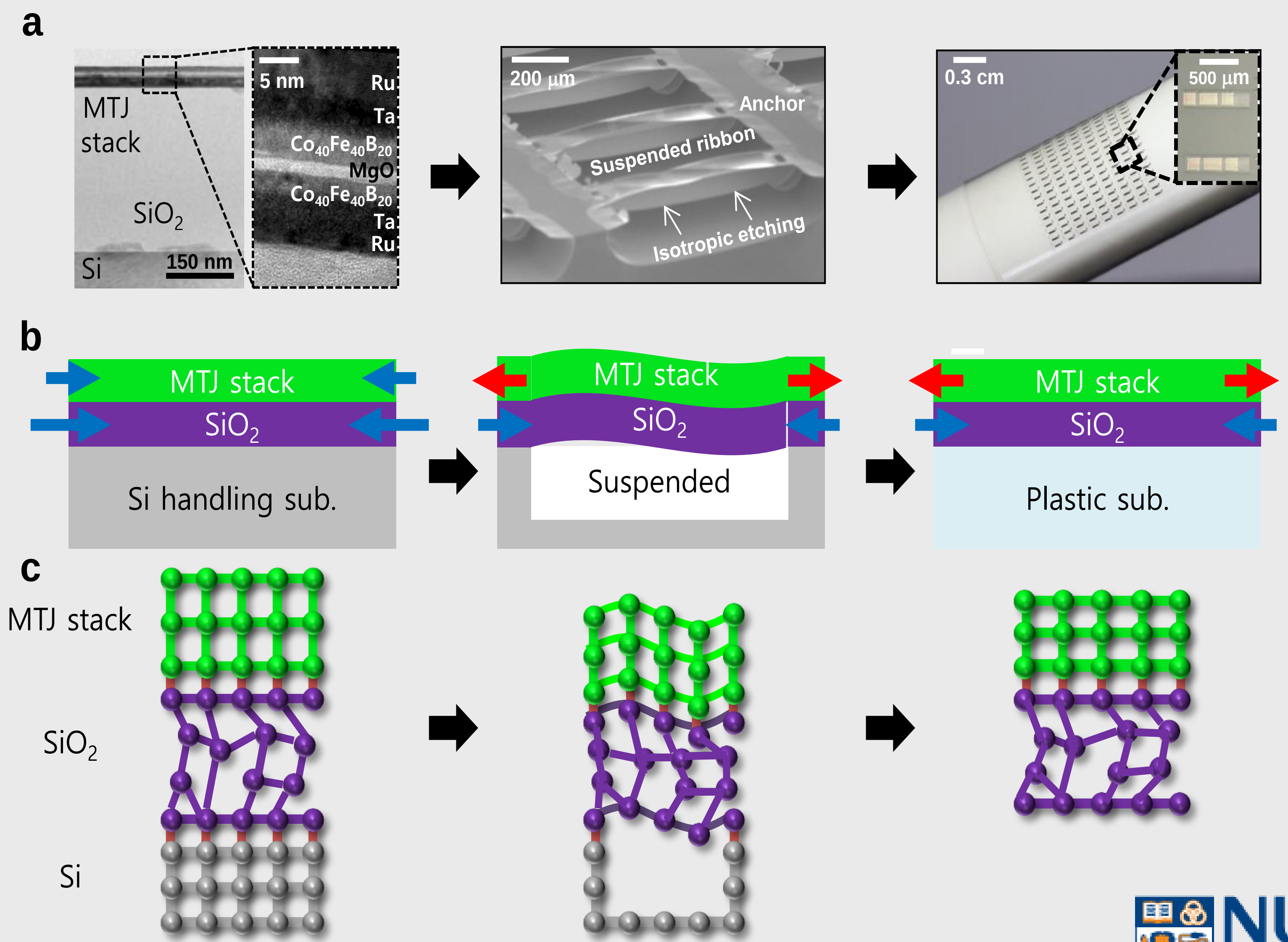

Adv. Mat. **28**, 4983 (2016)

Flexible MTJs

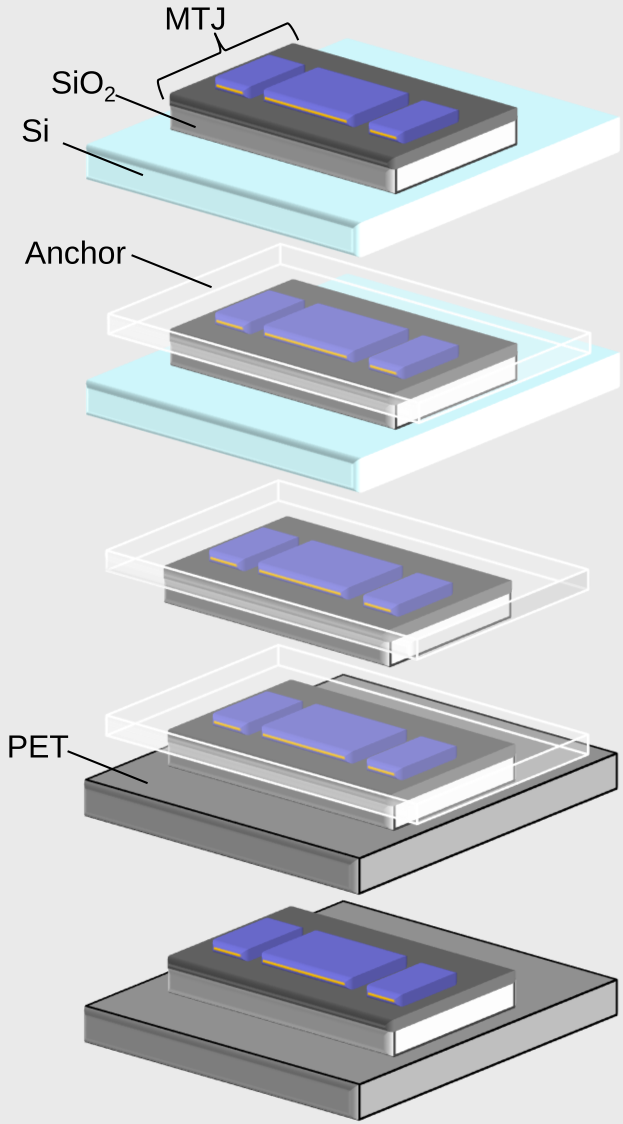

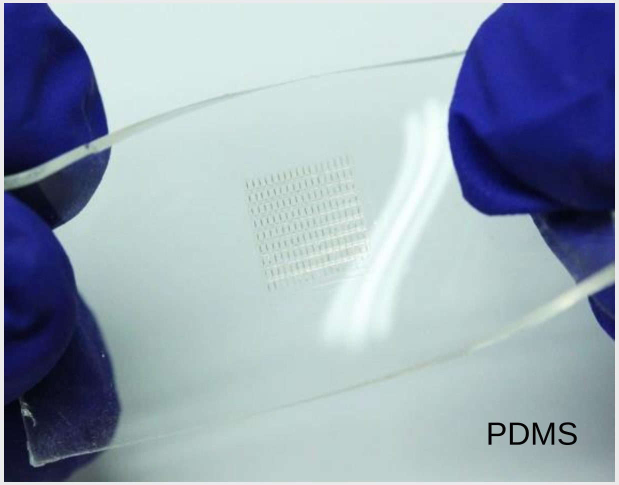

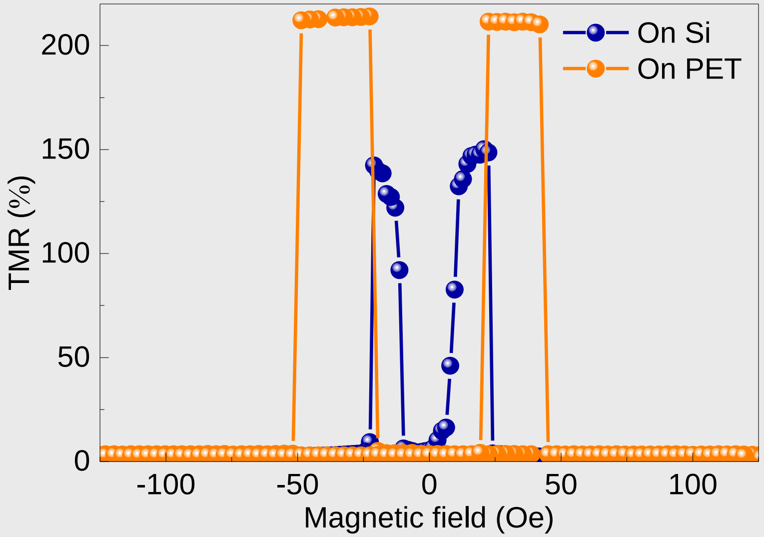

Adv. Mat. **28**, 4983 (2016)

TMR value is enhanced on PET due to tensile strain in the structure.
Lattice mismatch of ~4% b/w MgO and ferromagnets

$k_{//}$-resolved transmission spectra

Compressive strain

Tensile strain

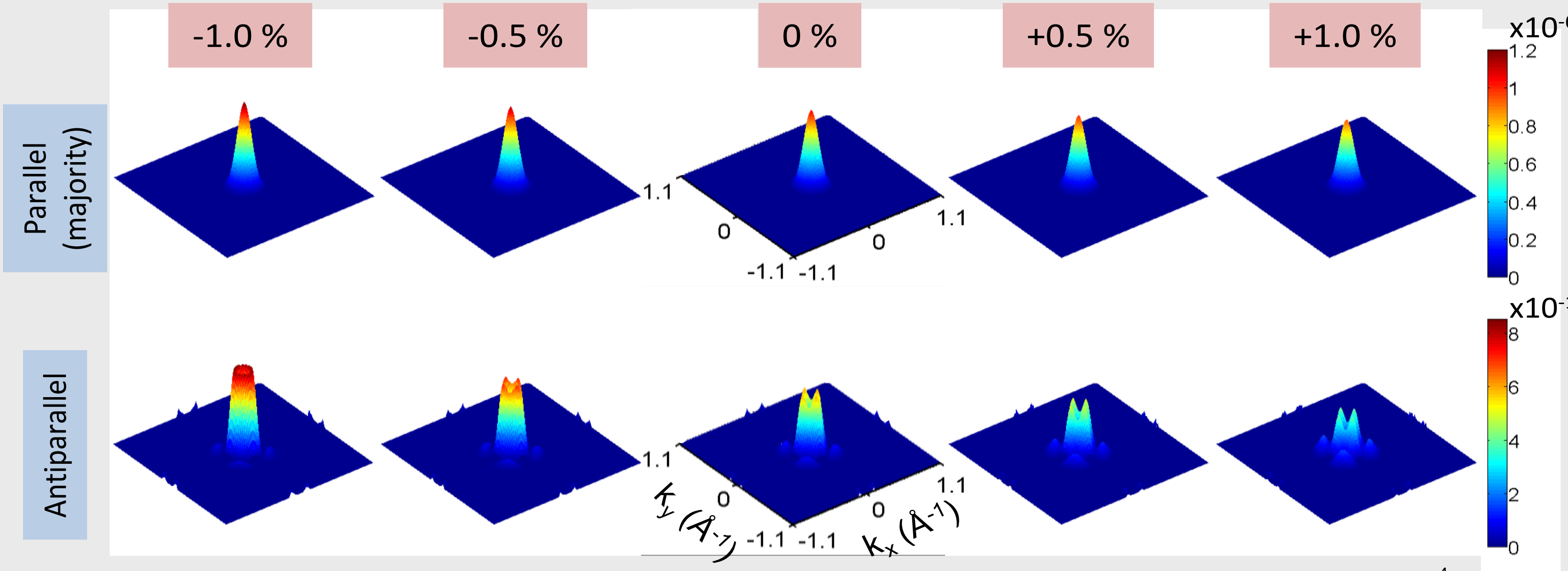

$$TMR = \frac{R_{AP} - R_P}{R_P}$$

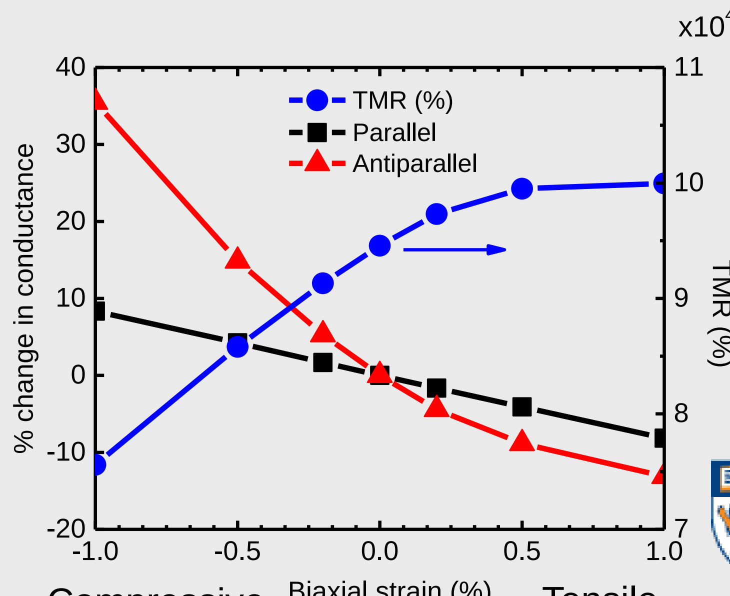

Adv. Mat. **28**, 4983 (2016)
APL **101**, 042407 (2012)

Flexible MTJs on various materials

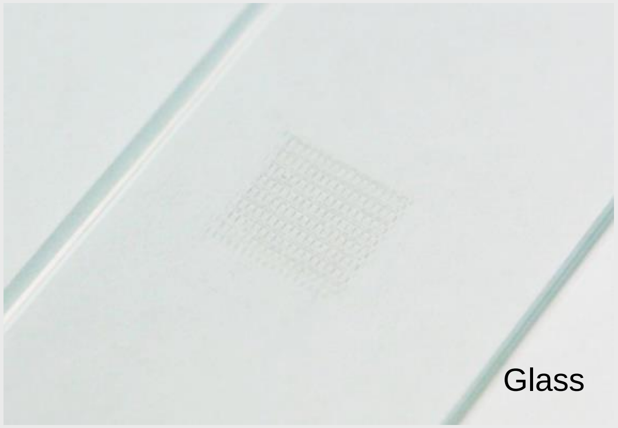

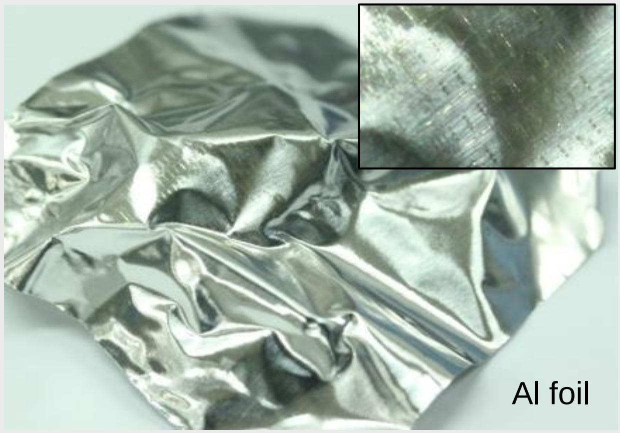

Al foil

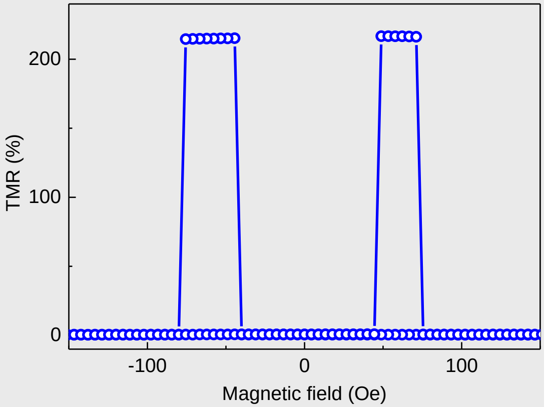

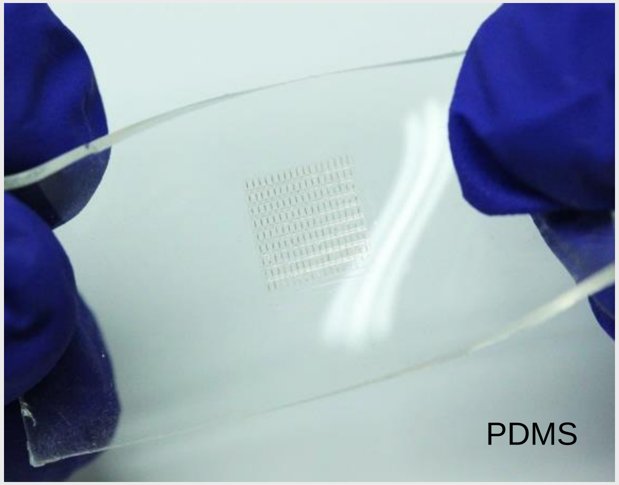

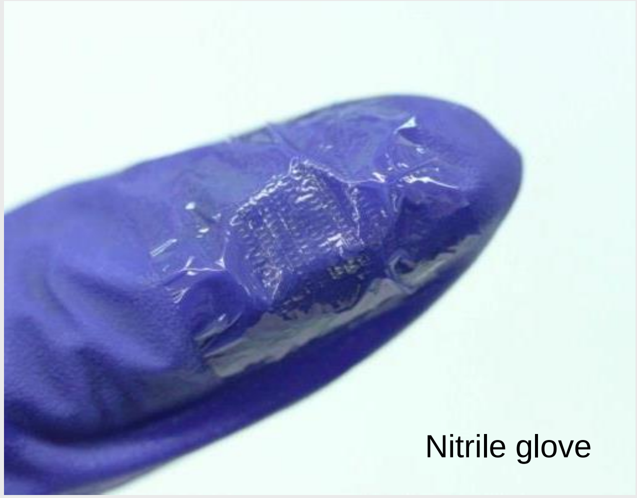

Adv. Mat. **28**, 4983 (2016)

Spin torque MRAM

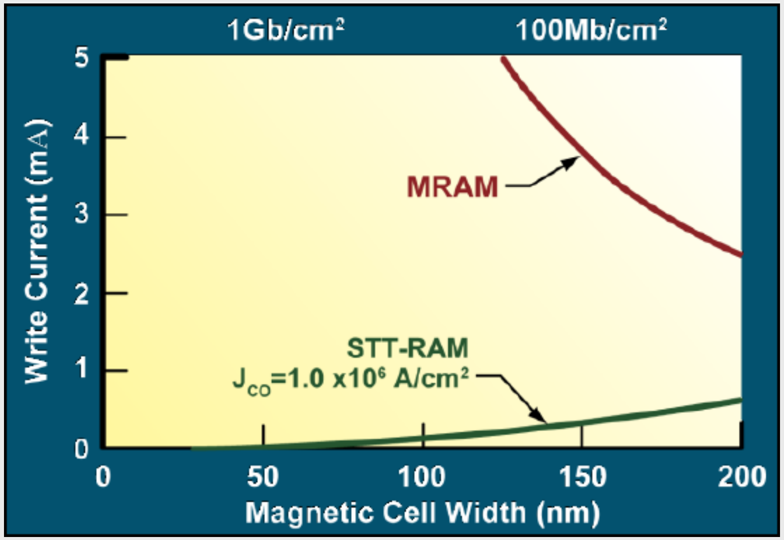

-Present STT-MRAM (Everspin) uses 90 nm node
-GF started to use 40, 28, 14 nm node
-TSMC, IBM, Samsung, TDK, Hynix, Sony, Avalanche, Toshiba, Intel, Qualcomm…

2019 March
Samsung
28 nm FD-SOI
embedded

Toggle-MRAM

STT-MRAM

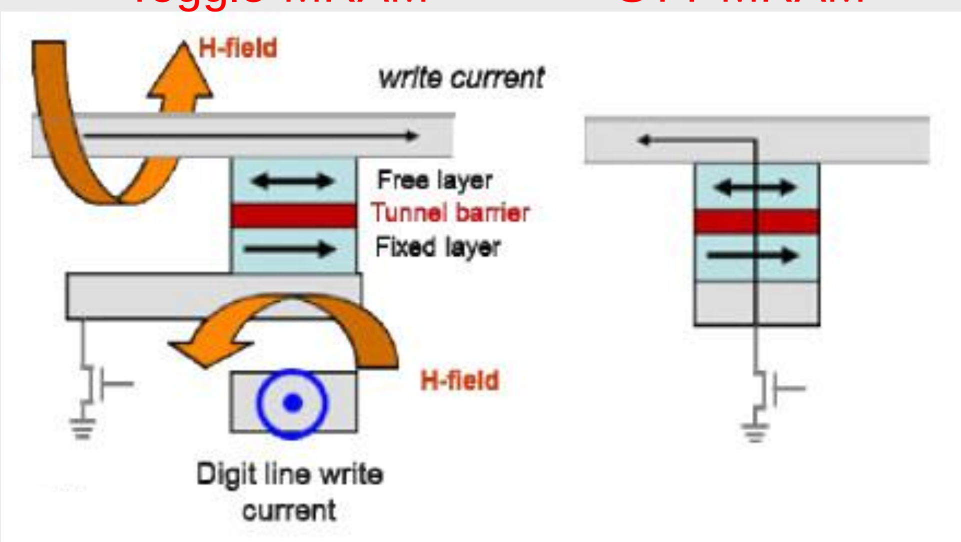

16 Mb

256 Mb

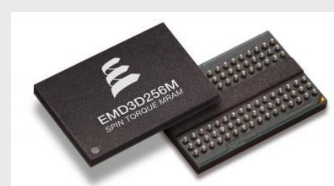

Everspin with
GlobalFoundries

SOT-MRAM

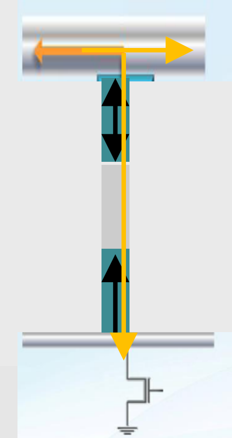

Spin deflection due to spin-orbit coupling

- Trajectory of a spinning ball depends on the direction of its spin.

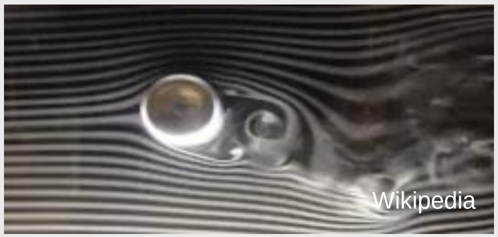

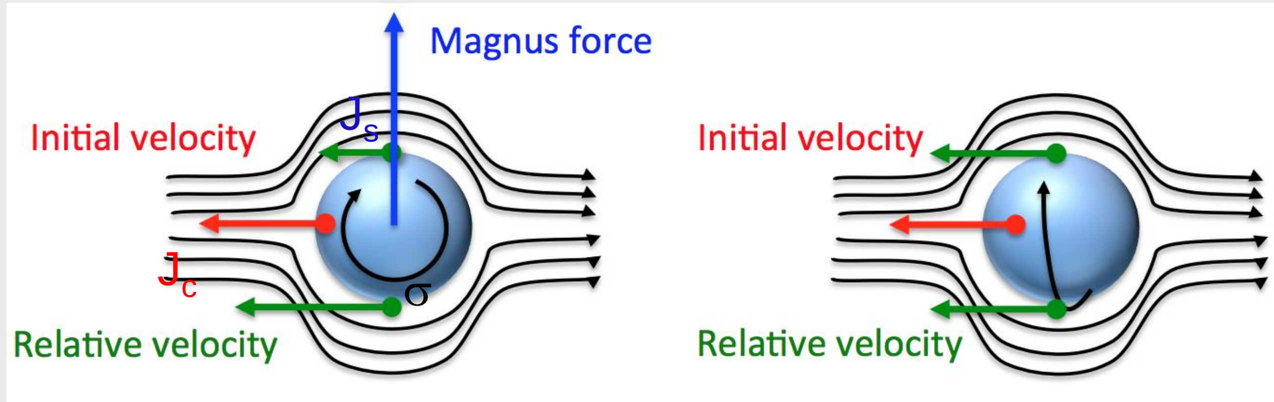

$J_c \perp J_s \perp \sigma$ $\quad$ $J_c \parallel \sigma \rightarrow J_s = 0$

- Electrons experience a transverse deflection depending on spin direction due to spin-orbit coupling.

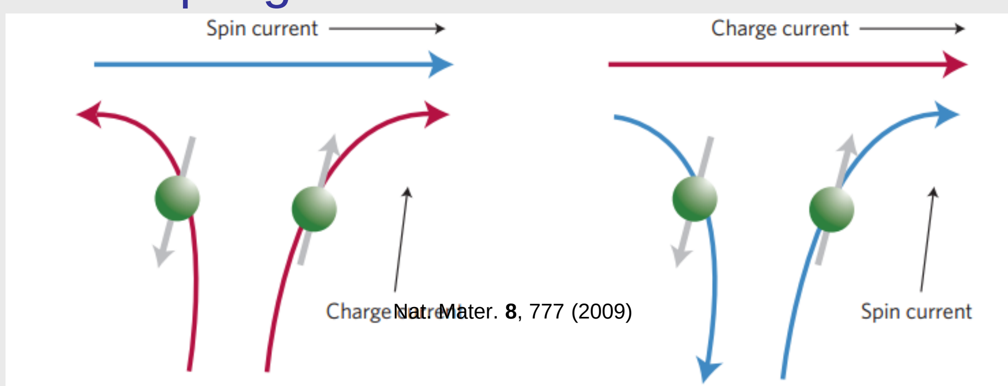

Nat. Mater. **8**, 777 (2009)

- Spin-charge interconversion: foundation of spin-orbitronics

Spin Hall and Inverse Spin Galvanic effects

Spin Hall effect

- Spin orbit coupling in the bulk of non-magnet.
- Can be from intrinsic or extrinsic (impurities).
- Quantified by spin Hall angle (SHA or θ_{sh})

$$\vec{j}_s = \theta_{sh}\left(\vec{j}_c \times \vec{\sigma}\right)$$

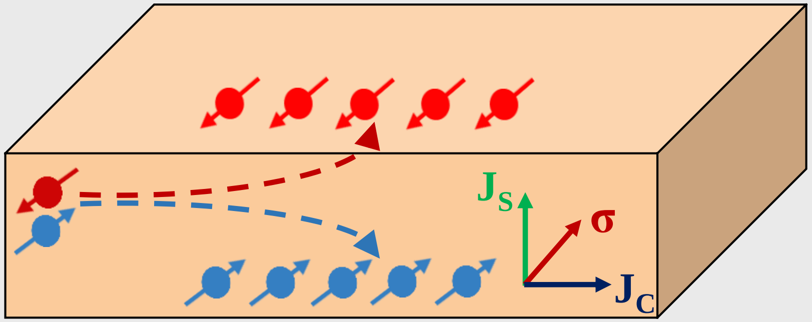

Rashba-Edelstein effect

- Structures with broken inversion symmetry
- Interfacial spin orbit coupling.
- Depends on the nature of the interface.
- Quantified by Rashba coefficient (∝ magnitude of **E=-∇V**)

$$\hat{H}_{so} = \xi \hat{\boldsymbol{\sigma}} \cdot \left(\nabla V \times \hat{\mathrm{p}}\right)$$

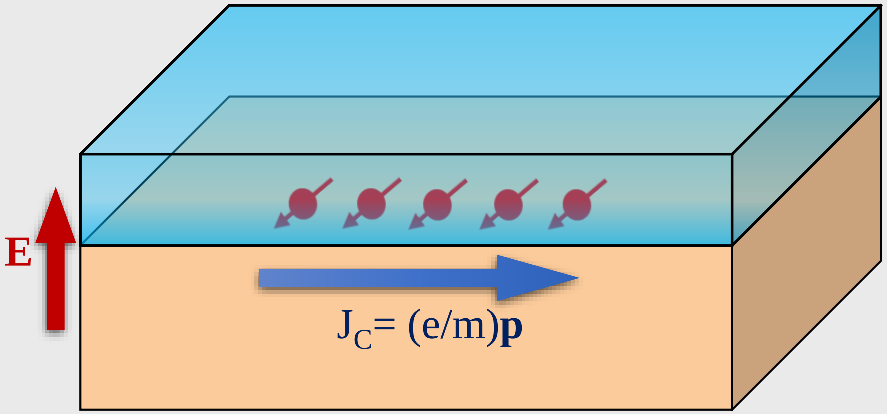

Theory: D'yakanov and Perel (1971), Hirsch (1999), Edelstein (2000), Zhang (2000), Murakami, Nagaosa, Zhang (2003), Sinova *et al.* (2004),…
Experiments: (semiconductors) Ganichev *et al.* (2002), Kato *et al.* (2004), Wunderlich *et al.* (2005) (metals) Valenzuela and Tinkham (2006), Saitoh *et al.* (2006), Kimura *et al.* (2007).

Observation of spin Hall effect in semiconductors

Magneto optical Kerr imaging
GaAs, T = 30 K

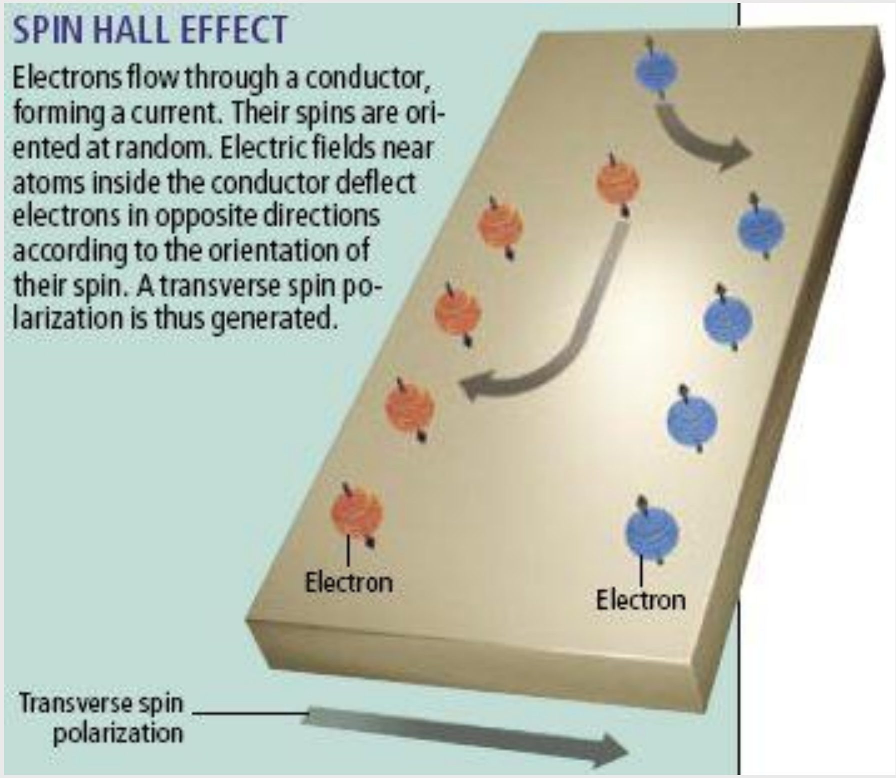

Y.K. Kato, Sci. Am. 2007

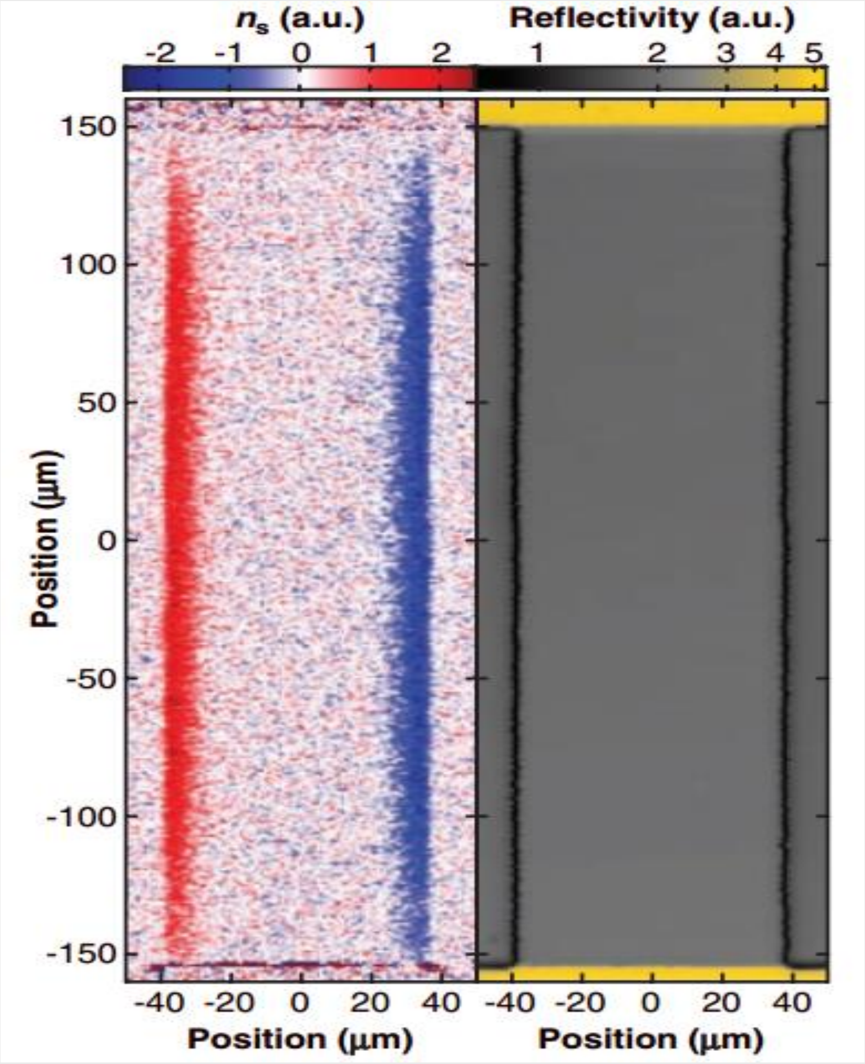

Science **306**, 1910 (2004)

Imaging is believing!
Easy for semiconductors, but difficult for metals.

NUS National University of Singapore

Scanning photovoltage microscope with currents

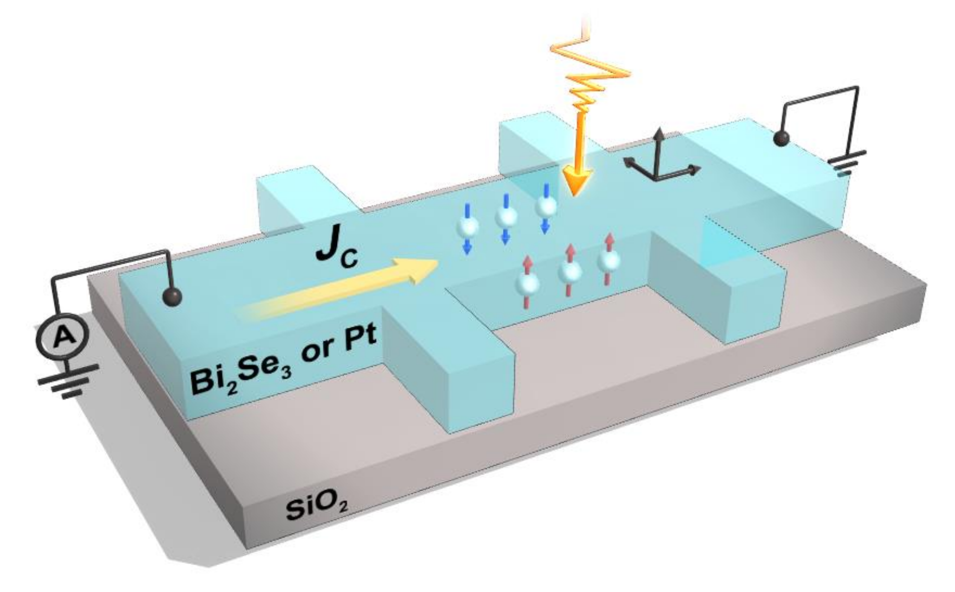

- DC current is applied to induce spin accumulation.
- Circularly polarized light normally incidents on the sample.
- Magnetic circular dichroism.
- Photovoltages are detected by lock-in amp.
- Piezo sample stage enables mapping.

- $V_{photovoltage} = V_{RCP} - V_{LCP}$

RCP light excites spin up electron, while LCP light excites spin down electron.

- $V_{photovoltage} > 0$ → local spin direction is spin down.
- $V_{photovoltage} < 0$ → local spin direction is spin up.

Nat. Comm. **9**, 2492 (2018); Adv. Opt. Mat. **4**, 1642 (2016)

Negligible spin accumulation in Cu

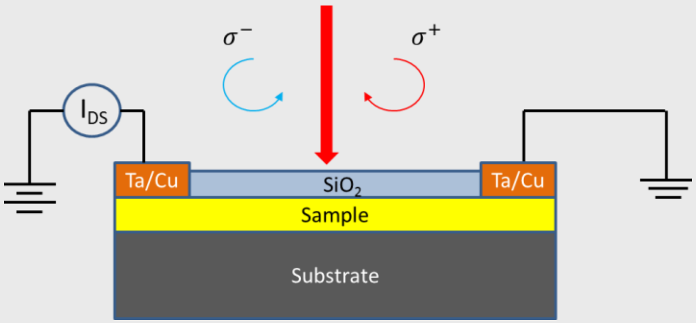

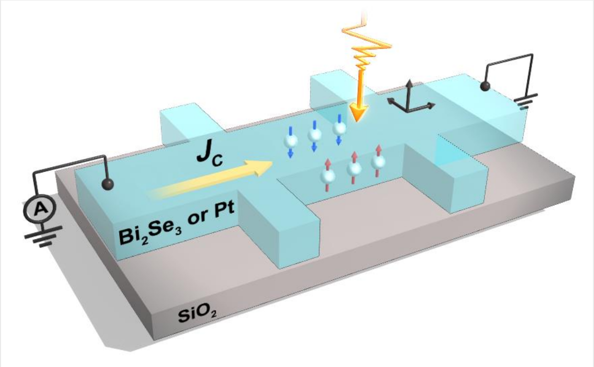

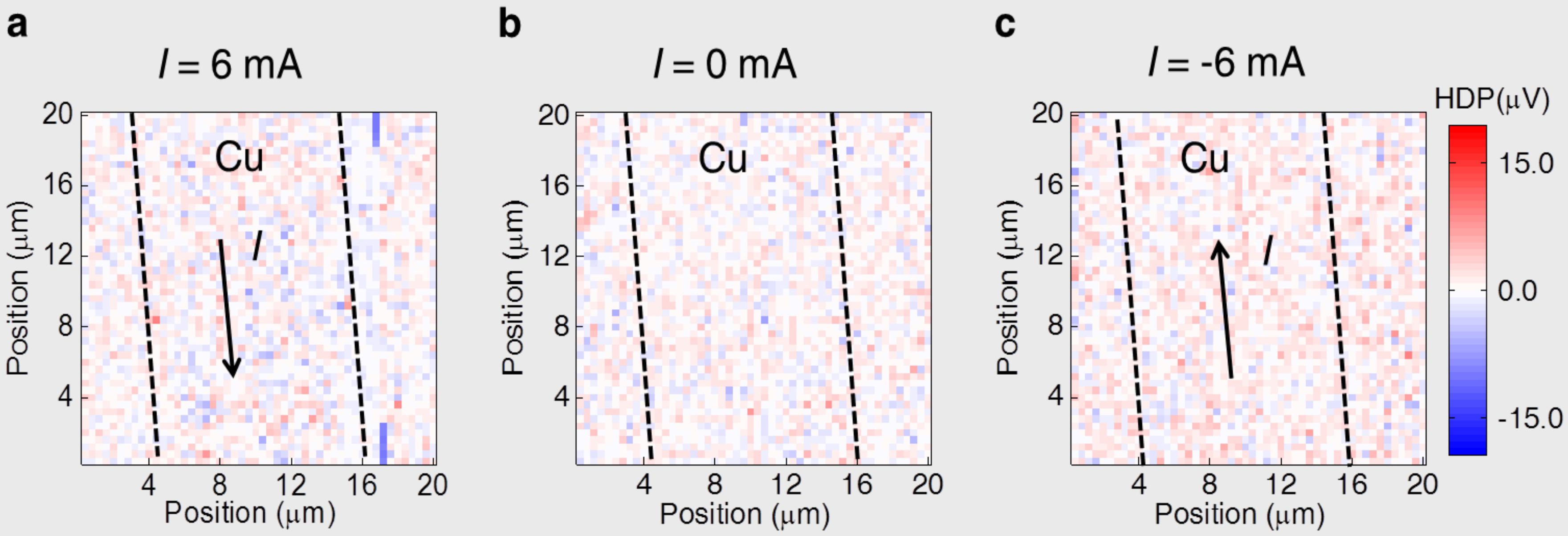

Bias dc current of 1 mA ~ 10^6 A cm^{-2}.
No signal regardless of currents.

Nat. Comm. **9**, 2492 (2018)

Accumulated spin imaging in Pt and Bi_2Se_3

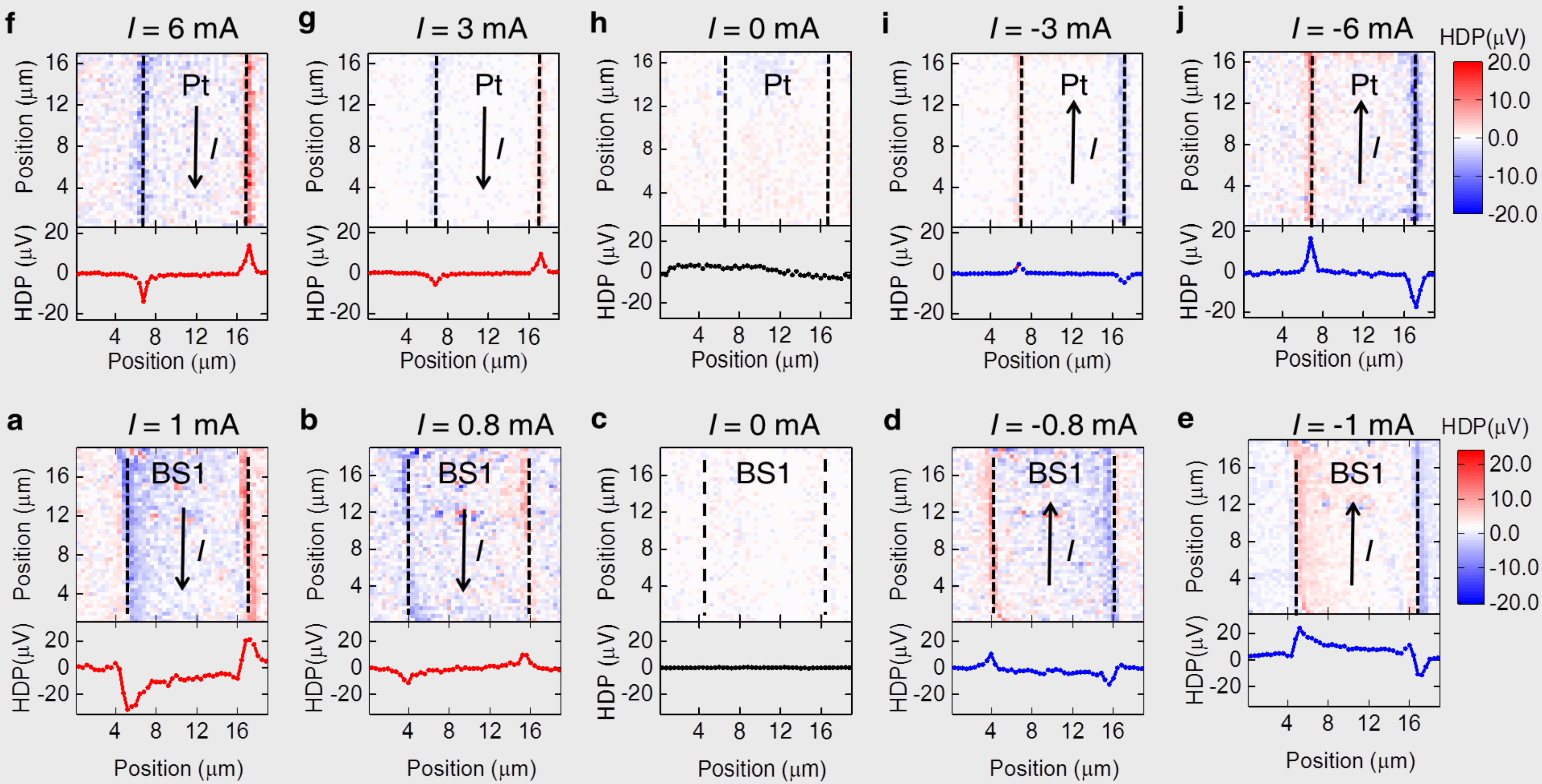

- Sign switches in opposite edges and with reversing currents.
- Both semiconductors and metals work.
- Can extract spin Hall angle and spin lifetime without a ferromagnet.

Nat. Comm. **9**, 2492 (2018)

Spin-orbit torque switching in metallic structures

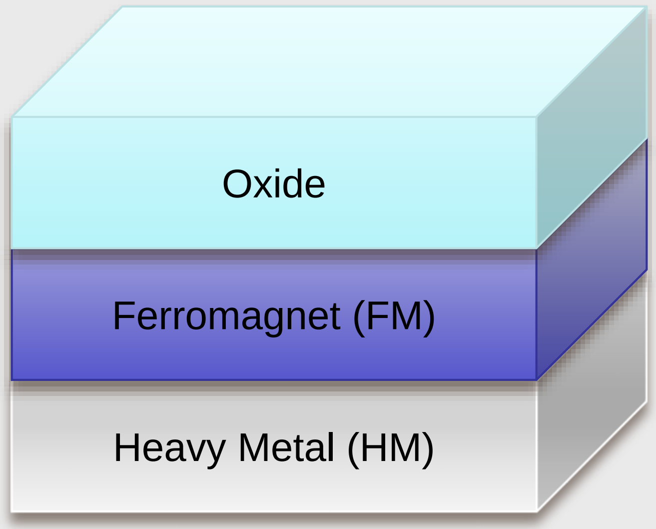

Strong Rashba field arises from asymmetric interfaces

Spin Hall effect arises from HM

In-plane currents can switch the magnetization (spin-orbit torques).

Spin-orbit torque has paved a novel way to manipulate the magnetization.

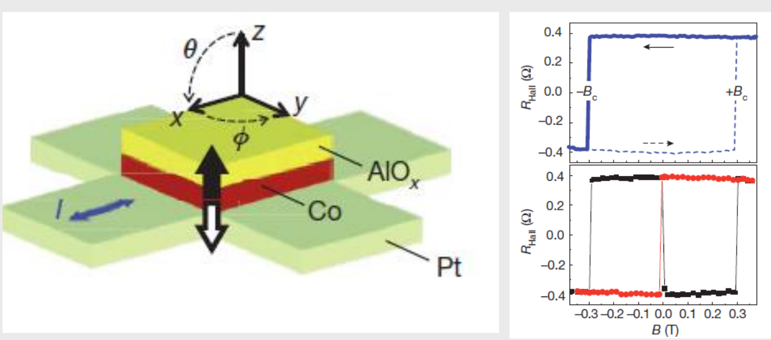

Nature **476**, 189 (2011)

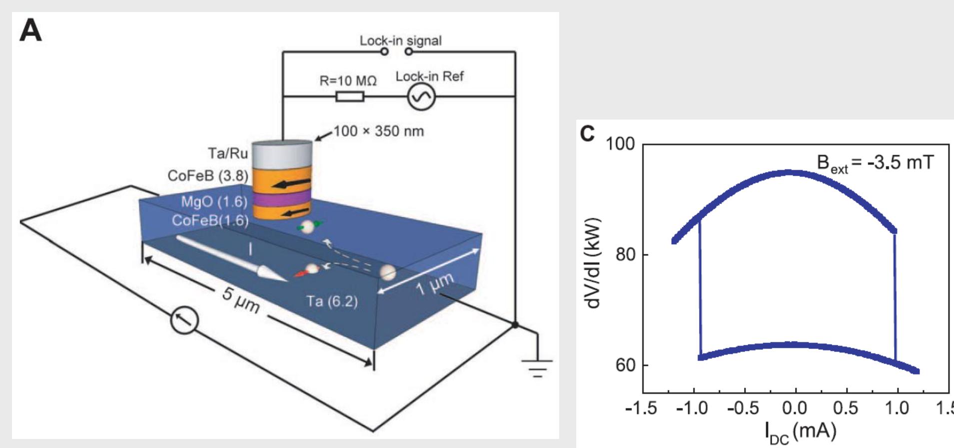

Science **336**, 556 (2012)

Spin orbit torque effective fields (H_L and H_T)

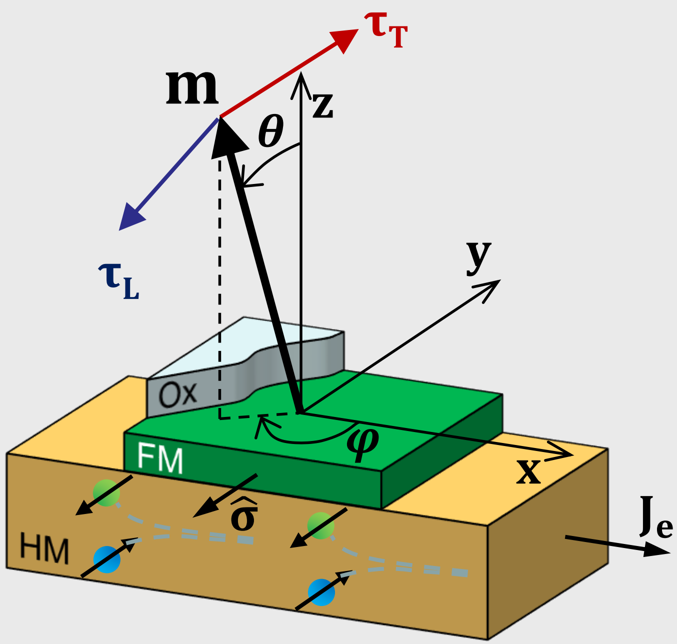

-Spins are generated in a nonmagnetic metal.

-Ferromagnet experiences a torque due to accumulated spins.

-In presence of SOT, the modified Landau-Lifshitz-Gilbert (LLG) equation

$$\partial_t \mathbf{m} = -\gamma\mu_0 \mathbf{m} \times \mathbf{H}_{\mathrm{eff}} + \alpha \mathbf{m} \times \partial_t \mathbf{m} + \boldsymbol{\tau}_{\mathrm{L}} + \boldsymbol{\tau}_{\mathrm{T}}$$

$$\boldsymbol{\tau}_{\mathrm{L}} = -\gamma\mu_0 \mathbf{m} \times \mathbf{H}_{\mathrm{L}}$$

$$\boldsymbol{\tau}_{\mathrm{T}} = -\gamma\mu_0 \mathbf{m} \times \mathbf{H}_{\mathrm{T}}$$

-Longitudinal field (H_L) along the y × m direction

-Transverse field (H_T) along the y direction

Review: *Adv. Mat.* **30**, 1705699 (2018)

Characterization of SOT - Second harmonic signal

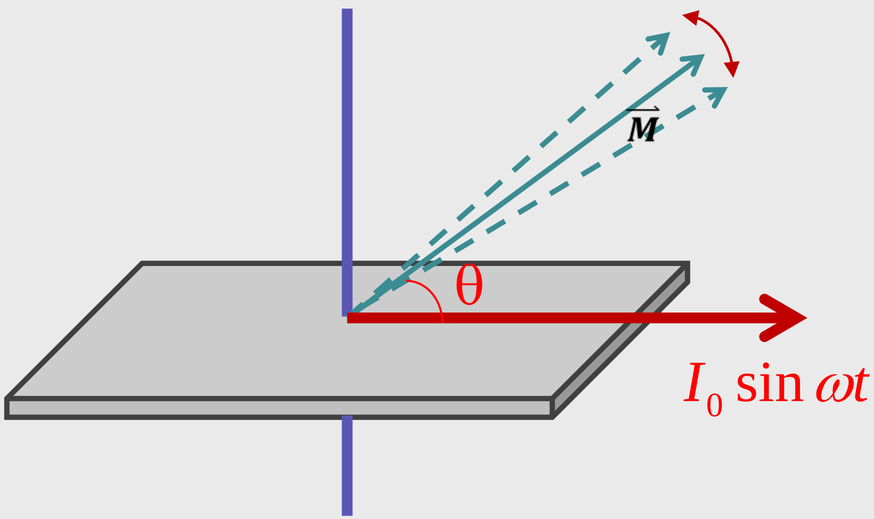

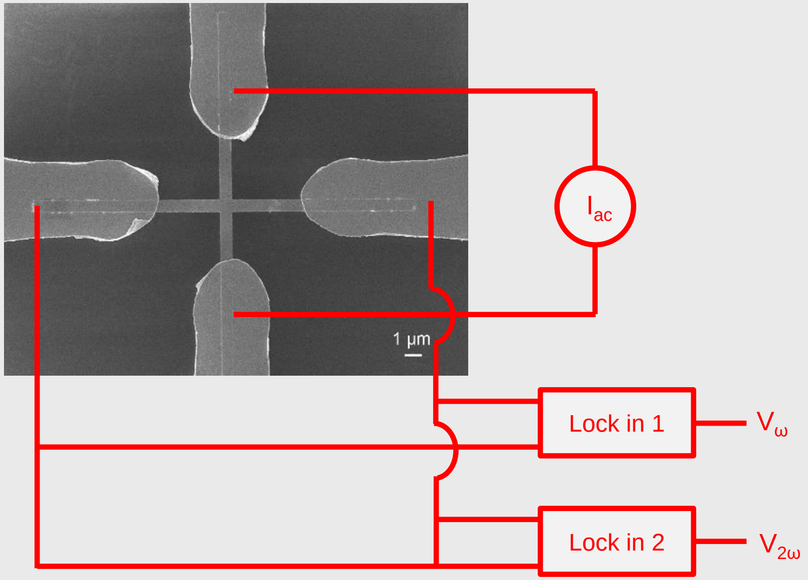

- In perpendicularly magnetized systems, a low frequency AC current is passed
  → Oscillating torques (SOT) on the magnet
  → Anomalous Hall resistance oscillates at same frequency.

$$V_H = I_{ac} R_{ac} = I_0 \sin \omega t (R_H + \Delta R_H \sin \omega t) = I_0 R_H \sin \omega t + \frac{I_0 \Delta R_H}{2} - \frac{I_0 \Delta R_H}{2} \cos 2\omega t$$

Pi *et al.*, Appl. Phys. Lett. **97**, 162507 (2010)

SOT effective field measurements (2nd harmonic)

SOT effective field : $H_L = \hbar\theta_{SH}|j_e|/(2|e|M_S t_F)$

Longitudinal configuration

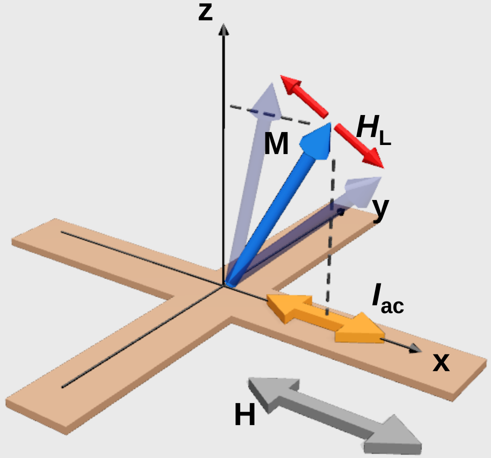

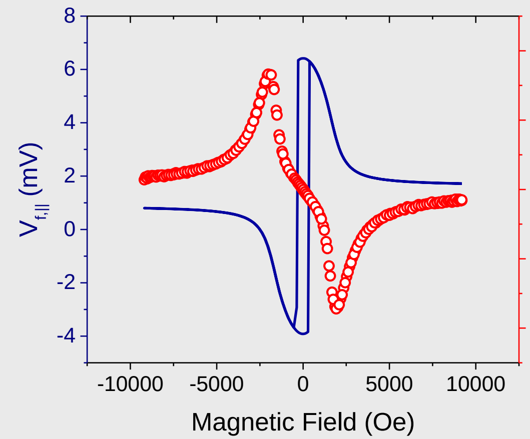

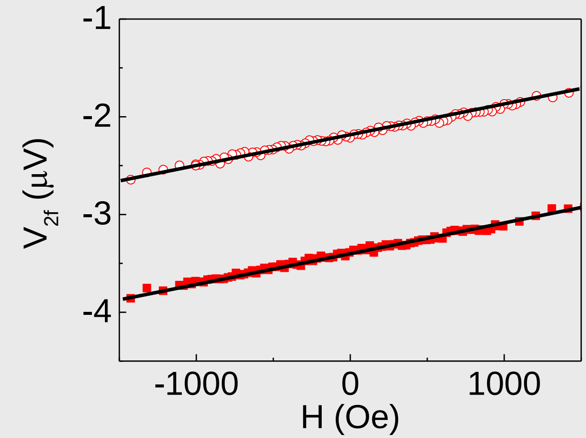

Transverse configuration

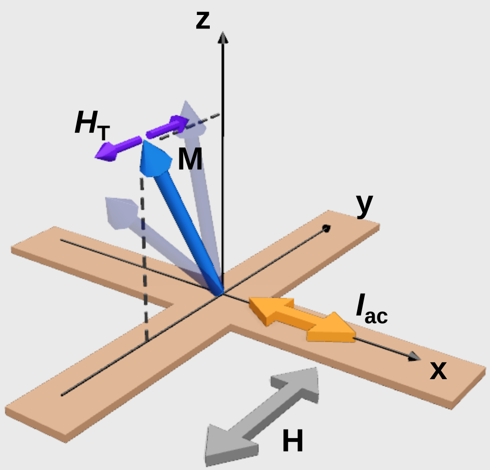

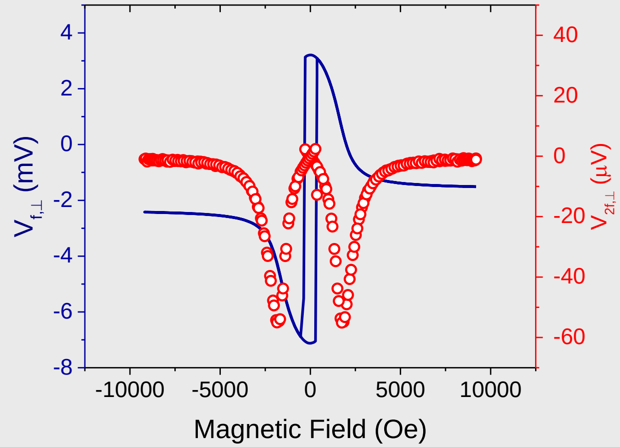

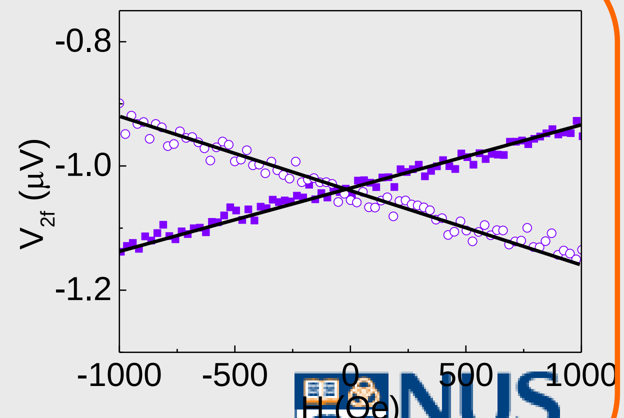

Garello *et al.* Nat. Nano. **8**, 587 (2013) PRL **111**, 246602 (2013), Sci. Rep. **4**, 4491 (2014). Kim *et al.* Nat. Mater. **12**, 240 (2013).

Spin Hall angle (θ_{SH})

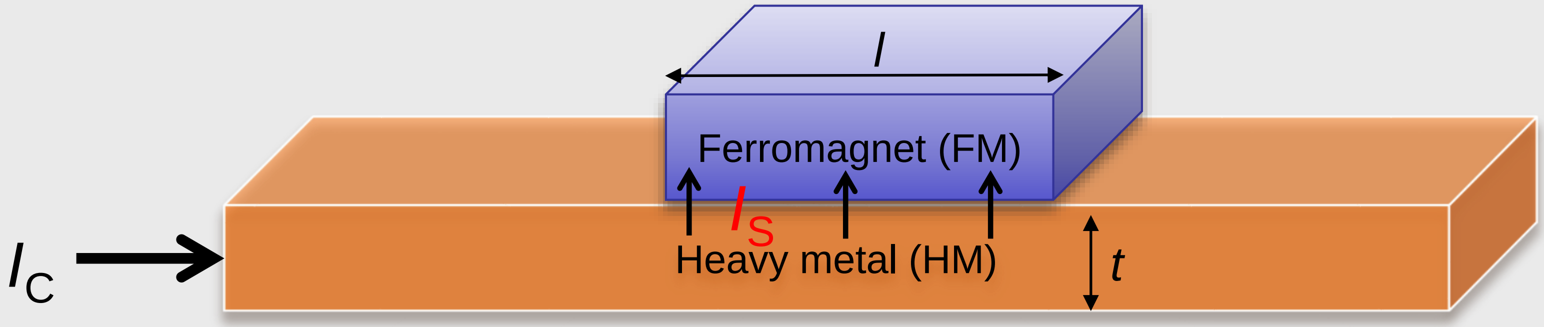

Spin currents can be very large, as the electron can interact with the FM many times (lateral scattering)

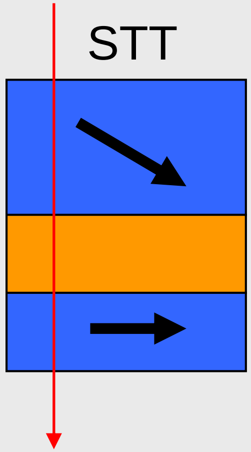

$$\theta_{SH} = \frac{\sigma_S}{\sigma_C}$$

$$\frac{I_S}{I_C} = \theta_{SH} \frac{l}{t} \quad l >> t$$

SOT effective fields (H_L and H_T) can be connected to θ_{SH}

$$\theta_{SH} = (2e/\hbar) M_S t_F H_{L,T}$$

Review: *Adv. Mat.* **30**, 1705699 (2018)

Spin torque ferromagnetic resonance (ST-FMR)

$$\frac{\partial \mathbf{m}}{\partial t} = -\gamma\mu_0 \mathbf{m} \times \mathbf{H}_{\mathbf{eff}} + \alpha \mathbf{m} \times \frac{\partial \mathbf{m}}{\partial t} + \boxed{\boldsymbol{\tau}_L + \boldsymbol{\tau}_T}$$

Use SOTs instead of $\boldsymbol{h}_{rf}$

- AC current $\mathbf{I}_{\mathbf{ac}}\mathbf{(t)}$ → AC spin orbit torques
- Magnetization oscillation → Resistance oscillation **R(t)**
- Spin rectification: DC voltage V_{mix} is detected as ST-FMR signal
- For a given frequency *f* of $\mathbf{I}_{\mathbf{ac}}$, H_{ext} is swept to meet the resonance

$I_{ac}(t)$ x R(t)

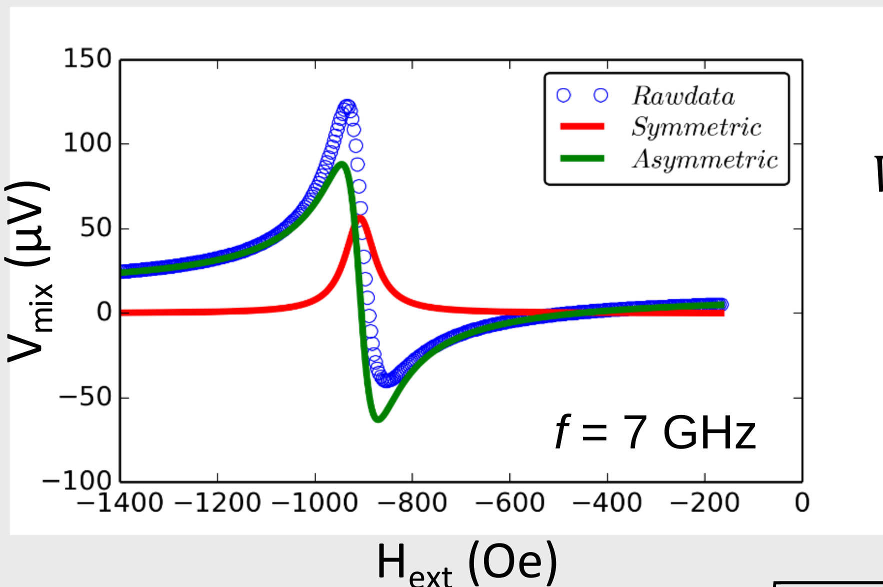

$$V_{\text{mix}} = V_S F_S(H_{ext}) + V_A F_A(H_{ext})$$

Symmetric Lorentzian

Antisymmetric Lorentzian

PRL **106,** 036601 (2011)

$$\theta_{SH} = (V_S/V_A)(e\mu_0 M_s t\, d/\hbar)\sqrt{1 + 4\pi\, M_{eff}/H_{ext}}$$

Review: J. Phys. D: Appl. Phys. **51**, 273002 (2018)

Current induced switching to evaluate θ_{SH}

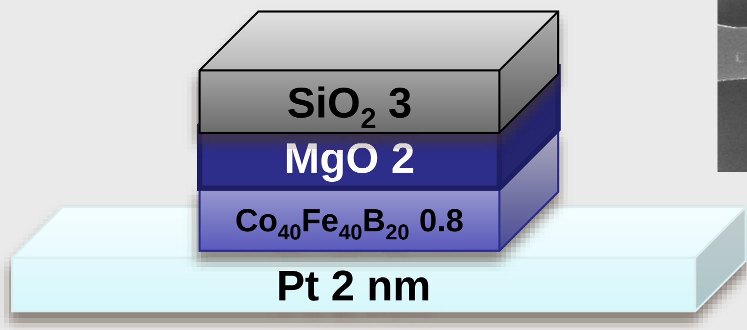

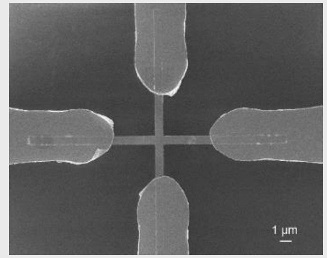

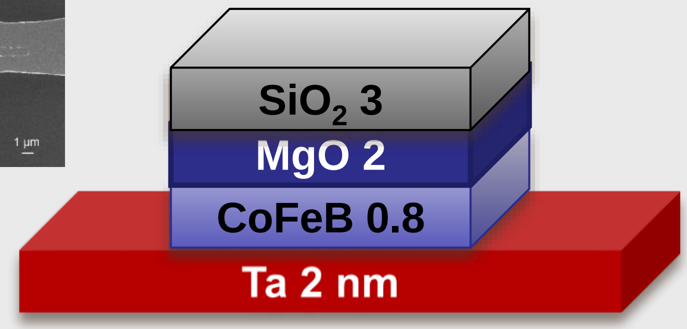

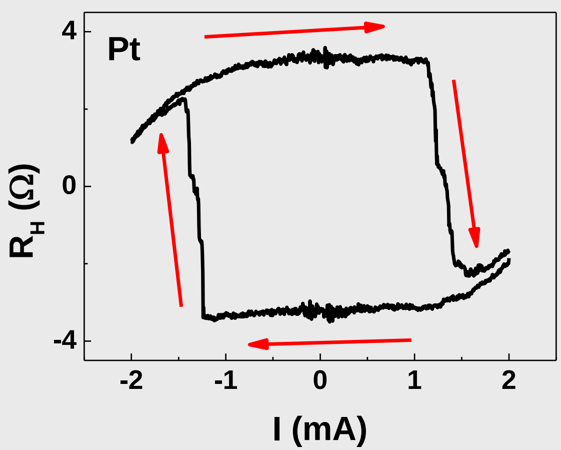

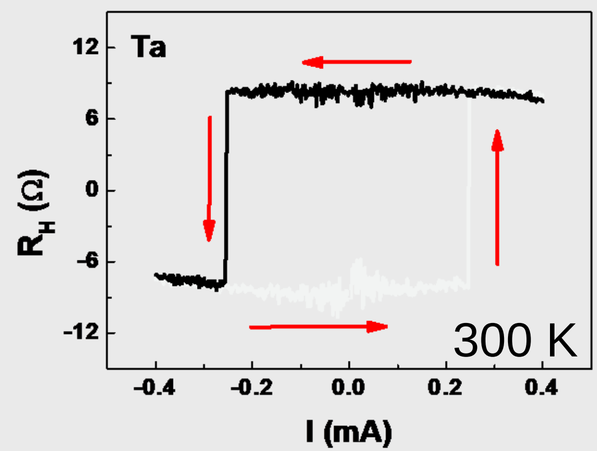

- Opposite switching polarity in Pt and Ta → opposite θ_{SH}
- Switching current in Ta is smaller than Pt nanowires

$$I_c \approx \frac{e}{\hbar}\left(\frac{M_S t_{FM} A_{HM}}{\theta_{SH}}\right) H_{eff}$$

Sci. Rep. **4**, 4491 (2014); APL **105**, 152412 (2014); APL **103**, 232408 (2013)

Spin orbit torque (SOT) engineering

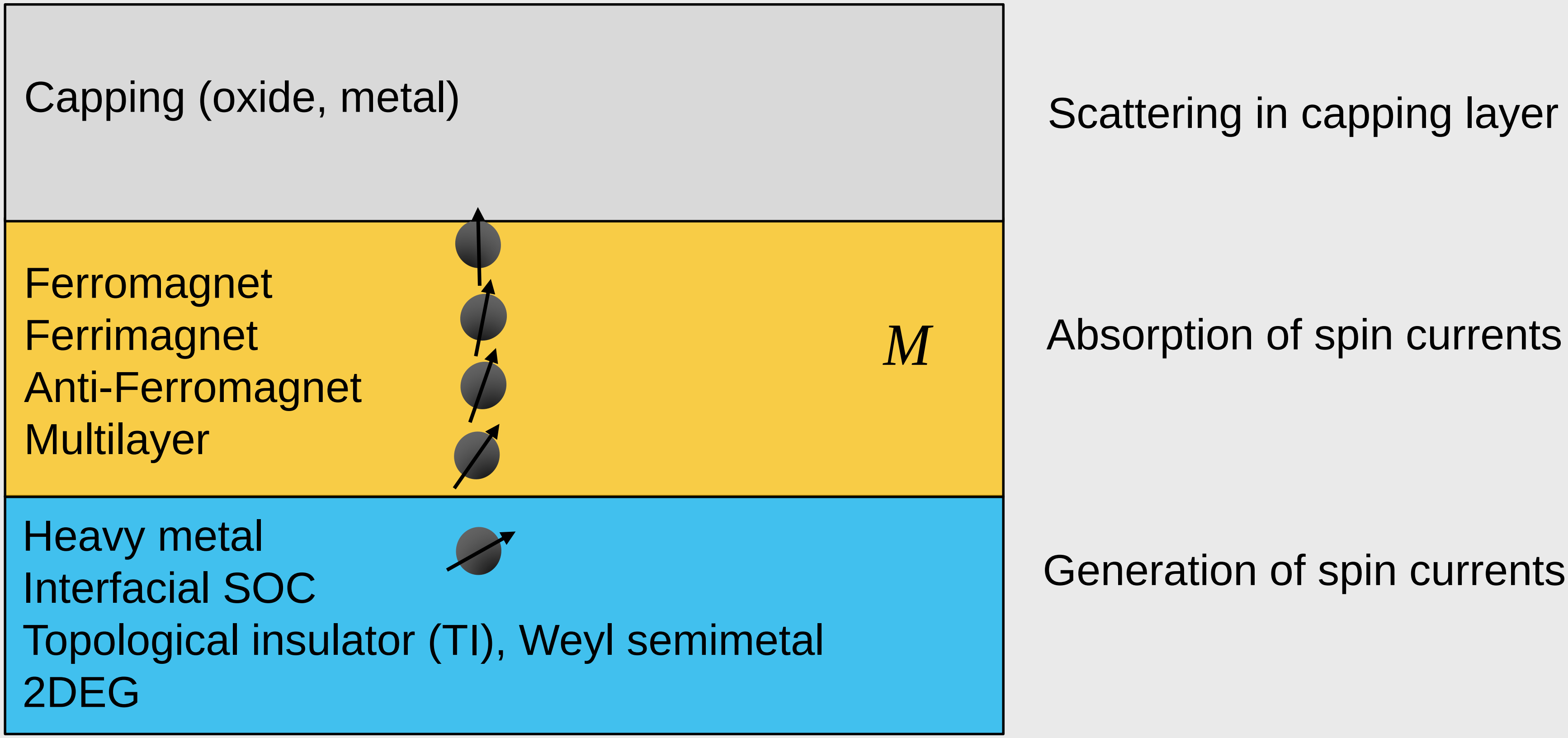

Search for large spin Hall angle (θ_{SH}) or effective fields (H_L and H_T)

Review: *Appl. Phys. Rev.* **5**, 031107 (2018)

NUS National University of Singapore

Spin Hall angle is a material parameter

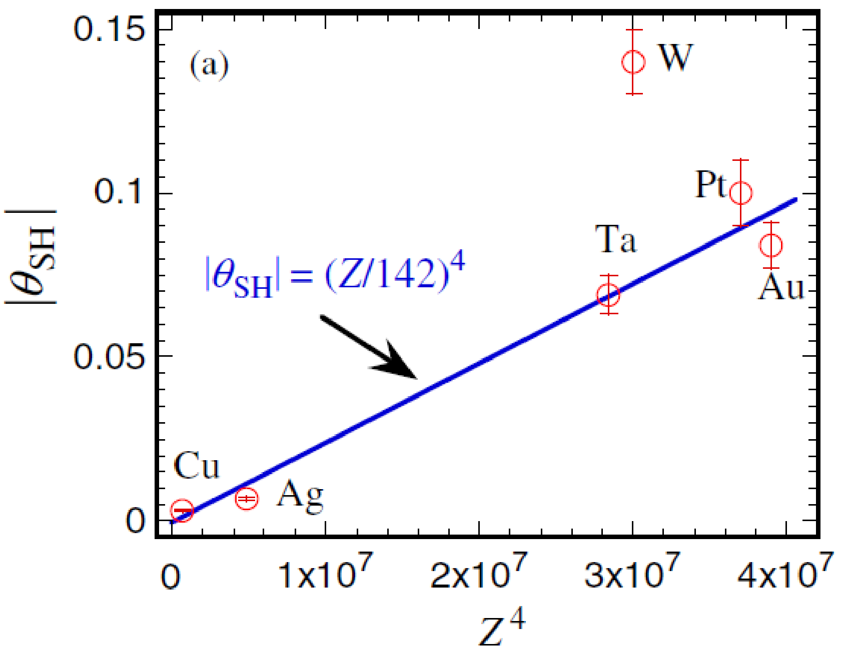

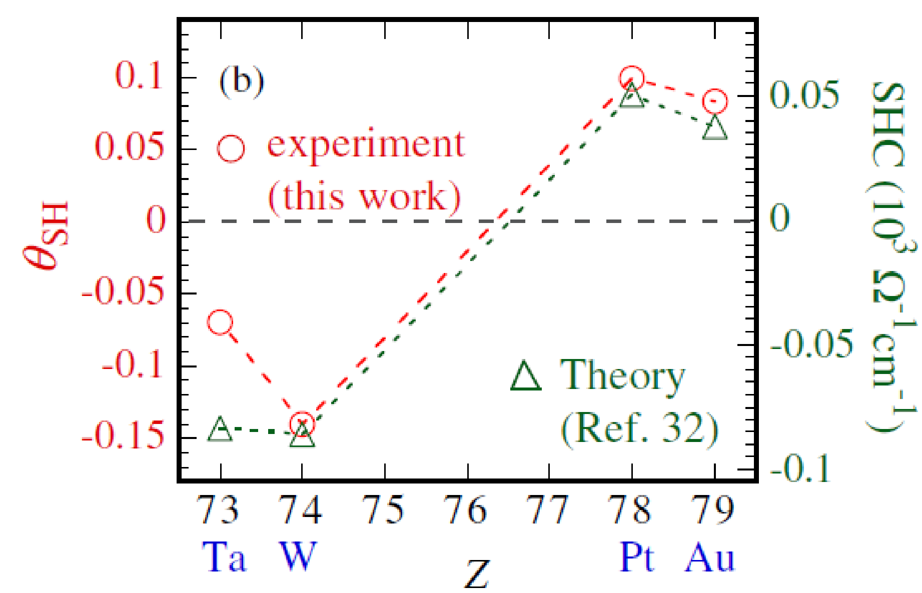

Z: atomic number

Number of d-electrons: Hund's rules

PRL **112**, 197201 (2014), PRB **77**, 165117 (2008), PRB **83**, 174405 (2011)

Heavy metals→ strong spin orbit coupling

Luckily some CMOS compatible materials show large spin Hall angles

Is θ_{SH} a fixed value for a given material?

Reported θ_{SH} from Pt using various methods

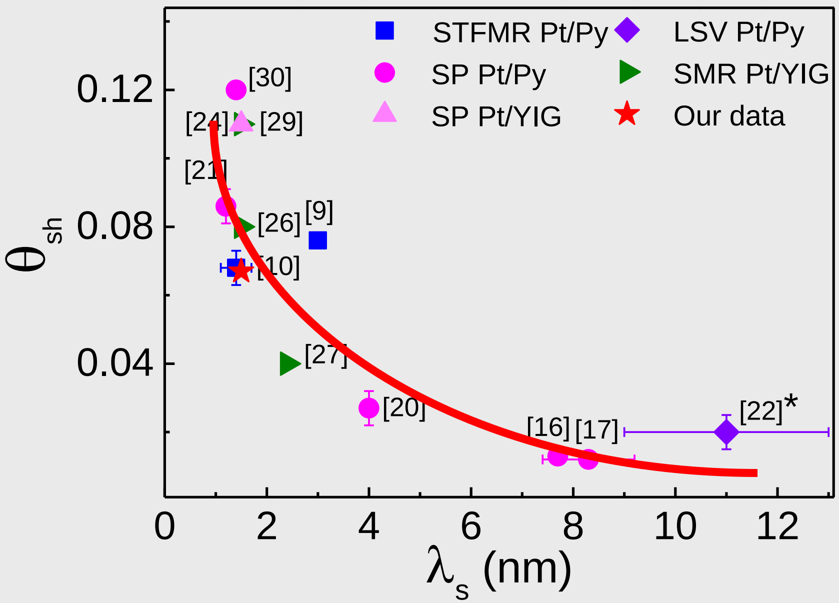

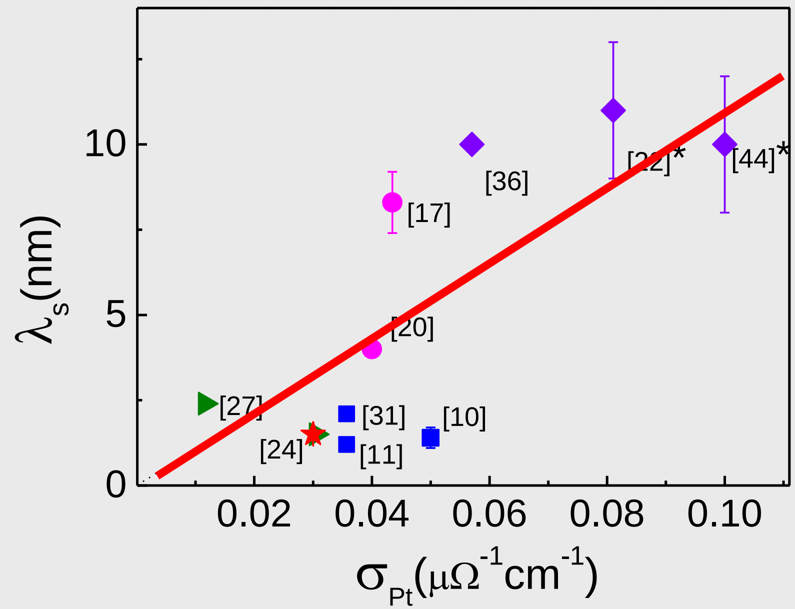

- Relationship of $\theta_{SH}\lambda_S$ ~ 0.13 nm [0.18 nm, PRL 112, 106602 (2014)]
- Large resistivity→ large θ_{SH} due to spin dependent scattering
- We can engineer θ_{SH} by changing σ_{Pt}
- Recent systematic measurements: Sagasta et al., PRB 94, 060412 (2016)

of Singapore

APL **105**, 152412 (2014)

Modulating polarity of SOTs

Ta

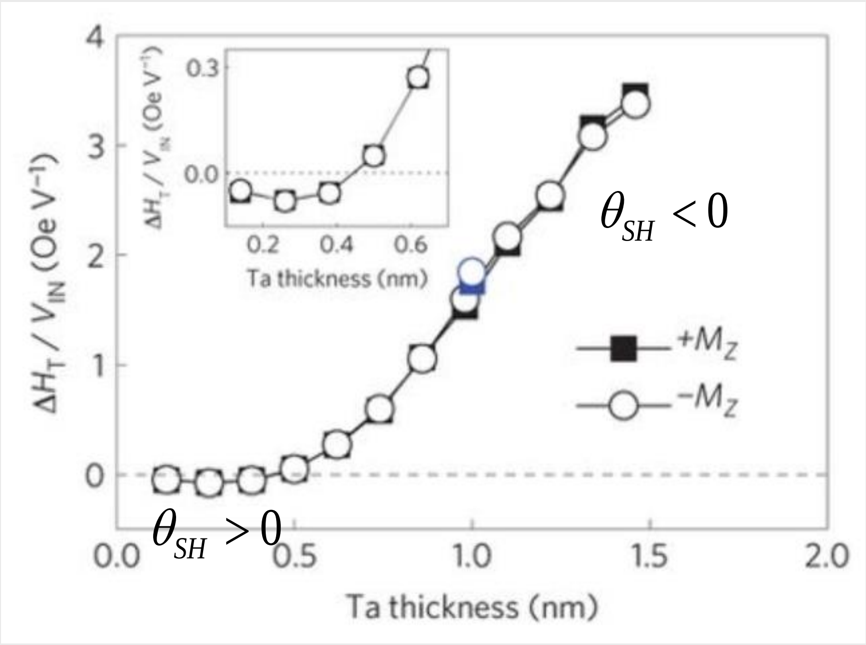

Nature Mater. 12, 240 (2013)

Hf

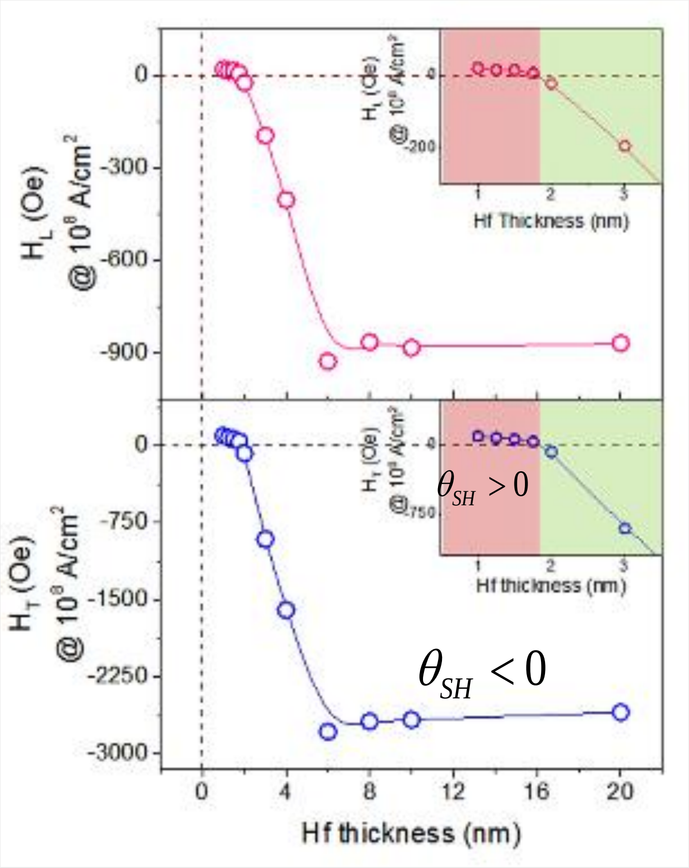

Appl. Phys. Lett. 108, 202406 (2016)

- The SOT polarity is a function of heavy metal thickness.
- Thick regime: spin Hall dominant
- Thin regime: interfacial spin-orbit with opposite sign to spin Hall

Is the sign of θ_{SH} fixed for a given material?

Reverse switching polarity by oxygen engineering

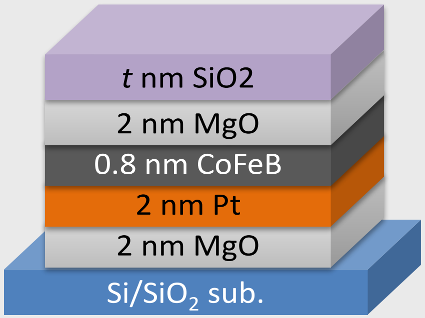

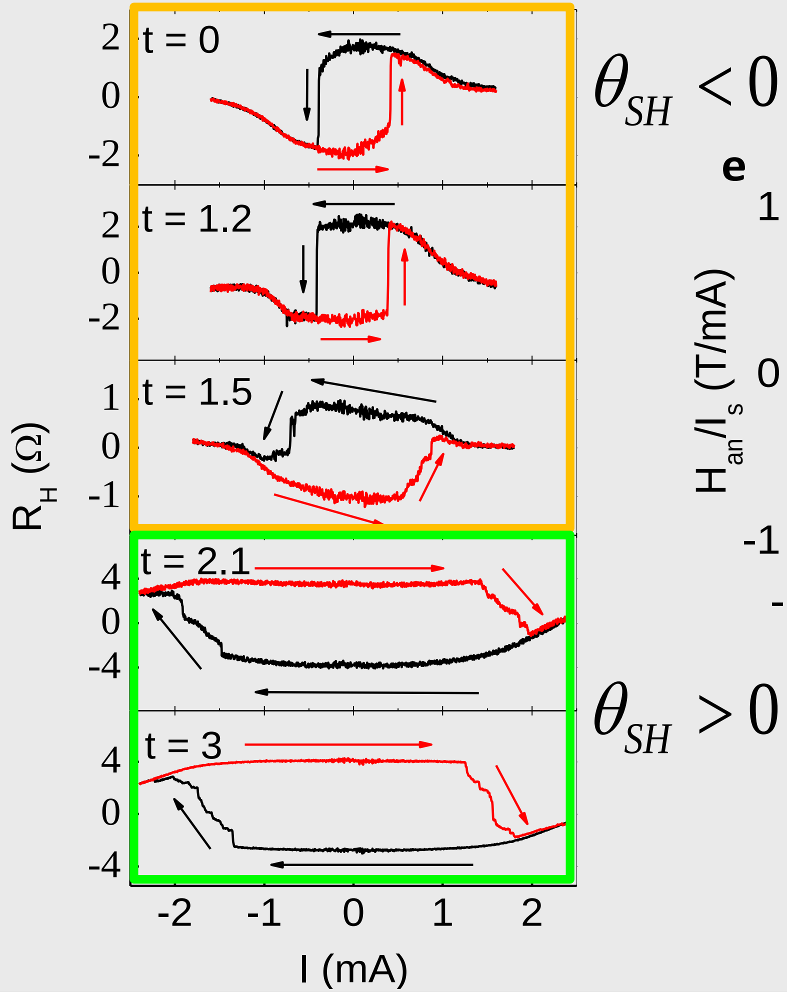

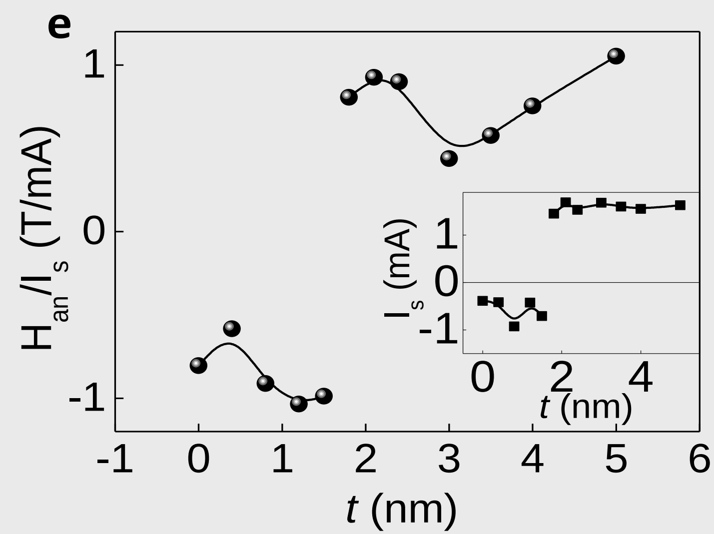

-Sign of spin Hall angle changes across a transition thickness of SiO_2 (*t* = 1.5 nm)

-Cannot be understood by spin Hall physics → suggest the role of interface

Nat. Nanotech. **10**, 333 (2015)

Electric-field control of effective spin Hall sign

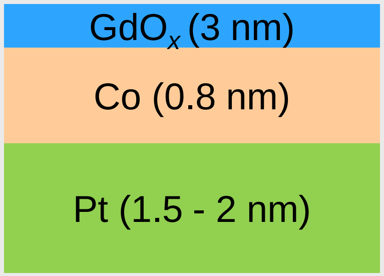

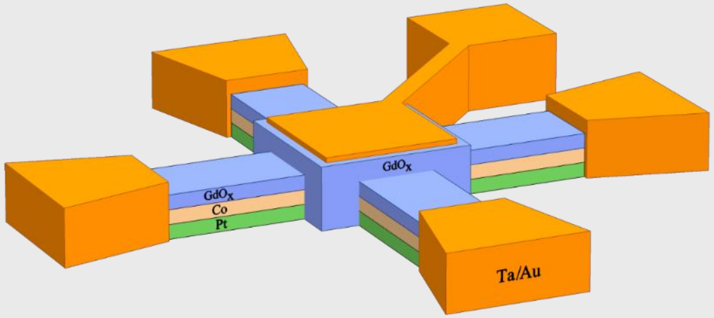

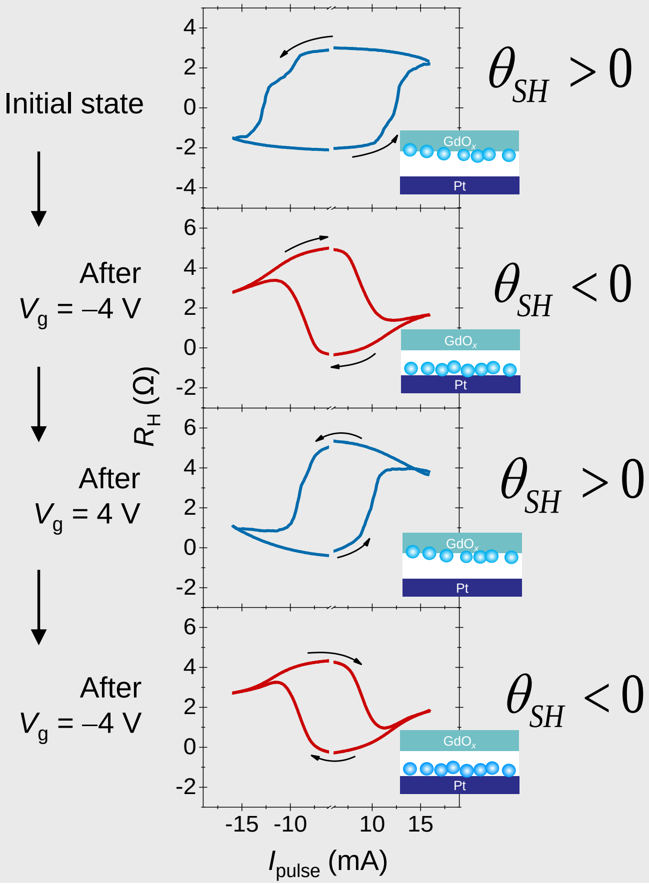

- Competition b/w bulk spin Hall vs. interfacial SOC with opposite sign
- Device can switch to either up or down depending on its programmed SOT state → reconfigurable spin logic

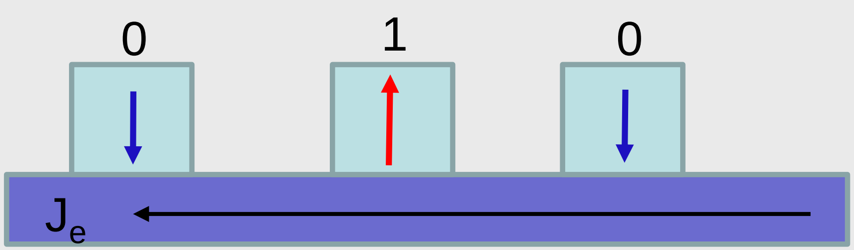

Nat. Commun. **10**, 248 (2019)

First principle calculations

First principle calculations performed in Prof. Nicholas Kioussis's group, *California State University.*

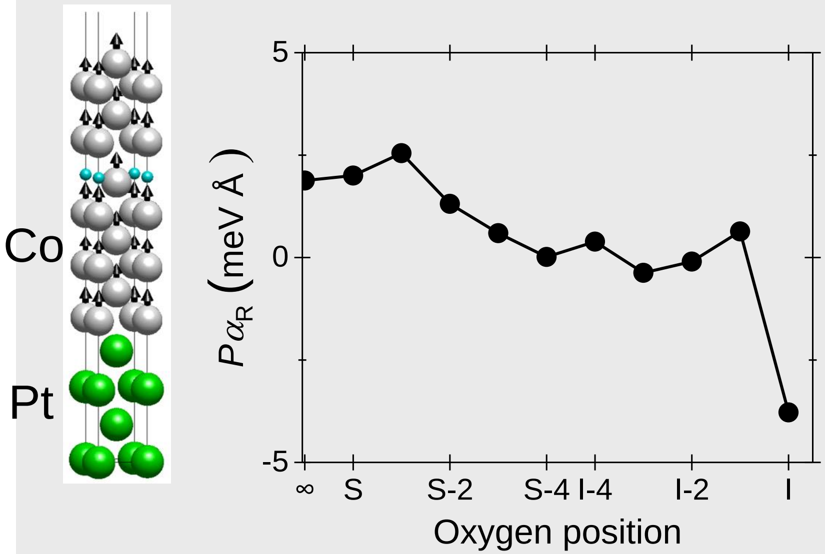

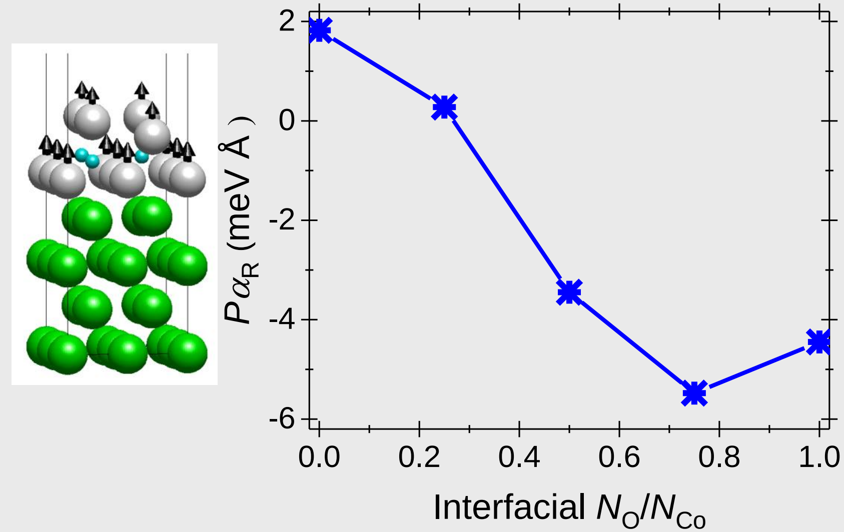

- The effective Rashba parameter ($P\alpha_R$) changes sign as oxygen is filled at the Pt/Co interface.
- The spin accumulation direction changes sign when the negative effective Rashba torque exceeds the spin Hall torque.

NUS National University of Singapore

Nat. Commun. **10**, 248 (2019)

Gradual modulation of SOTs

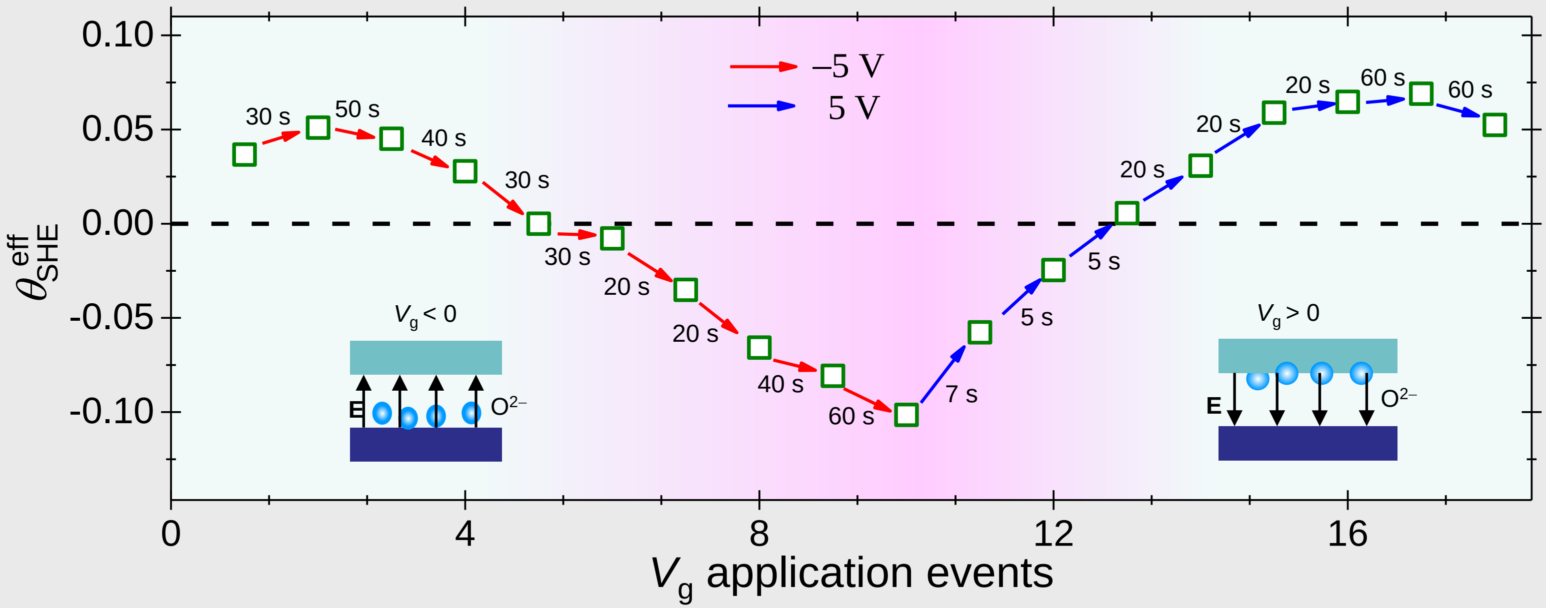

- Application of V_g pulses on a Pt (1.5 nm)/Co (0.8 nm) device.
- Thin gate oxide results in modulation at room temperature.
- The sign of effective spin Hall angle of the material can be changed using electric-field.
- Gradual modulation of SOTs can be applied to neuromorphic devices.

Nat. Commun. **10**, 248 (2019)

Illustration of Ru capping effect

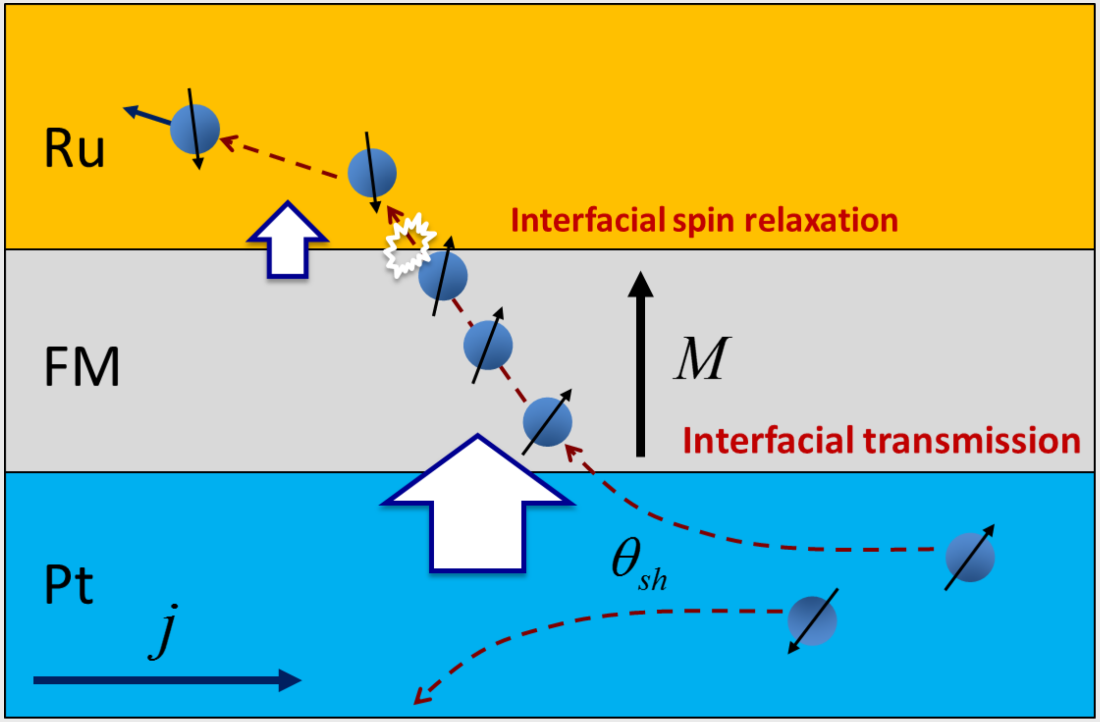

With a strong spin relaxation near the FM/Ru interface, the absorption of spin current from the Pt layer into FM is greatly enhanced. The white arrows denote the spin currents.

PRL **117**, 217206 (2016)

Ru capping effect in SOT

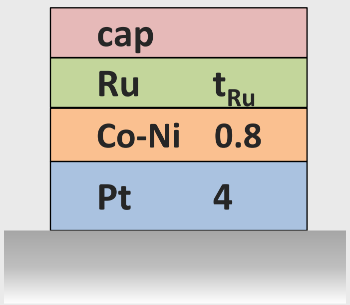

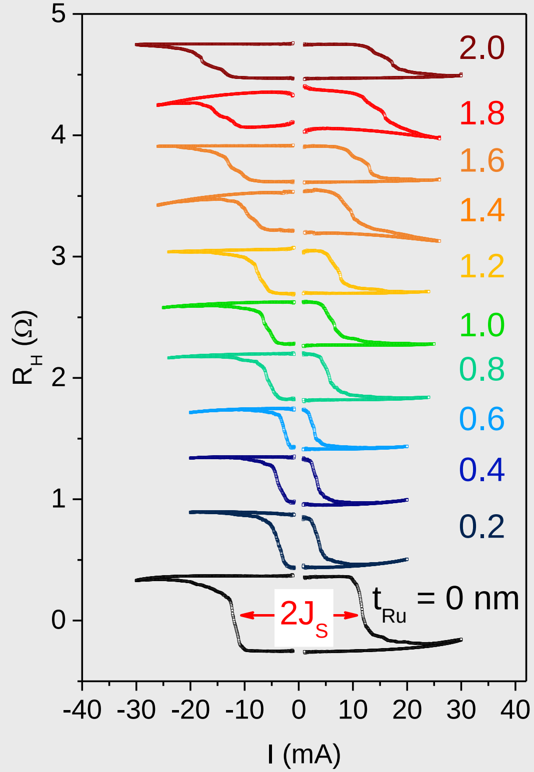

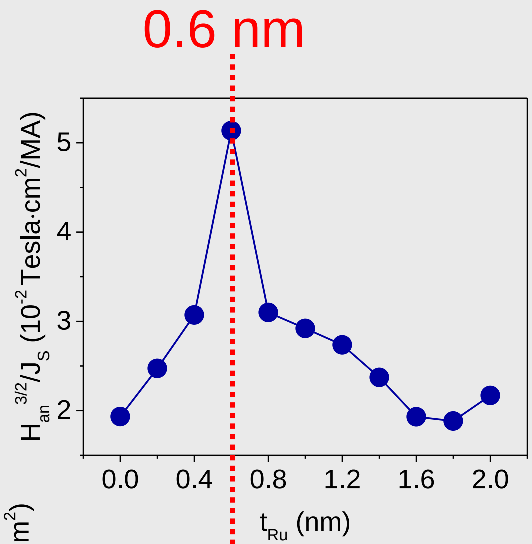

Large modulation of SOT by Ru (> 5 times reduction in J_S)

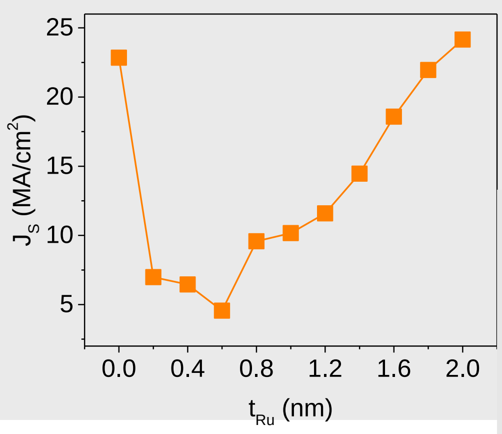

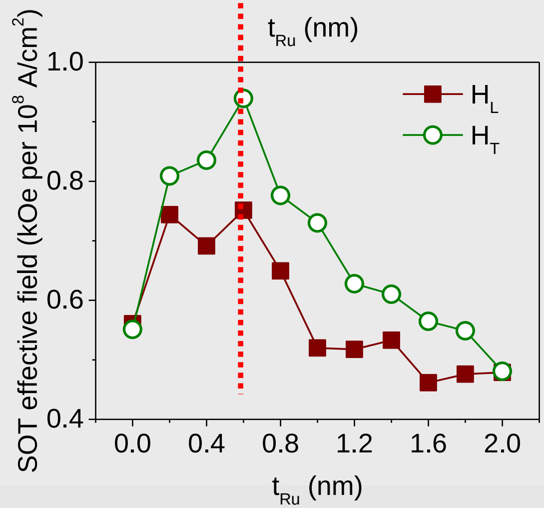

Both SOT switching efficiency and effective fields maximized with 0.6 nm Ru capping

PRL **117**, 217206 (2016)

Spin orbit torque in various magnets

Antiferromagnet

Ferromagnet

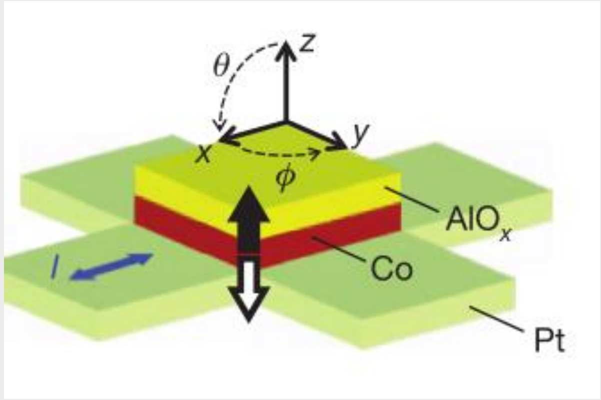

Nature **476**, 189 (2011)

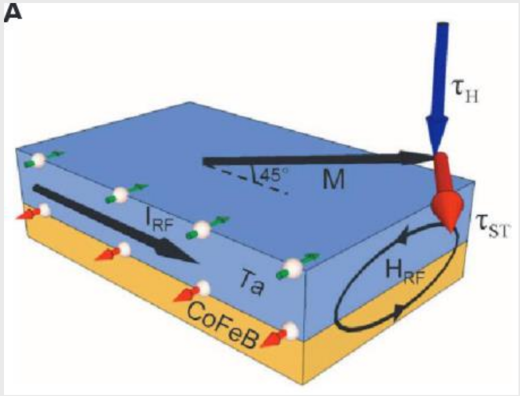

Science **336**, 555 (2012)

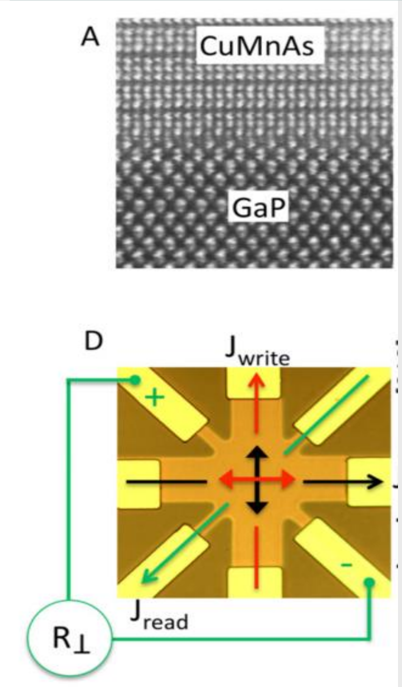

Science **351**, 587 (2016)

$1/t_{FM}$ dependence of spin torque (surface torque)
→ Limitation on FM thickness
→ Thermal stability issue

90 degree rotation
Small MR
Not compatible with MTJs

How about a **multilayer** or **ferrimagnet (FIM)**?
-Easy perpendicular anisotropy, enough magnetic volume

NUS National University of Singapore

Multilayer: structural asymmetry can be added up

TEM

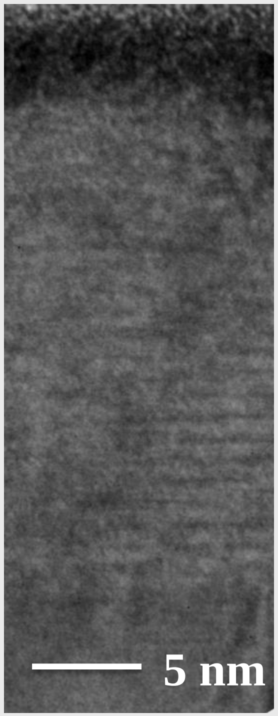

Ta (4 nm)

Co (0.2 nm)/
Pd (0.7 nm)/
multilayer
(22 times)

Ru

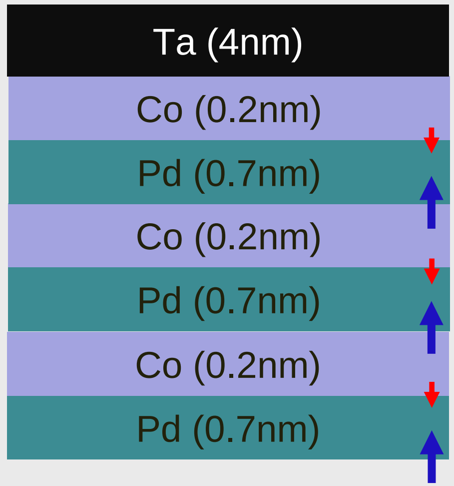

$\theta_{SH} = 4$

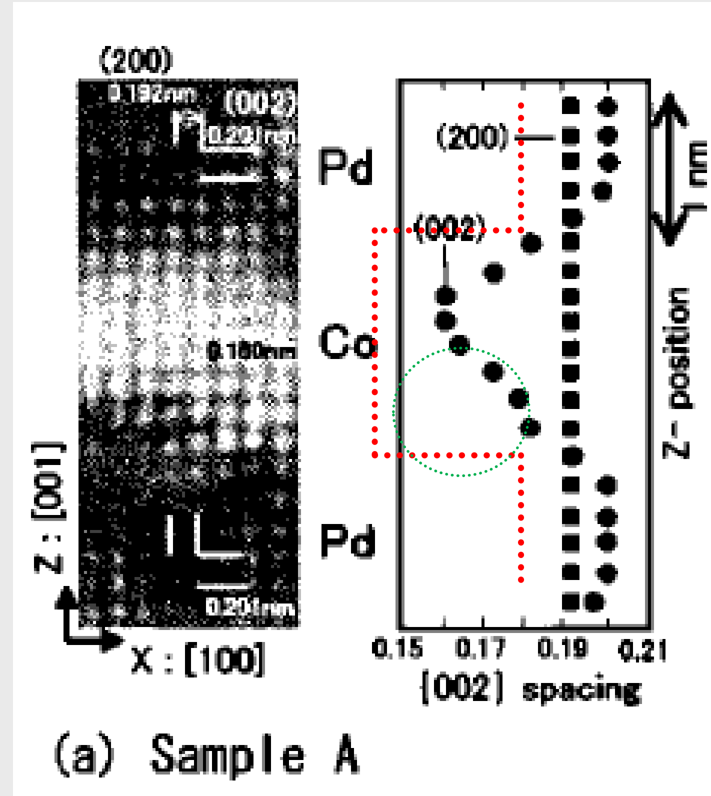

Maesaka, IEEE Trans. Magn. 38, 2676 (2002)
Kim, PRB 53, 11114 (1996)

-Two successive Co/Pd and Pd/Co interfaces are structurally dissimilar.

-Lattice mismatch (9%) between Pd and Co → Strain engineering

-This distortion is 30% stronger for Co/Pd than for Pd/Co interfaces

Phys. Rev. Lett. **111**, 246602 (2013)

SOT in ferrimagnet : CoGd

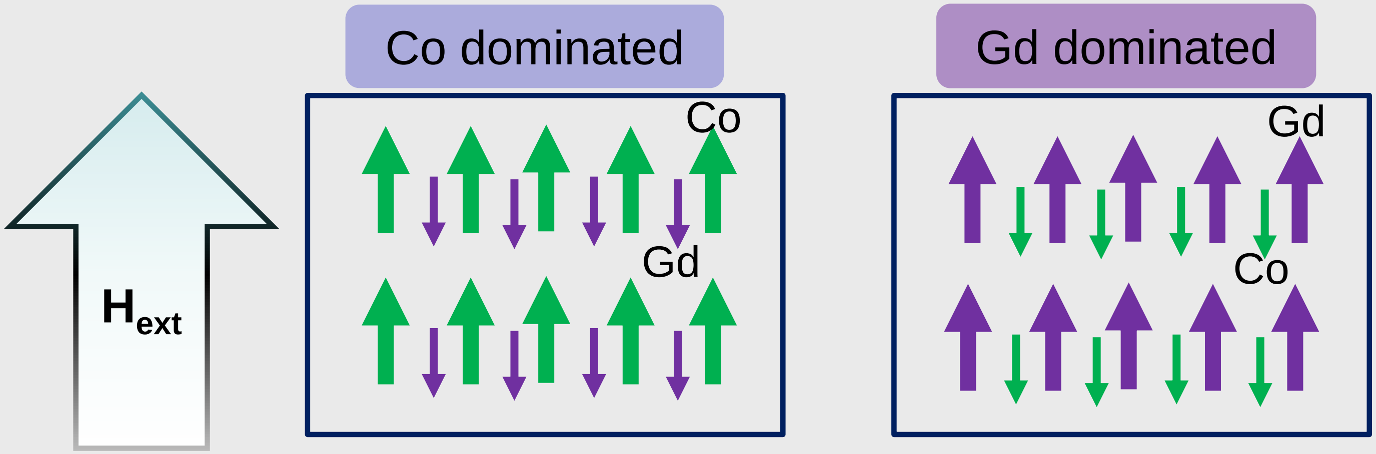

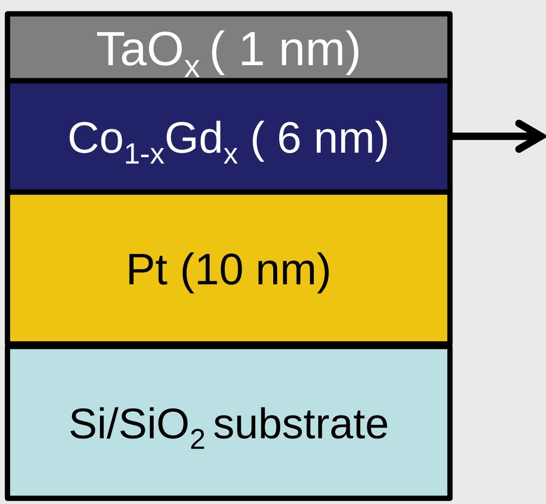

- Films deposited with varying Co and Gd compositions.
- CoGd has bulk PMA.
- Thermally stable thick magnetic layer is grown.

Phys. Rev. Lett. **118**, 167201 (2017)

Anomalous scaling of SOT in ferrimagnets

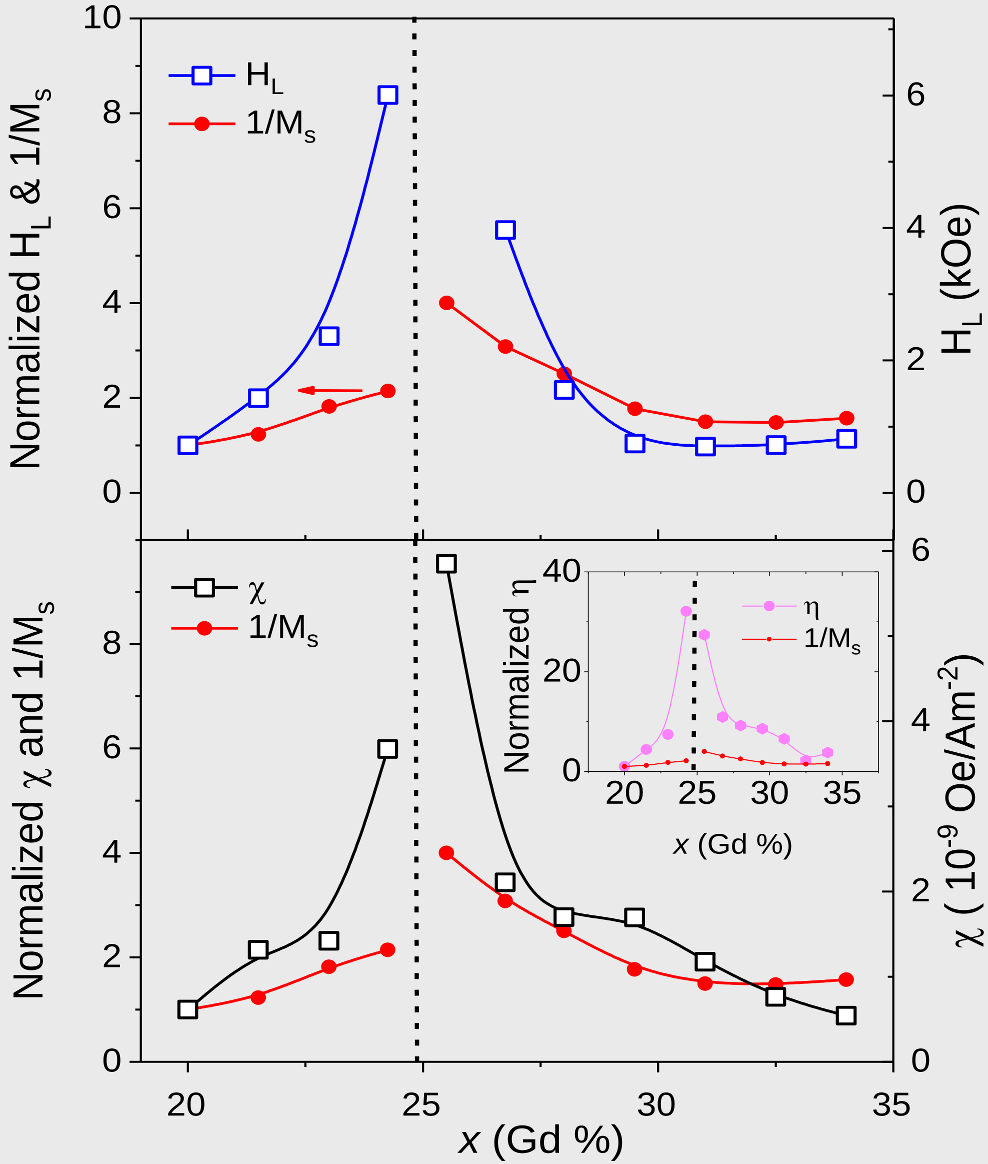

- Switching efficiency ($\chi = H_p / J_s$), H_L and $1/M_s$ are normalized with respect to their respective values for $Co_{80}Gd_{20}$.
- Exceptional and disproportionate (to $1/M_S$) change of η and H_L cannot be explained by existing SOT understanding.
- x10 times increase in θ_{SH} due to negative exchange coupling

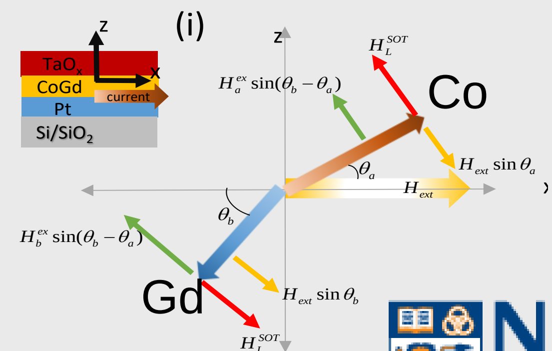

Phys. Rev. Lett. **118**, 167201 (2017)

Ferromagnet vs. ferrimagnet

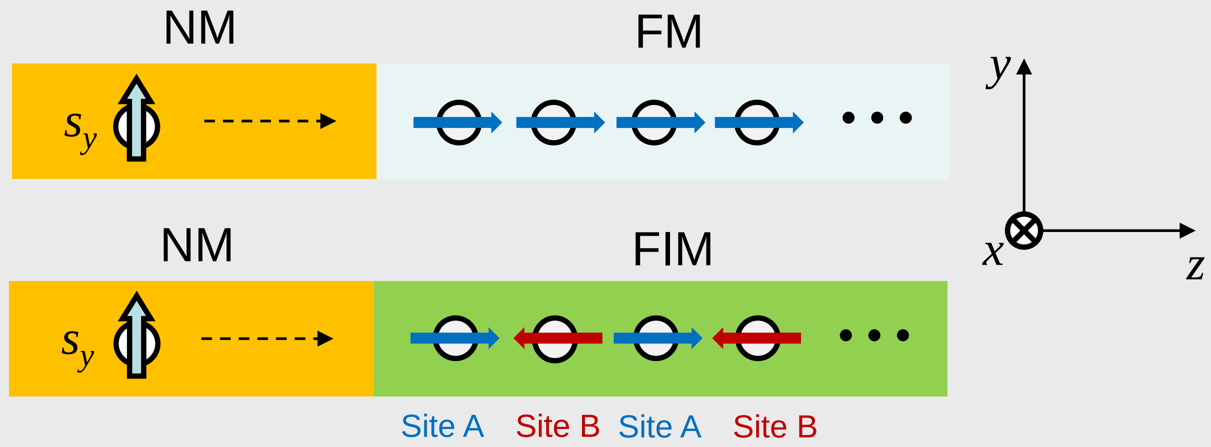

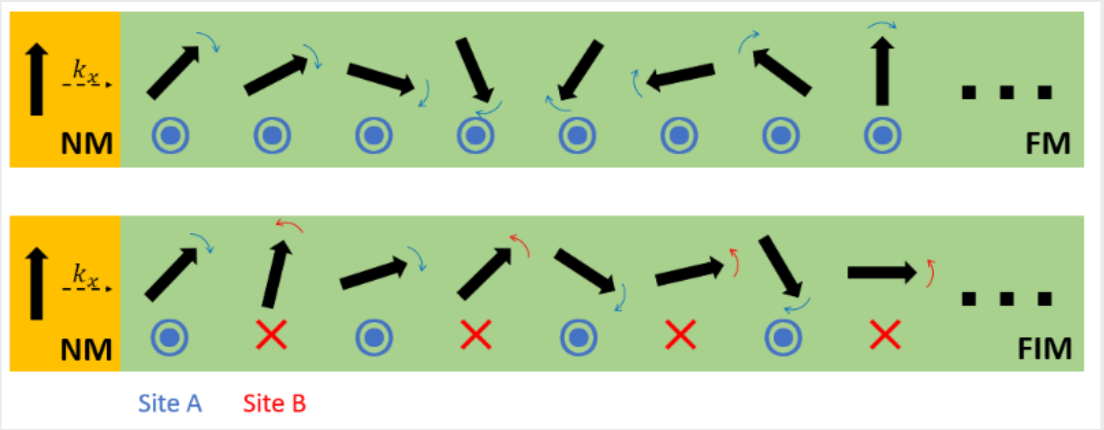

Alternating exchange fields in ferrimagnet (FIM) on an atomic scale
→ much less spin dephasing → long spin coherence length
→ Bulk-like torque in FIM

Nat. Mater. **18**, 29 (2019)

SOT effective fields

Ferromagnet

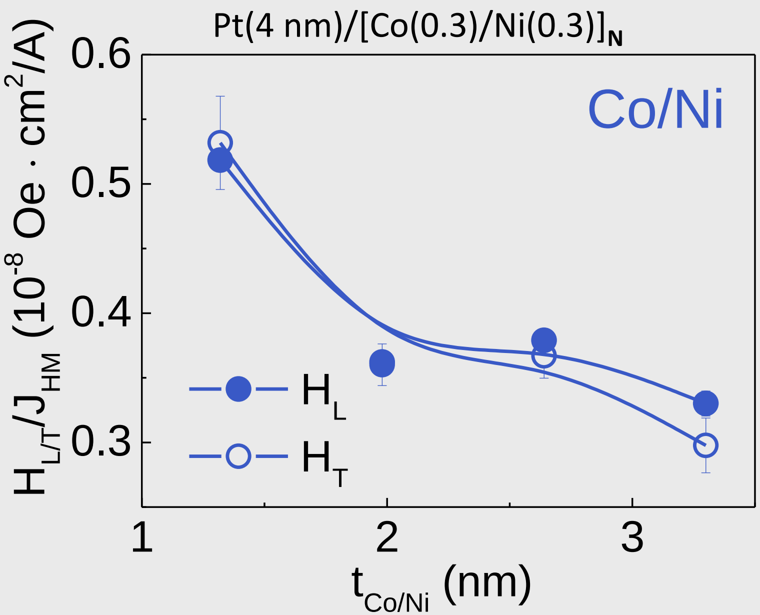

Ferrimagnet

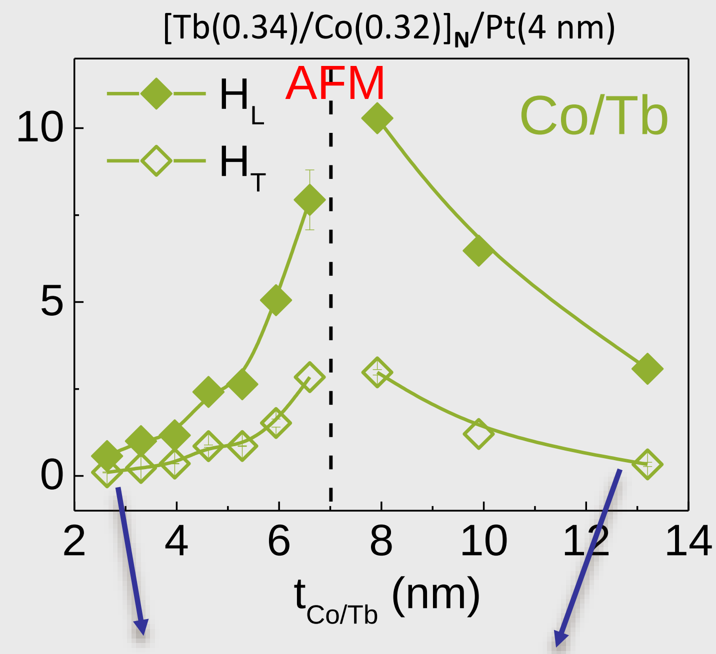

poor compensation

$$H_L = \frac{\hbar}{2e}\frac{J_{HM}}{M_S t_{FM}}\theta_{HM}\left[1-\mathrm{sech}\left(\frac{t_{HM}}{\lambda_{HM}}\right)\right]$$

- FM Co/Ni: ***$t_{Co/Ni}$*** ↑ → **SOT** ↓.
- FIM Co/Tb: SOT **diverges** at **compensation**.
- SOT in FIM is **~20 times larger** than that in FM.
- SOT in FIM shows **bulk-like-torque** characteristic.

NUS National University of Singapore

Nat. Mater. **18**, 29 (2019)

SOT current induced switching efficiency

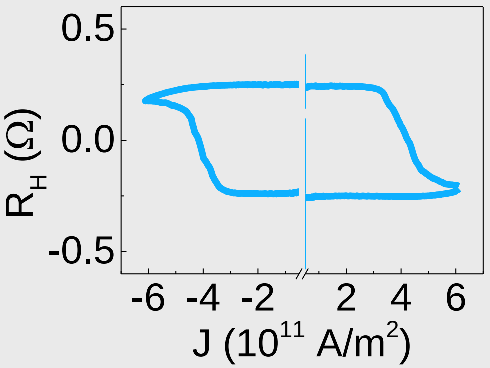

Most switching through DW nucleation and propagation

SOT switching efficiency: $\eta = H_P / J_W$

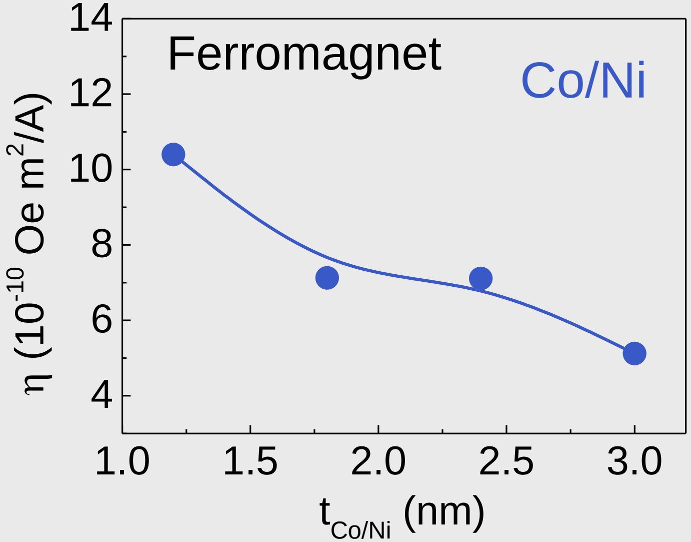

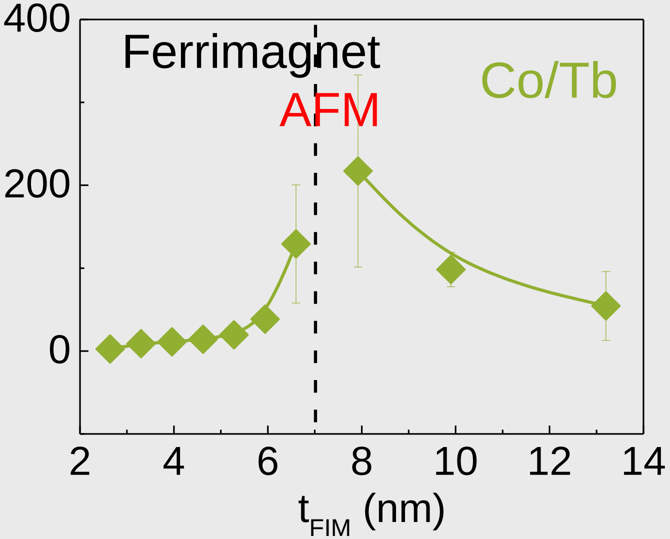

- *η* is in line with that of SOT effective fields, decreasing for FM and **diverging** at **compensation.**
- In FIM system, *η* is ~**20 times higher** than FM system.

Nat. Mater. **18**, 29 (2019)

M_S & $t_{FM/FIM}$ effect?

$$H_L = \frac{\hbar}{2e}\frac{J_{HM}}{M_S t_{FM}}\theta_{HM}\left[1-\mathrm{sech}\left(\frac{t_{HM}}{\lambda_{HM}}\right)\right] \rightarrow \eta, H_L \propto 1/(M_S t)$$

Ferromagnet

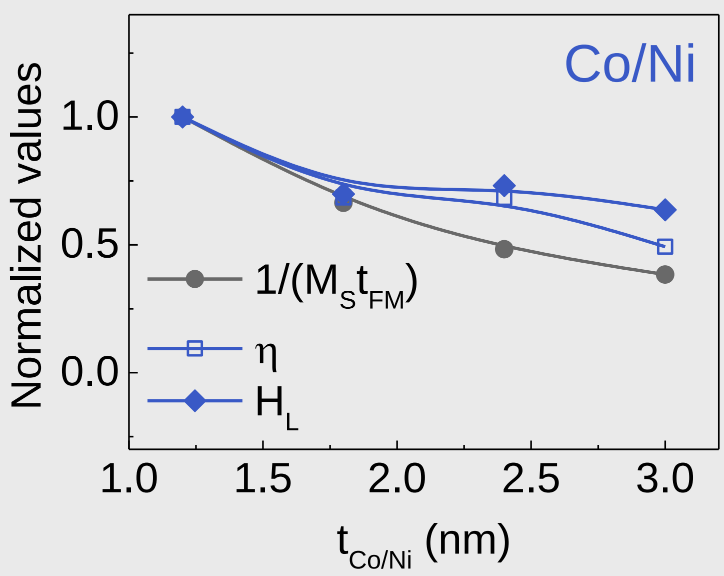

Ferrimagnet

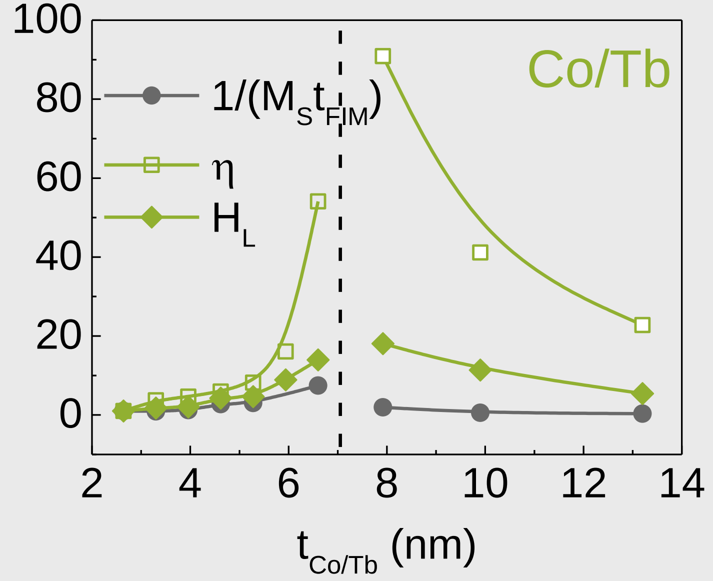

Surprisingly in FIM, the scaling trend of η and H_L **contradicts** SOT governing equation.

Nat. Mater. **18**, 29 (2019)

Spin pumping in a ferrimagnet

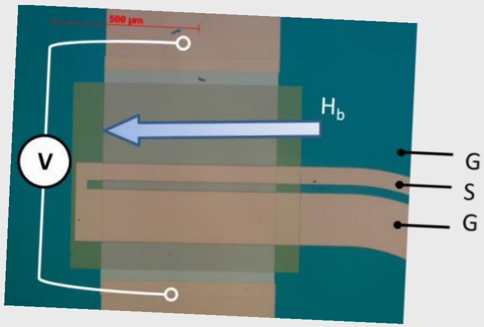

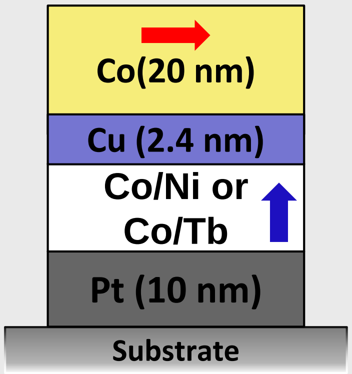

-If spin coherence length is long, a transverse spin current passes through the Co/Ni or Co/Tb layer.
-V_{ISHE} is generated.

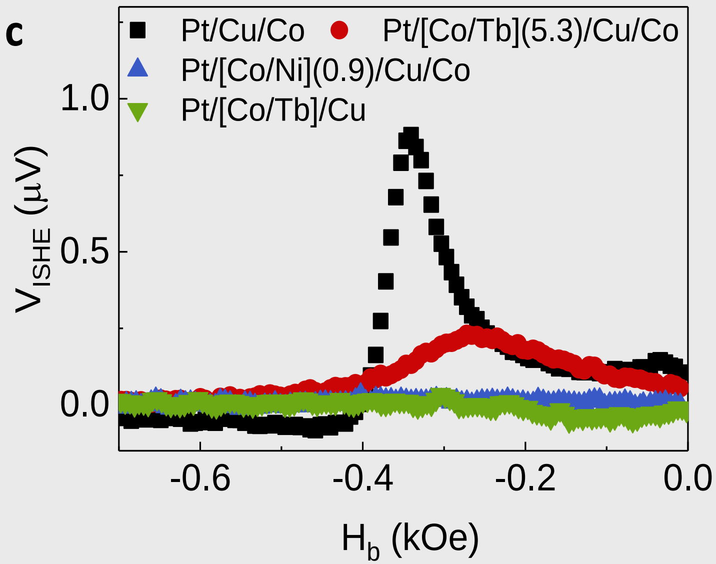

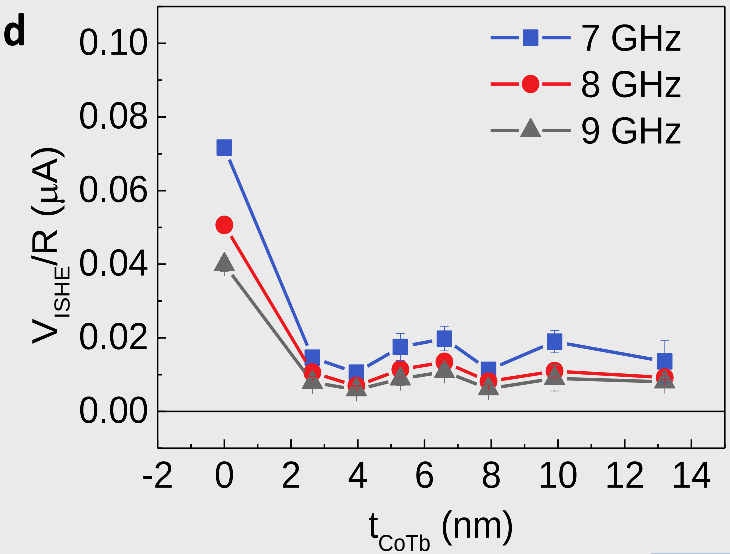

Long spin dephasing length in Co/Tb

NUS National University of Singapore

Nat. Mater. **18**, 29 (2019)

SOT dynamics with two torque terms

Landau-Lifschitz-Gilbert equation in macrospin approximation

$$\frac{\partial \mathbf{m}}{\partial t'} = -\mathbf{m}\times(\cos(\theta)\hat{\mathbf{z}} + h_x\hat{\mathbf{x}}) + \alpha\mathbf{m}\times\frac{\partial \mathbf{m}}{\partial t'} - h^{\parallel}\left[\mathbf{m}\times(\mathbf{m}\times\hat{\boldsymbol{\sigma}})\right] - h^{\perp}(\mathbf{m}\times\hat{\boldsymbol{\sigma}})$$

- $t' = \gamma\mu_0 H_{ani} t$
- *uniaxial anisotropy*
- $h_x = 0$
- *Gilbert damping*
- *Slonczewski torque* $\boldsymbol{\tau}^{\parallel}$
- *field-like torque* $\boldsymbol{\tau}^{\perp}$

$$h^{\parallel,\perp} = \frac{H^{\parallel,\perp}}{H_{ani}} = \frac{\gamma\hbar}{2|e|M_S t_{FM} H_{ani}} c^{\parallel,\perp} J_e$$

$c^{\parallel,\perp}$ *: efficiency*
~ *spin Hall angle*

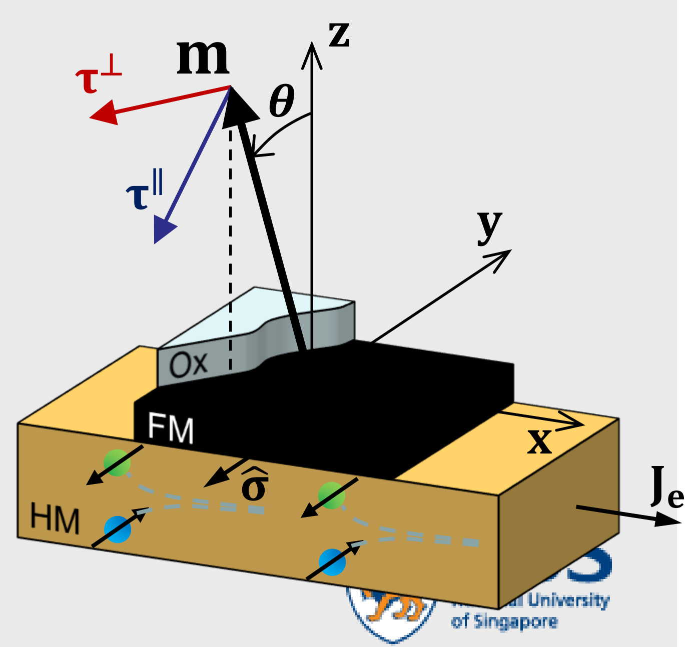

Example : Ta/CoFeB/MgO	Kim *et al.*, Nat. Mat. **12** *240* ('13)	Avci *et al.*, PRB **89** *214419* ('14)	Qiu *et al.*, Sci Rep. **4** *4491* ('14)
$H^{\parallel}$ at 10^8 A cm^{-2}	62 Oe	200 Oe	440 Oe
$H^{\perp}$ at 10^8 A cm^{-2}	185 Oe	950 Oe	1940 Oe
$\tau^{\parallel}/\tau^{\perp}$	0.3*	0.21	0.23

* from -0.3 to 1.2 varying with thicknesses

Phys. Rev. Appl. **3**, 064012 (2015)

Complex spin-dynamics

Phys. Rev. Appl. **3**, 064012 (2015)

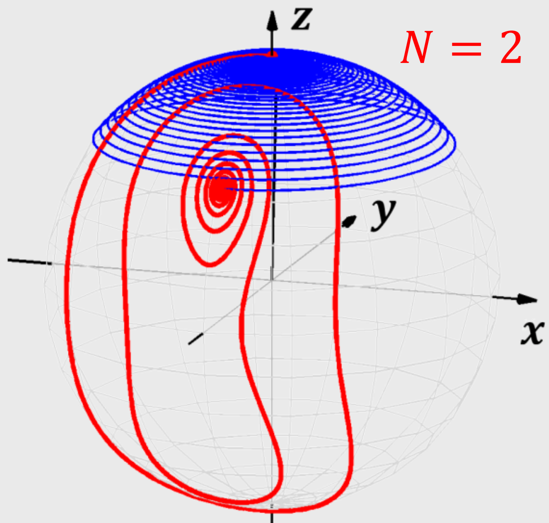

$h^{\parallel} = 0.04 \quad h^{\perp} = 0.8$

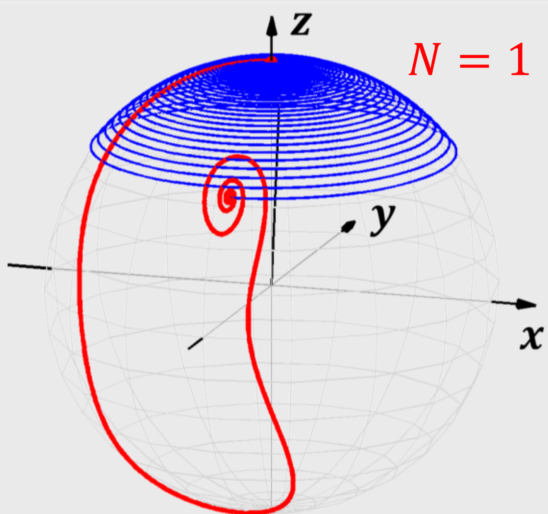

$h^{\parallel} = 0.1 \quad h^{\perp} = 0.8$

Still, $\alpha = 0.01$ and $h^{\perp} = 0.8$,

Let us $\uparrow h^{\parallel}$

$\boldsymbol{\tau}^{\parallel}$ is an effective damping

$\propto \cos(\hat{\boldsymbol{\sigma}}, \mathbf{m})$

Precession order $N \downarrow$

Half-precession switching

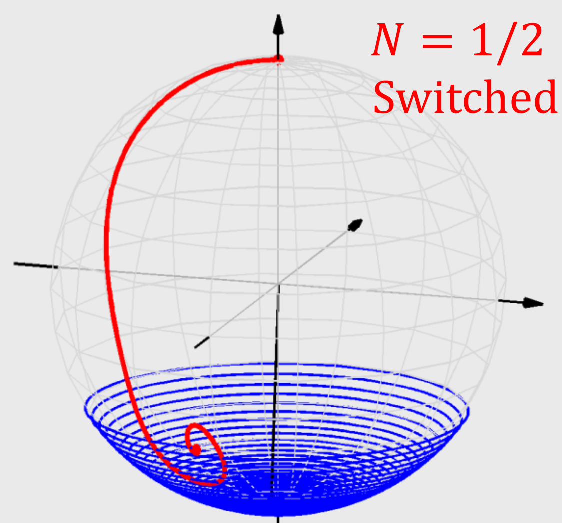

$h^{\parallel} = 0.2 \quad h^{\perp} = 0.8$

$\boldsymbol{h^{\parallel}/h^{\perp} = 0.25}$

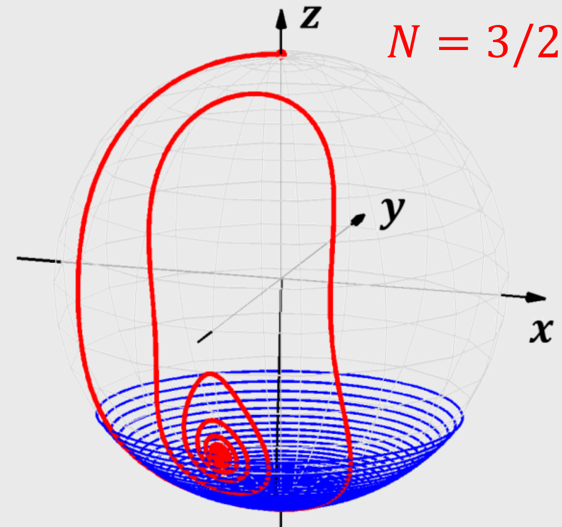

$h^{\parallel} = 0.05 \quad h^{\perp} = 0.8$

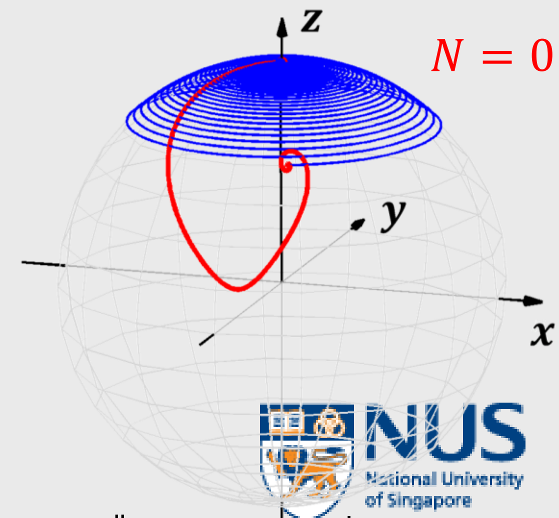

$h^{\parallel} = 0.3 \quad h^{\perp} = 0.6$

National University of Singapore

Time resolved SOT dynamics measurements

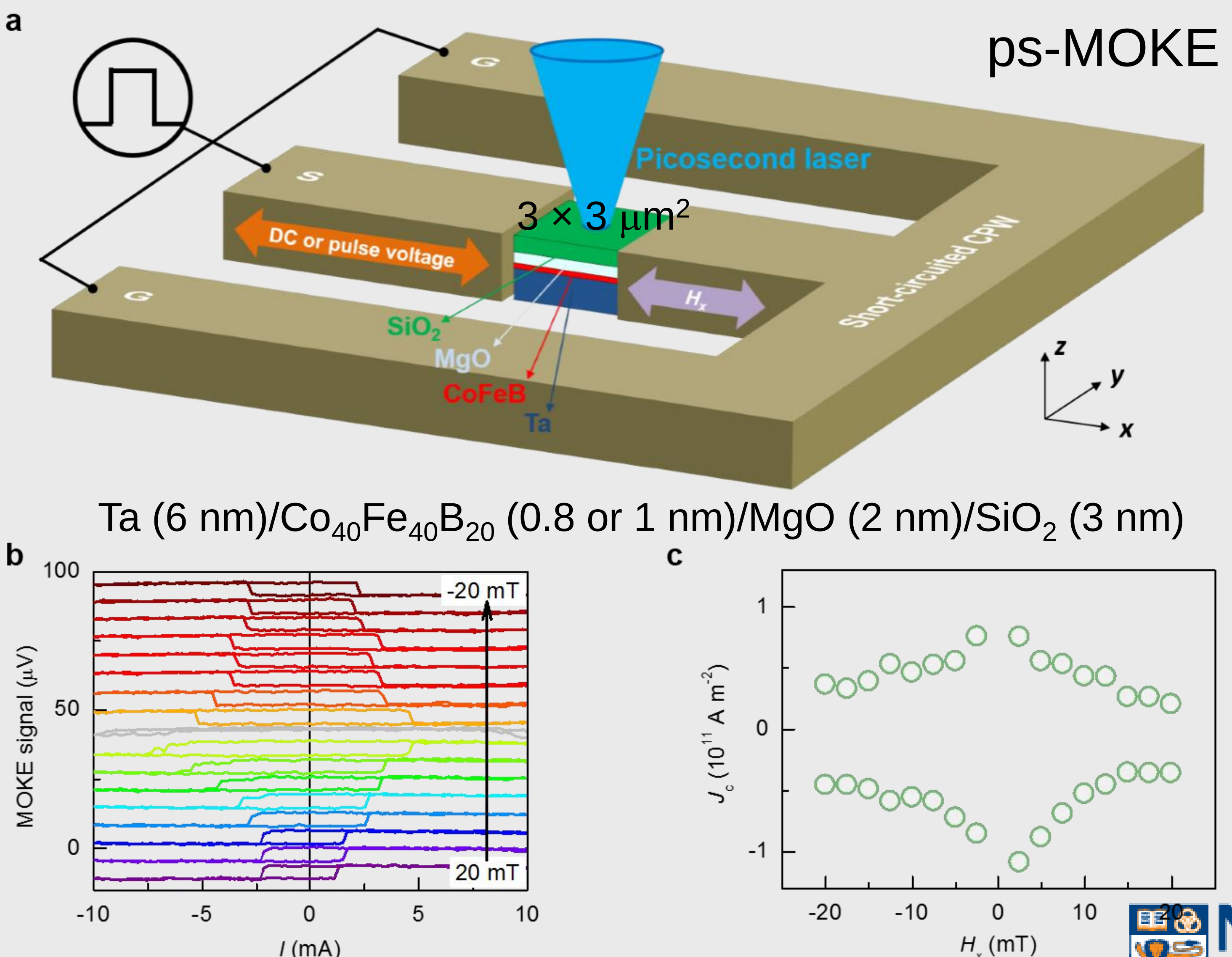

Sci. Adv. **3**, e1603099 (2017)

Anomalous back-switching with longer pulses

First time-domain SOT data

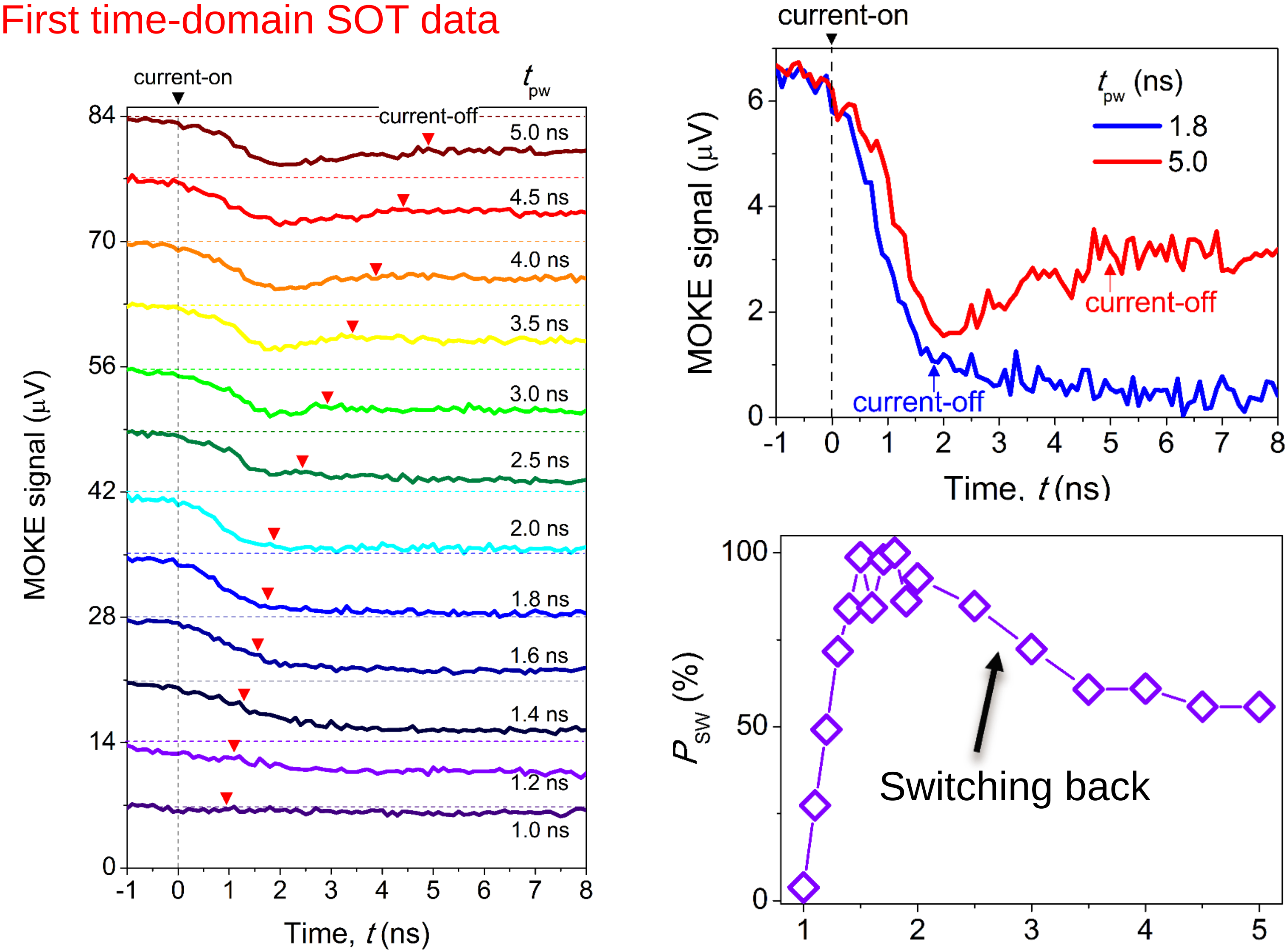

$J_c = 5.2 \times 10^{11}$ A·m^{-2}, $H_x = -168$ mT

Sci. Adv. **3**, e1603099 (2017)

Field-like torque induced switching back process

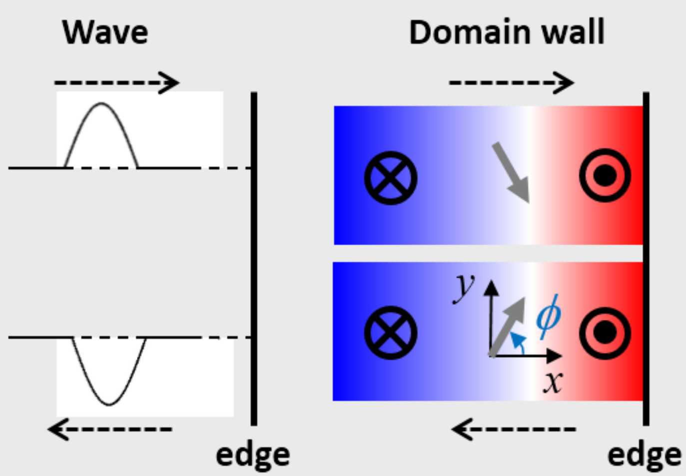

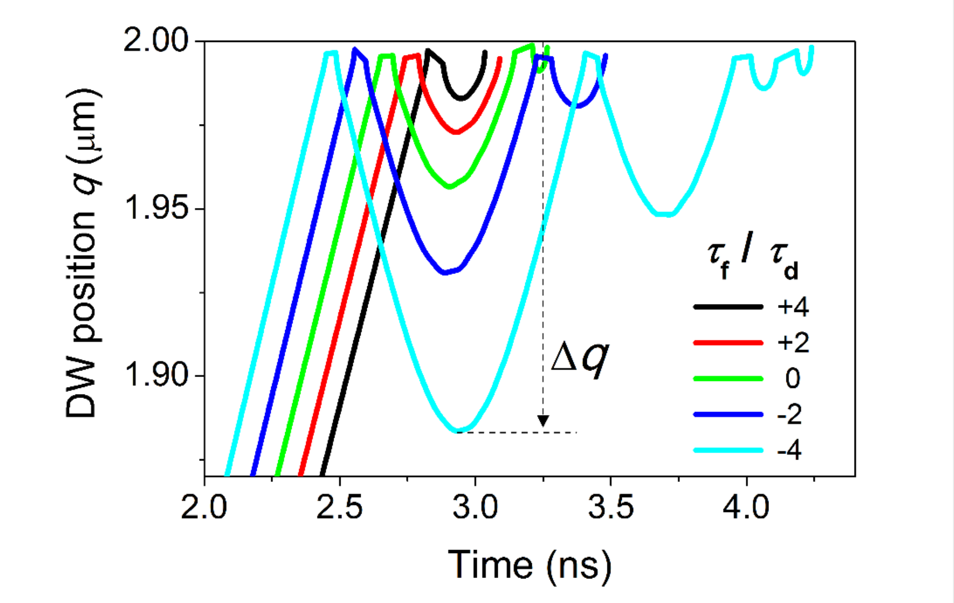

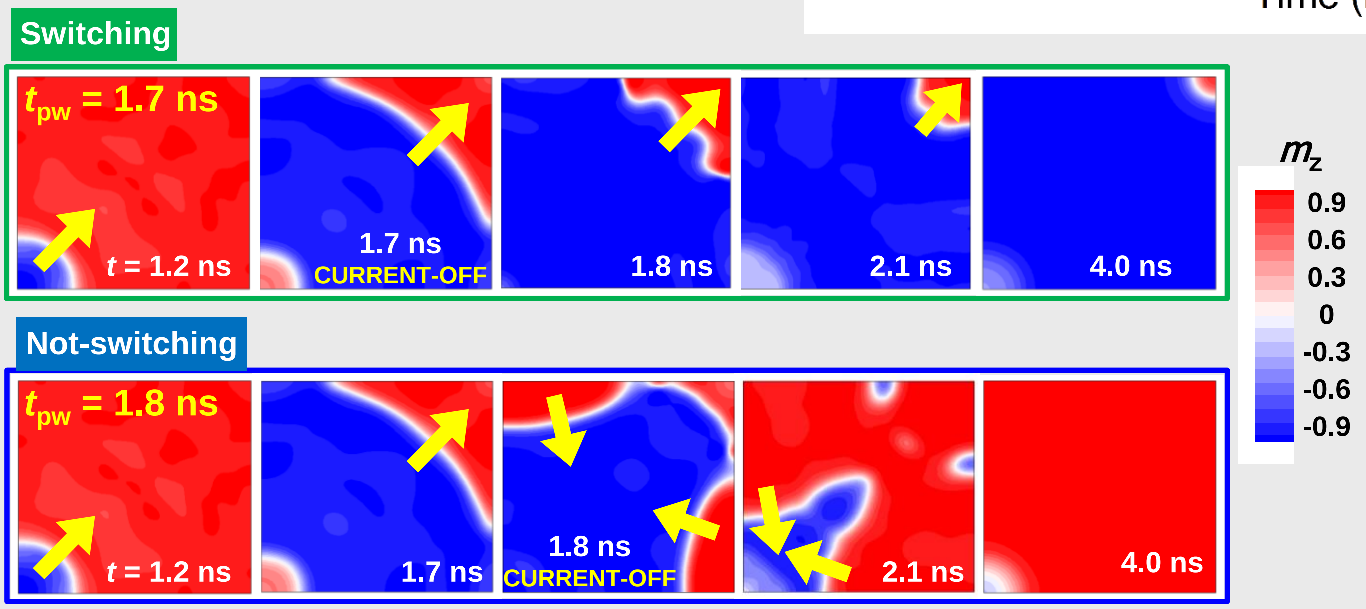

Sci. Adv. **3**, e1603099 (2017)

Oscillatory spin-orbit torque switching

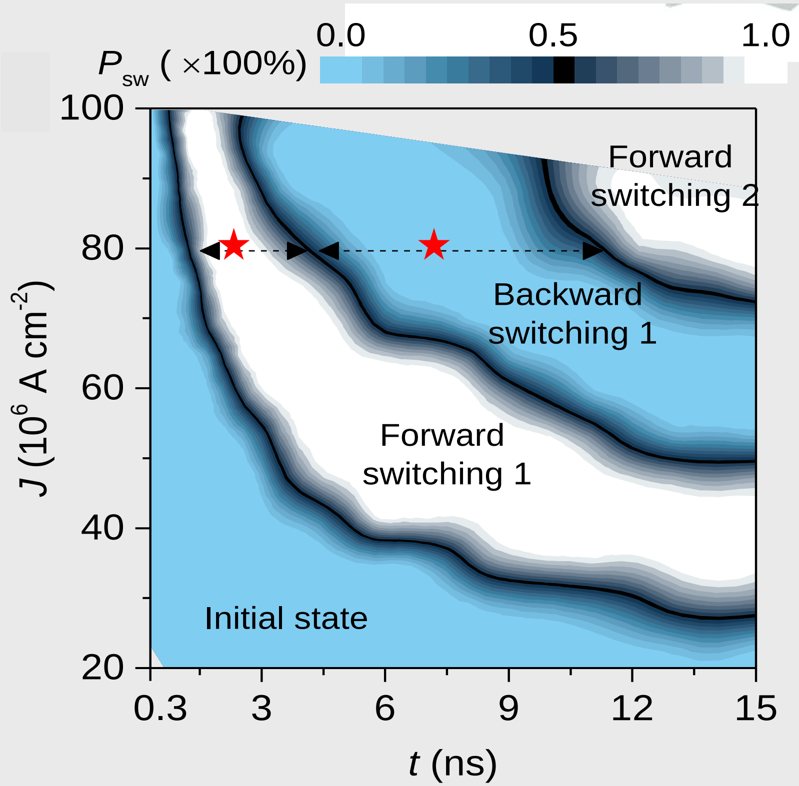

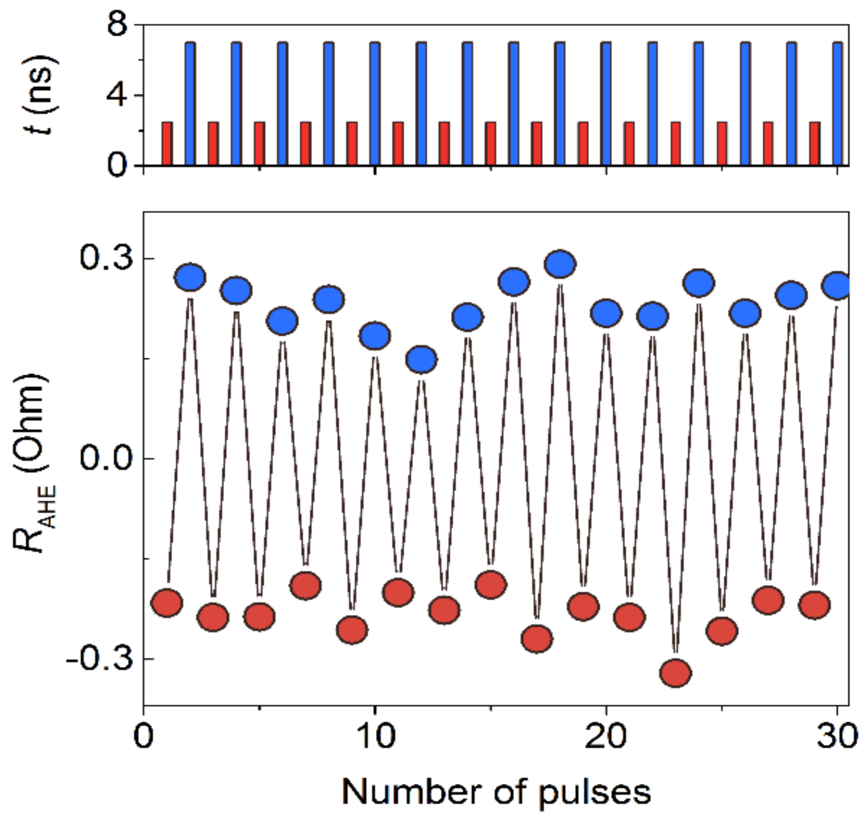

-Unipolar switching of PMA CoFeB dot.

-Positive current pulses with alternating duration of 2.5 ns and 7.5 ns.

-Driving transistors can be replaced by diodes → smaller size

NUS National University of Singapore

Communications Physics **1**, 2 (2018)

3D topological insulators (TIs)

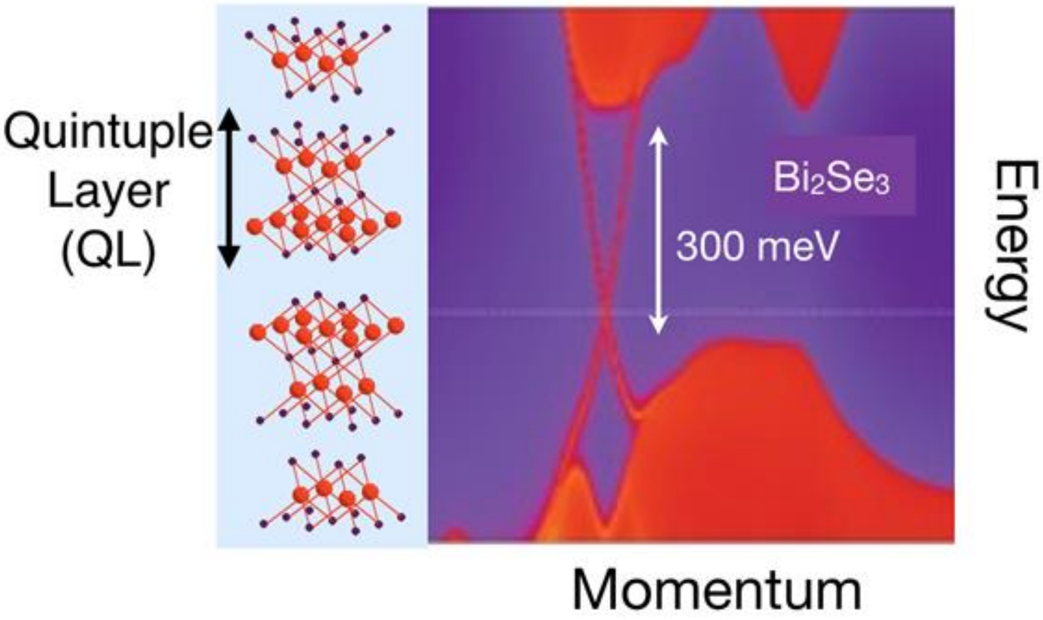

H. Zhang, C.-X. Liu, *et al., Nature Physics* **5**, 438 (2009)

Fu & Kane, *Phys. Rev. B* **76**, 045302 (2007)
Moore & Balents, *Phys. Rev. B* **75**, 121306(R) (2007)
Roy, *Phys. Rev. B* **79**, 195321 (2009)

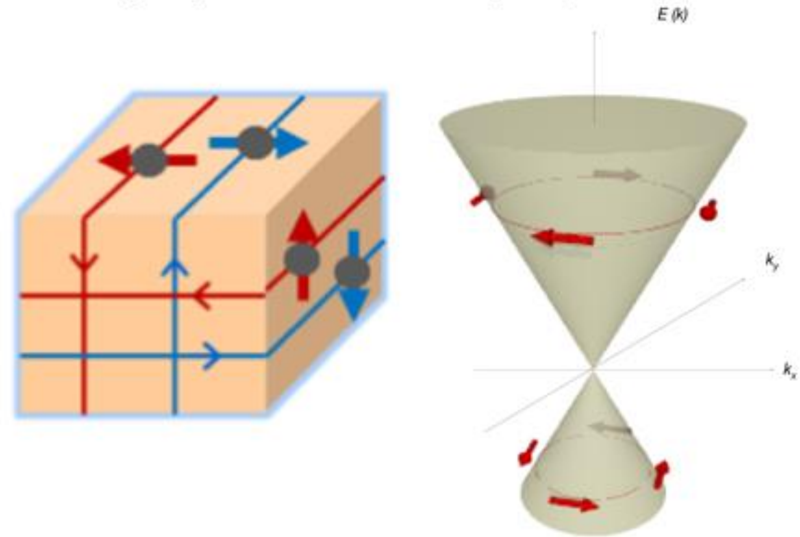

- ❑ Spin polarized surface currents
- ❑ Spin-momentum locking → giant spin Hall angle?

Exotic spin Hall angles from topological insulators

spin Hall angle (θ_{SH}) = 2~3.5
ST-FMR (Cornell)

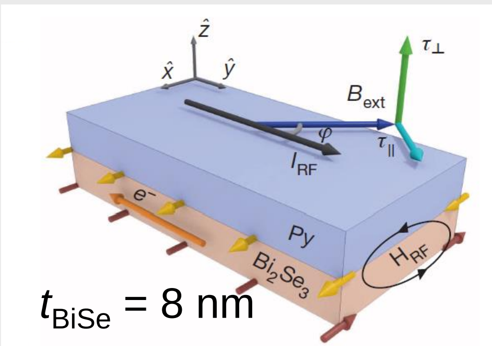

t_{BiSe} = 8 nm

Nature **511**, 449 (2014)

θ_{SH} = 0.42 (low temp)
ST-FMR (NUS)

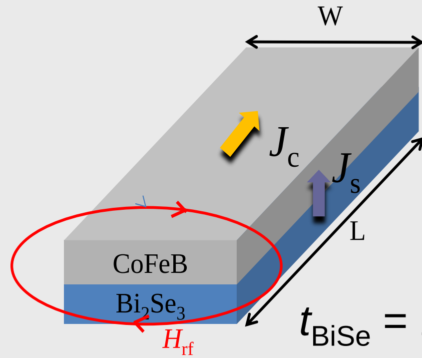

t_{BiSe} = 20 nm

PRL **114**, 257202 (2015)

θ_{SH} = 140-425 (low temp)
spin-orbit switching (UCLA)

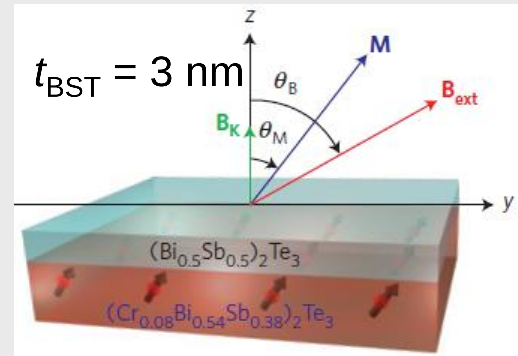

t_{BST} = 3 nm

Nat. Mater. **13**, 699 (2014)

θ_{SH} ~ 1 × 10^{-4}
Spin-pumping (Tohoku)

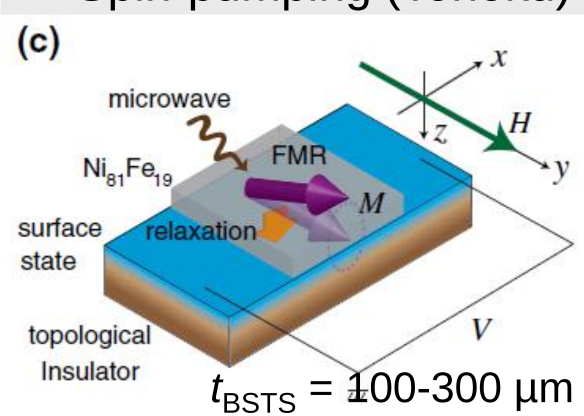

t_{BSTS} = 100-300 μm

PRL **113**, 196601 (2014)

θ_{SH} = 0.01
Spin-pumping (NUS)

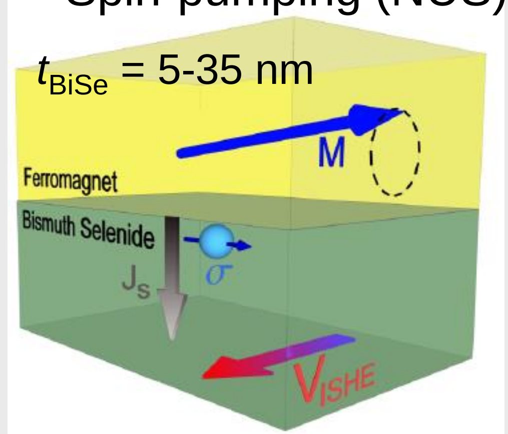

t_{BiSe} = 5-35 nm

PRB **90**, 094403 (2014)

θ_{SH} = 0.01-0.4
Spin-pumping (Minnesota)

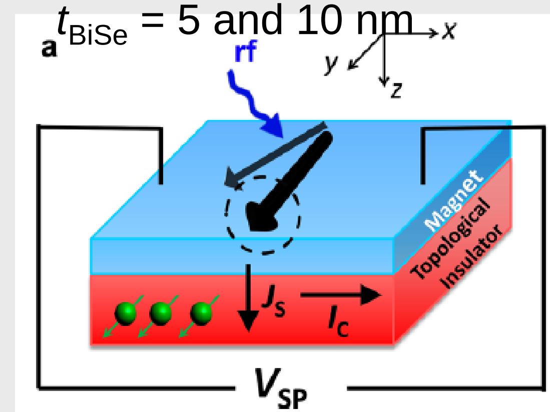

t_{BiSe} = 5 and 10 nm

Nano Lett **15**, 7126 (2015)

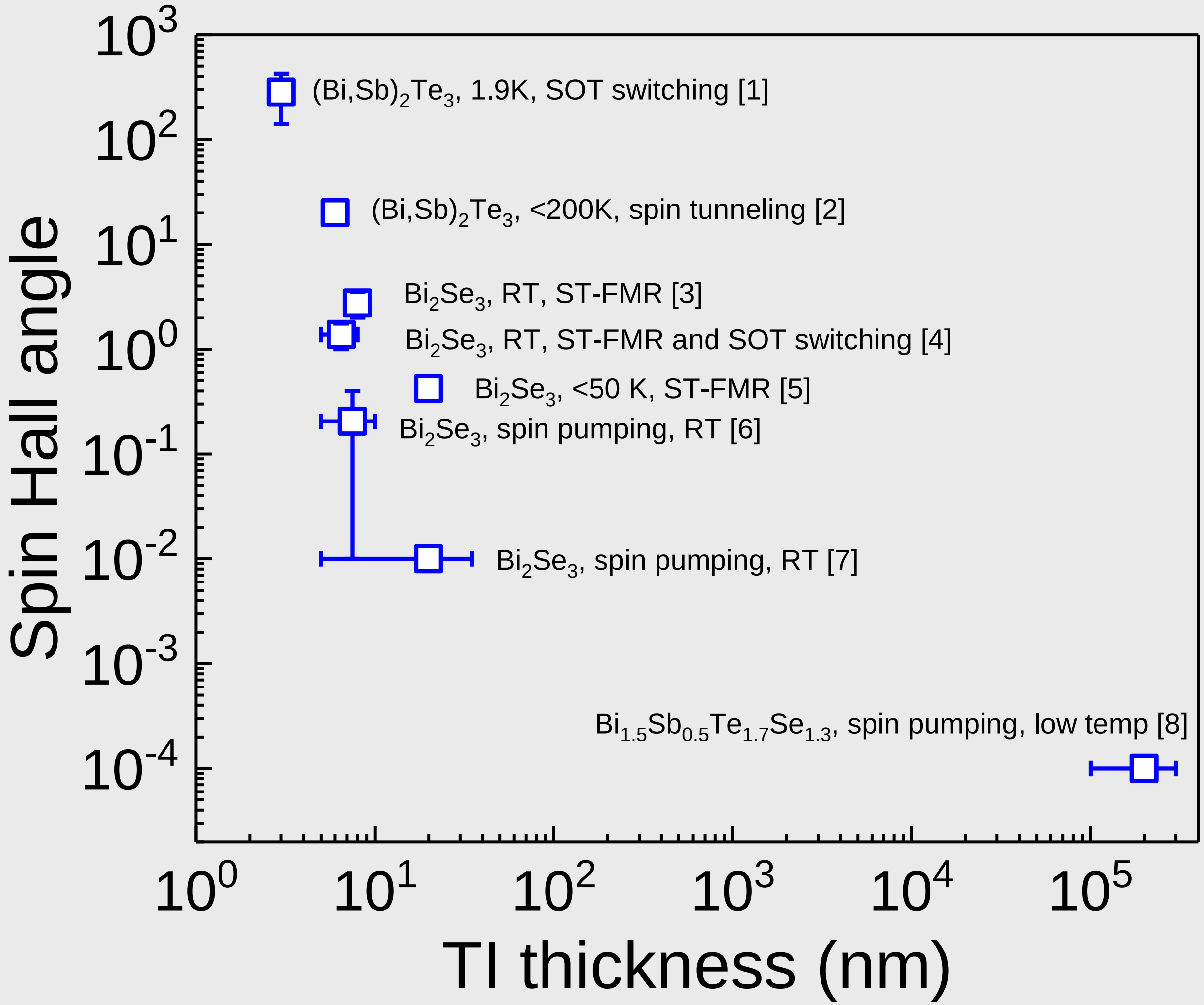

-TI is not a good insulator.

-E_F is pinned in conduction band.

-Current shunting thru bulk reduces the efficiency!

[1] Nat. Mater. **13**, 699 (2014)
[2] PRB **91** 235437 (2015)
[3] Nature **511**, 449 (2014)
[4] Nat. Commun. **8** 1364 (2017)
[5] PRL **114**, 257202 (2015)
[6] PRB **90**, 094403 (2014)
[7] Nano Lett **15**, 7126 (2015)
[8] PRL **113**, 196601 (2014)

Review: J. Phys. D: Appl. Phys. **51**, 273002 (2018)

Thickness dependent spin torques in Bi_2Se_3/CoFeB

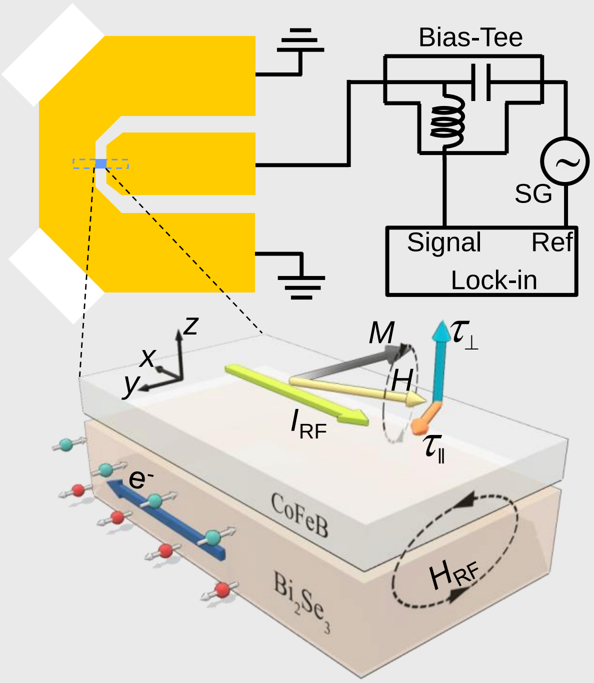

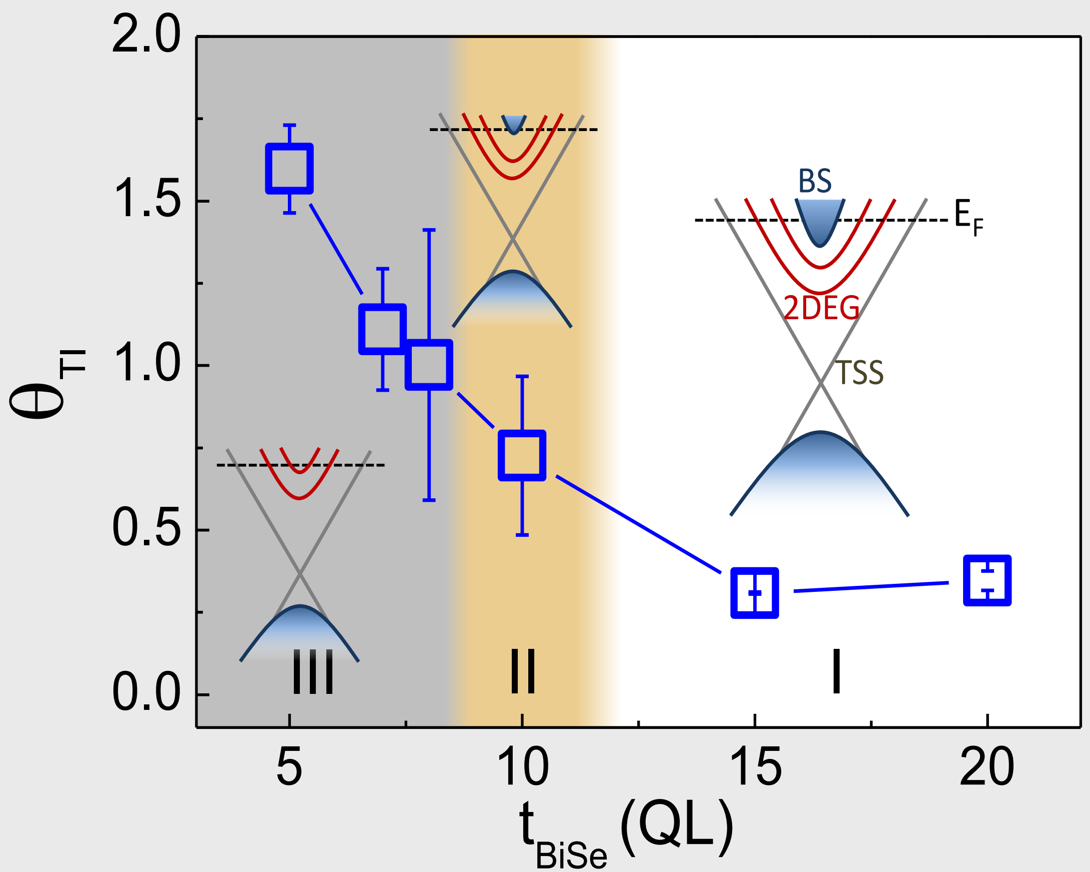

- Used spin torque ferromagnetic resonance (ST-FMR) measurements.
- Identify the optimum thickness range of Bi_2Se_3 to be 5–8 quintuple layers (QL) to maximize the spin torque effect.
- A giant SOT efficiency (θ_{TI}) of ~1–1.75 at room temperature.

Nat. Comm. **8**, 1364 (2017)

NUS National University of Singapore

Current induced magnetization switching in Bi_2Se_3/Py

Bi_2Se_3 (8 QL)/NiFe (6 nm)/MgO (1 nm)/SiO_2 (4 nm)

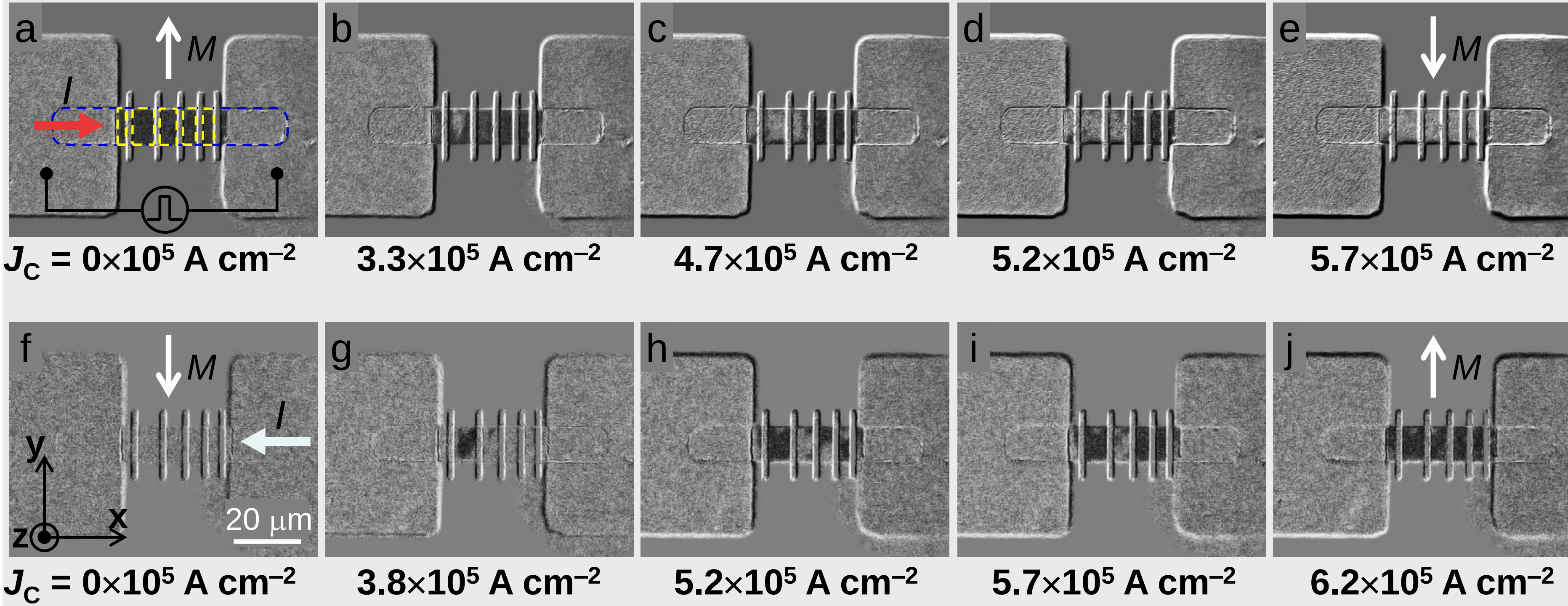

- TI magnetization switching reported in a Cr doped TI at 1.9 K with an external magnetic field [Nat. Mater. 13, 699 (2014)].
- Demonstrated magnetization switching of Bi_2Se_3/NiFe at room temp with a low critical current density (J_C~6×10^5 A/cm^2) and without a magnetic field.
- A giant θ_{TI} = 1.75.

NUS National University of Singapore

Nat. Comm. **8**, 1364 (2017)

LAO/STO – 2DEG formation

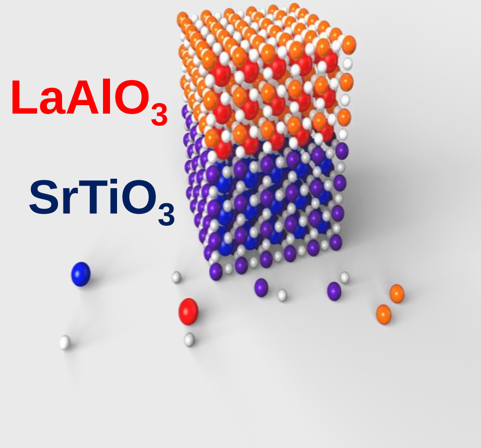

$LaAlO_3$ grown on TiO_2 terminated $SrTiO_3$ (100)

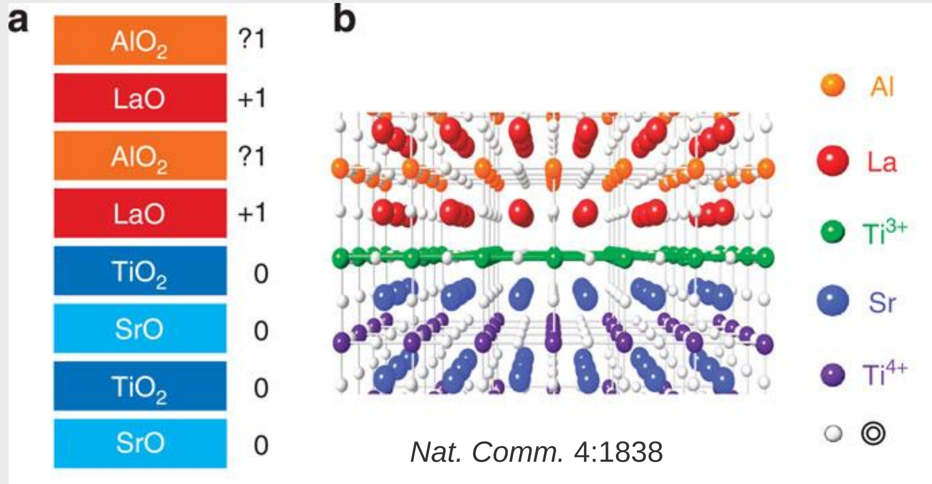

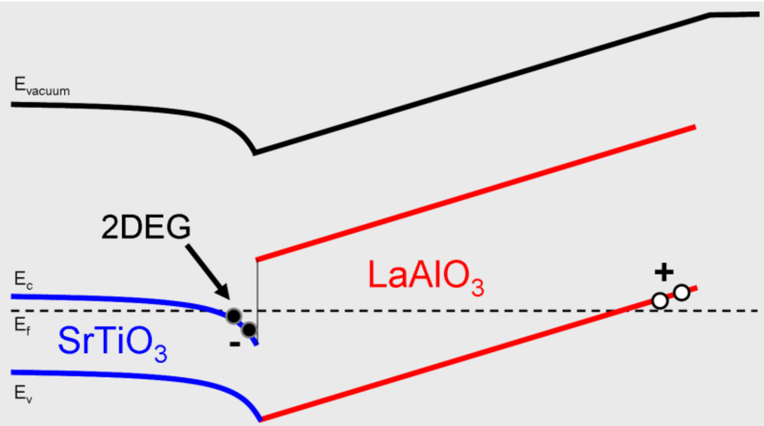

- ❑ $SrTiO_3$ (Insulator 3.2 eV)
- ❑ $LaAlO_3$ (Insulator 5.6 eV)

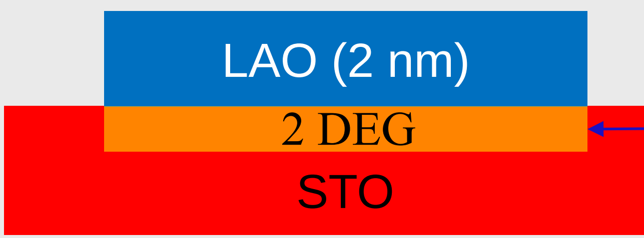

2 DEG formed inside the STO side

NUS National University of Singapore

Spin-orbit fields in $LaAlO_3/SrTiO_3$ heterostructures

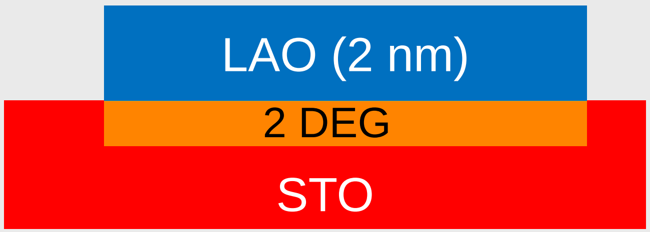

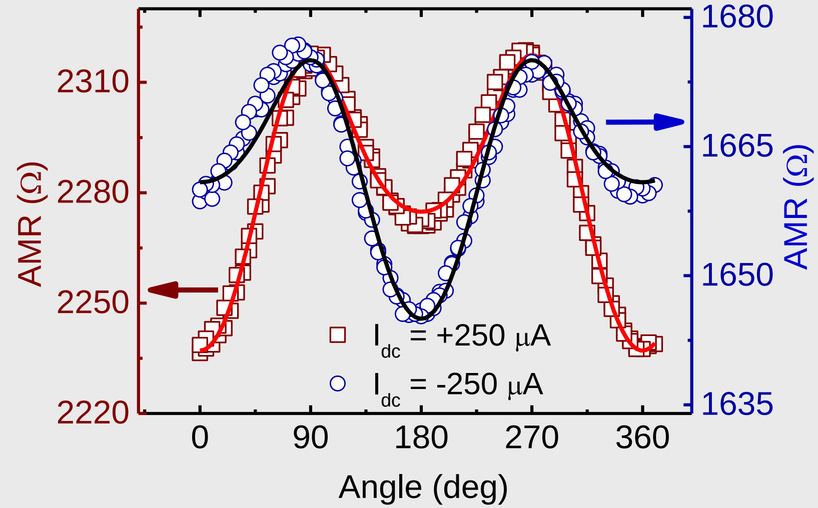

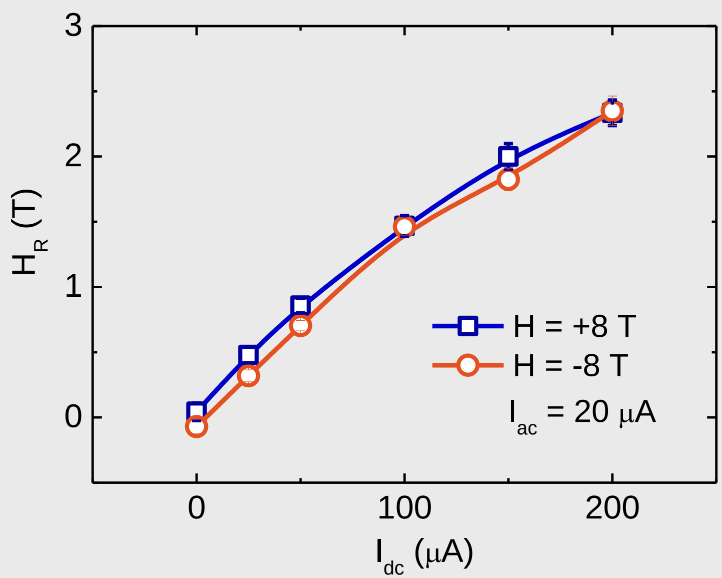

Assuming thickness of 2DEG

t_{2DEG} = 7 nm

Nat. Mater. **7**, 621 (2008)

current density = 7.14×10^8 A/m^2

2.35 T @ 200 μA

→ **3** T/(10^5 A/cm^2)

$\boldsymbol{\theta_{SH}}$ ~ 2 (M_s = 50 emu/cc)

NUS National University of Singapore

Appl. Phys. Lett. **105**, 162405 (2014)

Spin Hall magnetoresistance

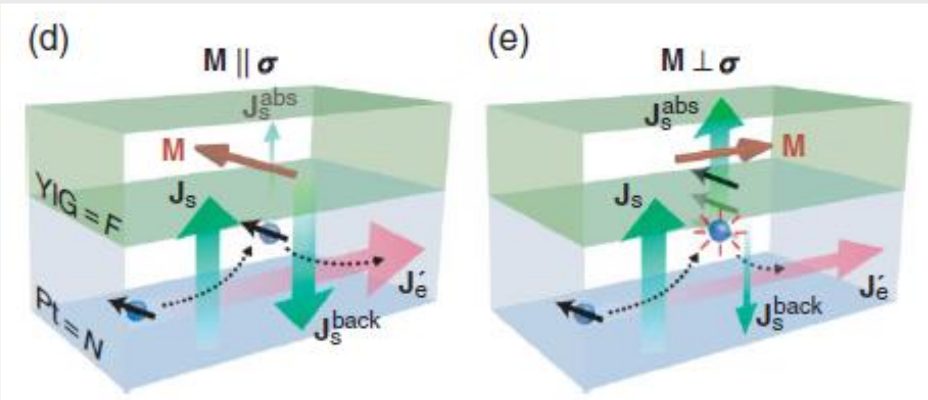

PRL 110, 206601 (2013)

→ SHE and ISHE

→Depends on spin mixing conductance

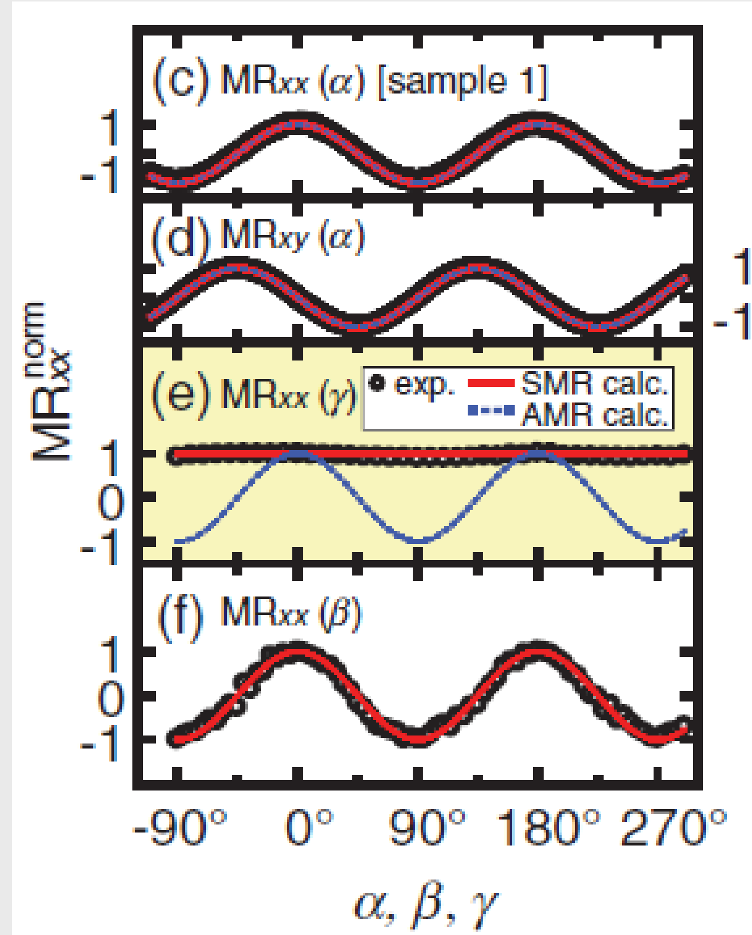

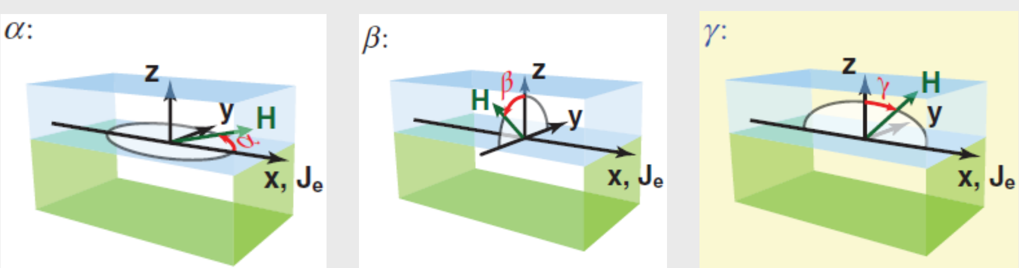

Rashba magnetoresistance in LAO/STO

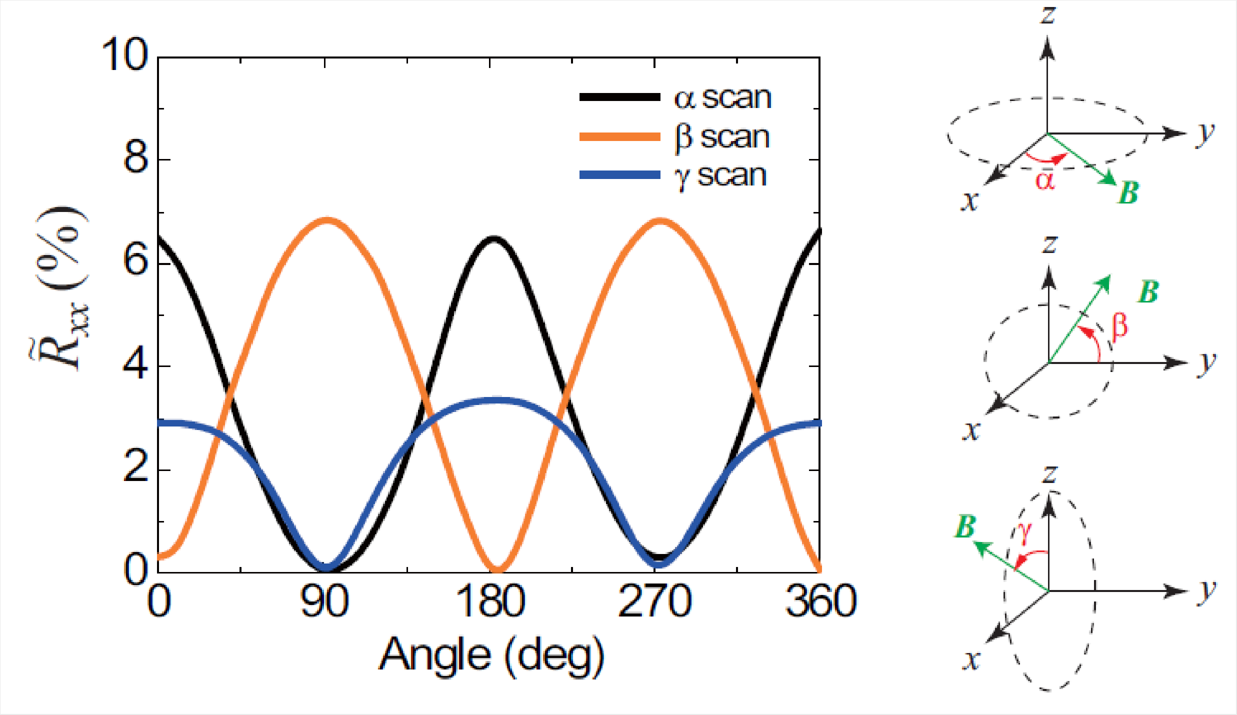

Interfacial nature of STO/LAO → Rashba MR
Spin Hall MR from FM/heavy metal is 0.01-1%
Rashba MR is 1-2 order magnitude larger than spin Hall MR

PRB **96**, 064401 (2017)

Giant charge-to-spin conversion at STO/LAO interface

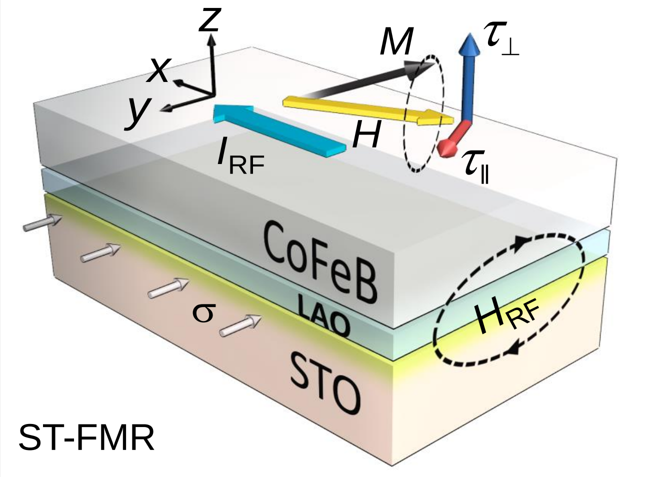

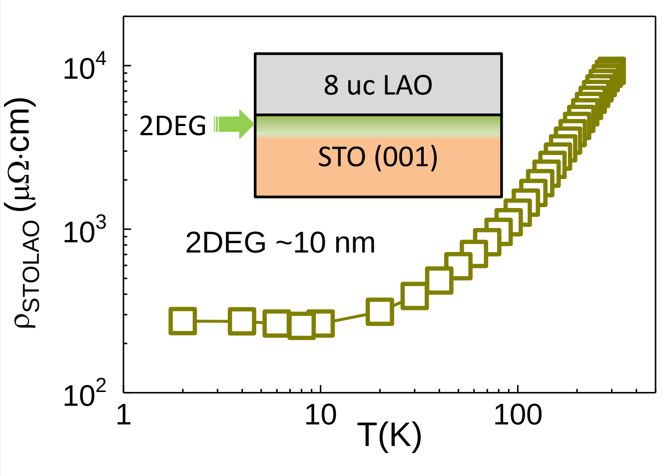

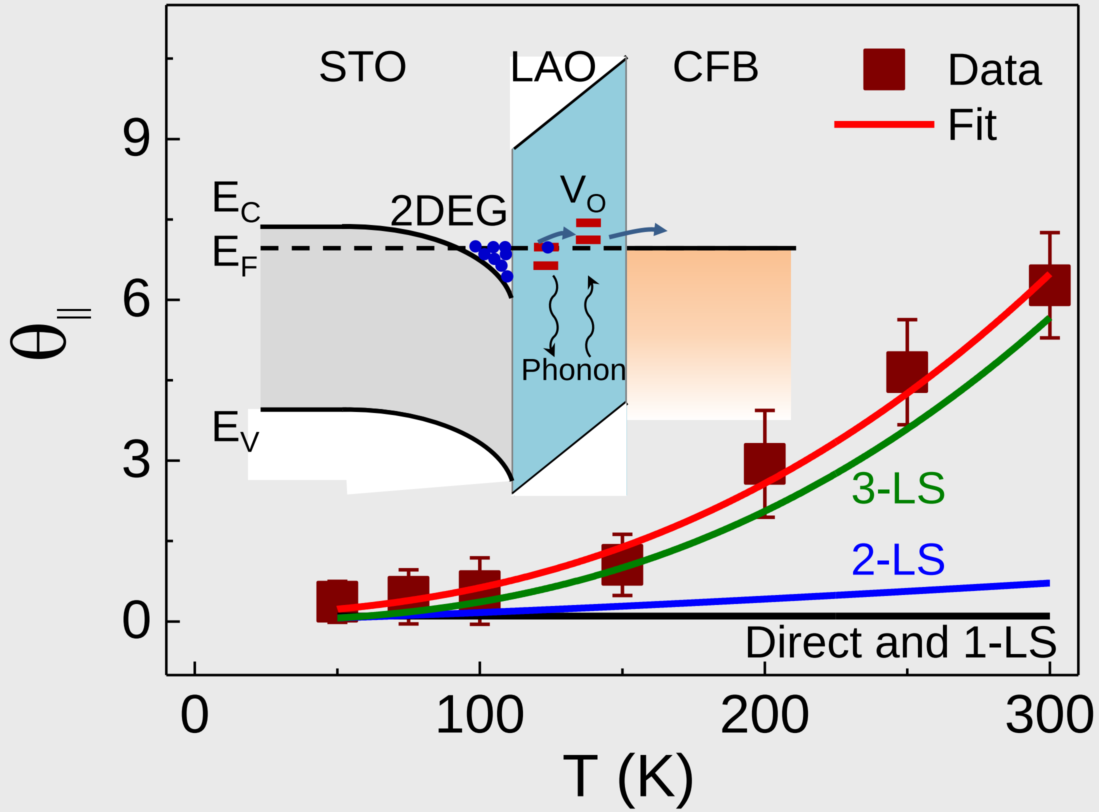

- Possible inelastic tunneling via localized states for spin transmission
- θ_{SH} = 6.3 (room temp)

Nano Lett. **17**, 7659 (2017)

NUS National University of Singapore

Eliminate LAO → $SrTiO_3$ (111)

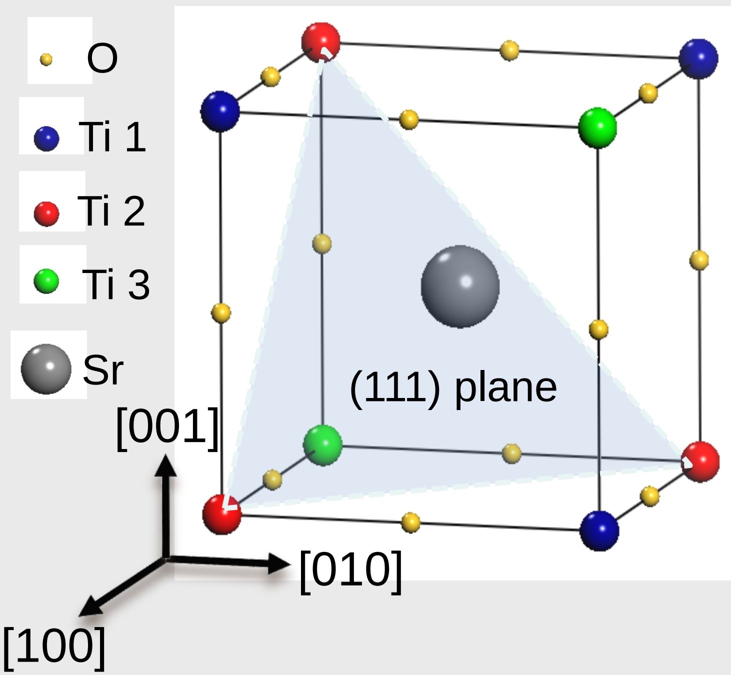

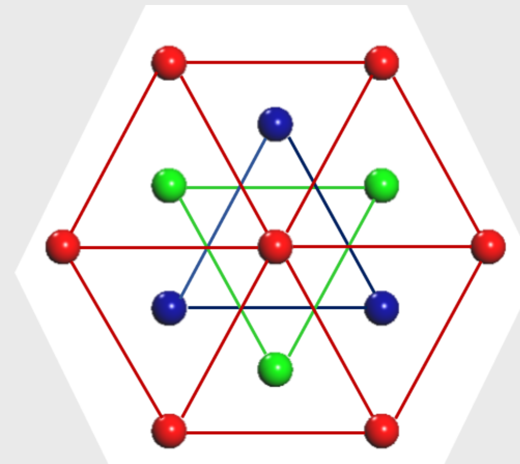

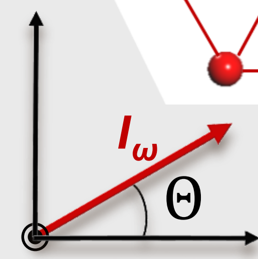

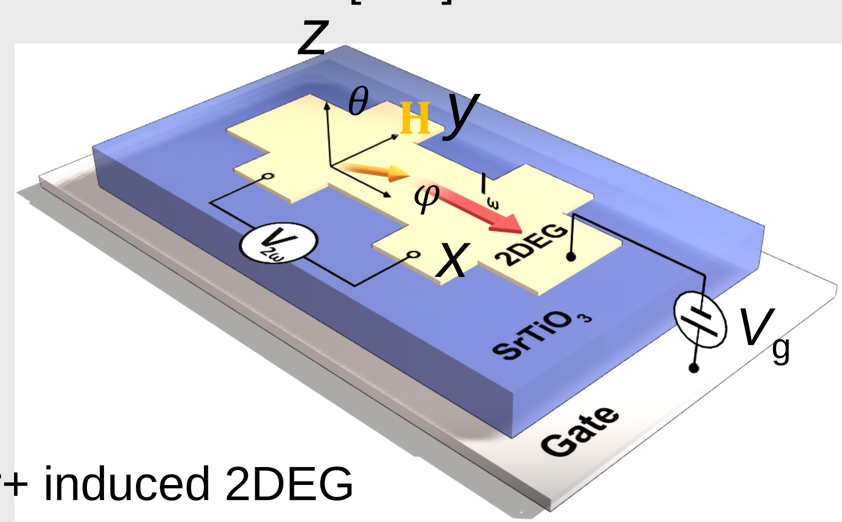

Ar+ induced 2DEG

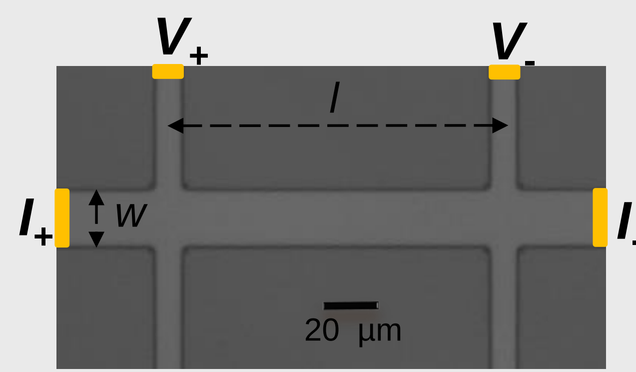

n~ 0.5 - 1.3 × 10^{14} cm^{-2}

NUS National University of Singapore

PRL **120**, 266802 (2018)

Observation of BMER in Bi_2Se_3

Bilinear magneto-electric resistance (BMER)

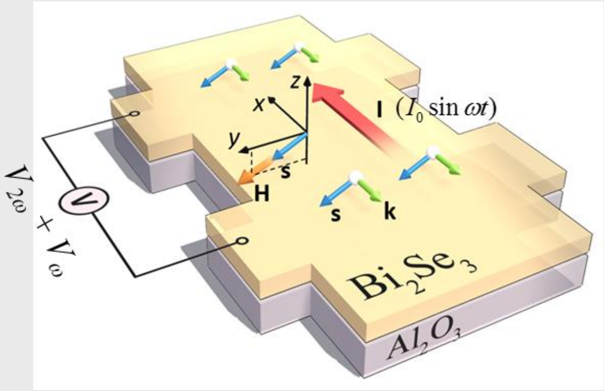

MBE grown Bi_2Se_3 (20 QL)/Al_2O_3 (0001)

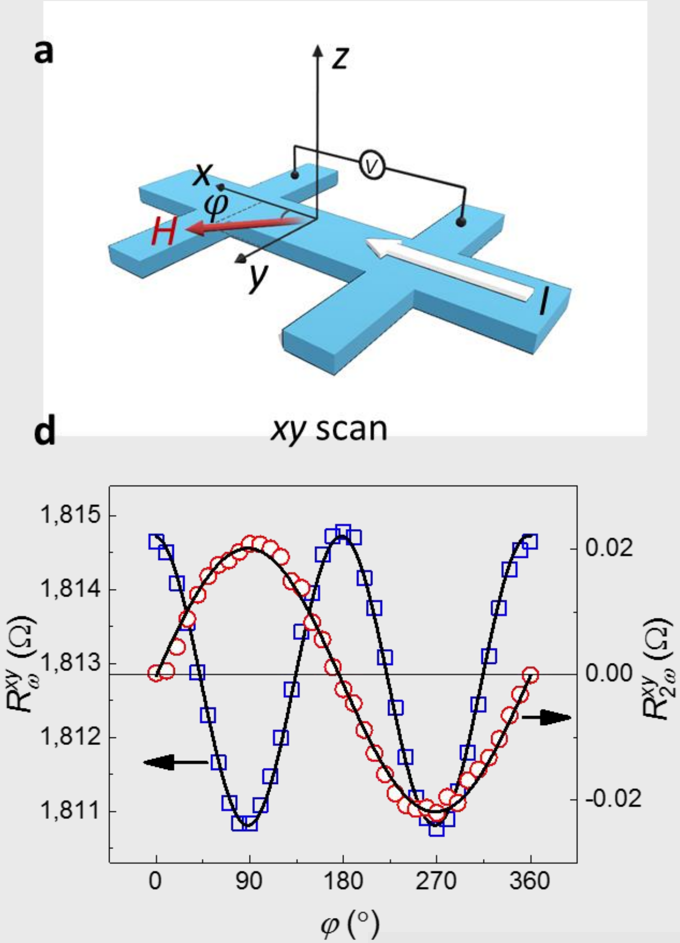

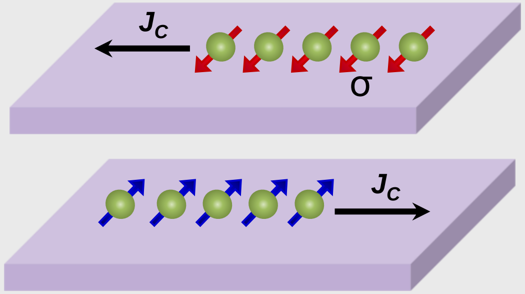

$R_{2\omega} \propto \boldsymbol{s} \cdot \boldsymbol{H}$

Blue curves: $R_\omega(-\boldsymbol{H}) = R_\omega(\boldsymbol{H})$

Red curves: $R_{2\omega}(-\boldsymbol{H}) = -R_{2\omega}(\boldsymbol{H})$

A new spin-dependent nonlinear MR

R_ω represents the current-independent resistance, while $R_{2\omega}$ is the current-dependent resistance.

Nat. Phys. **14**, 495 (2018)

Bi_2Se_3 (20 QL, 125K, 9T, 0.55mA)

National University of Singapore

BMER features

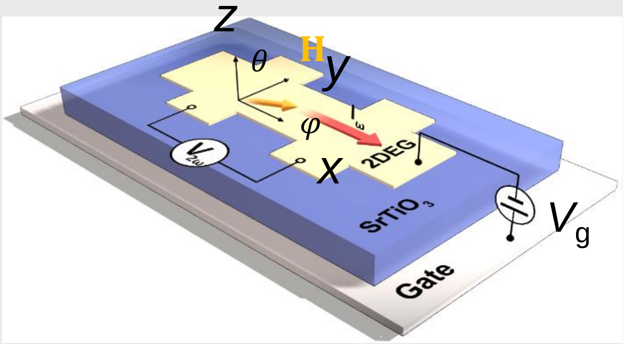

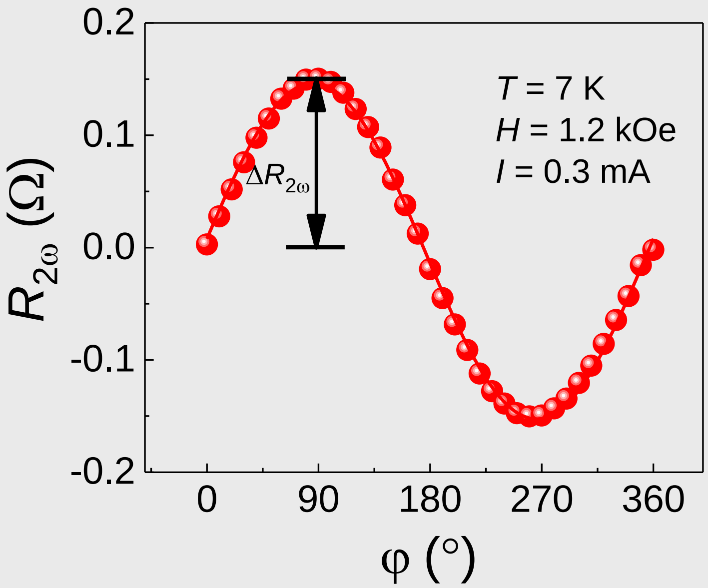

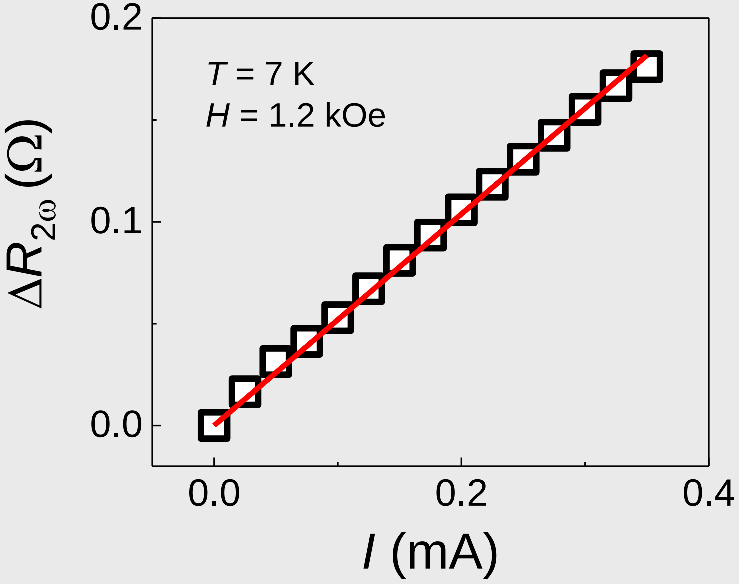

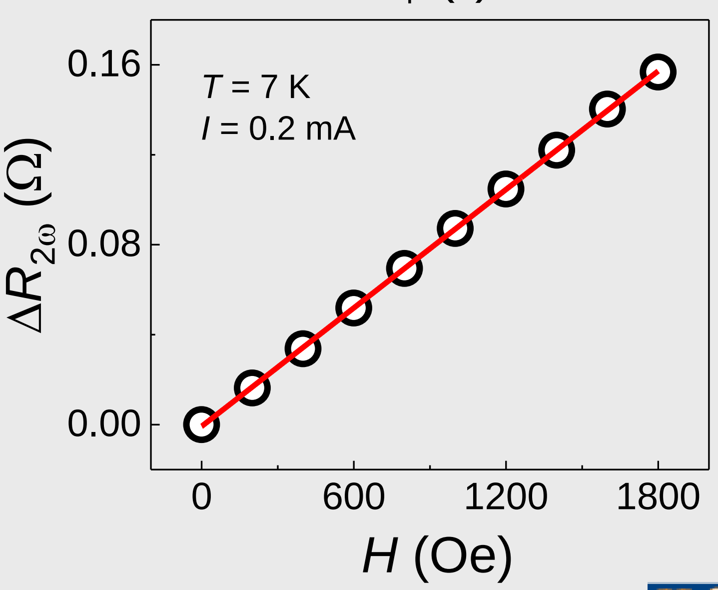

2ω signals are linear with the current and magnetic field → BMER

PRL **120**, 266802 (2018)

Out-of-plane spin canting in $SrTiO_3(111)$

z-y scan

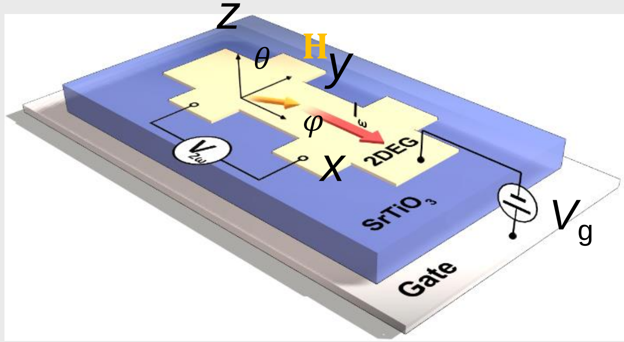

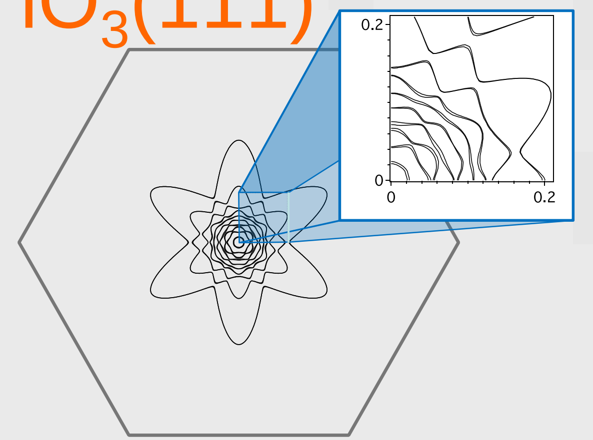

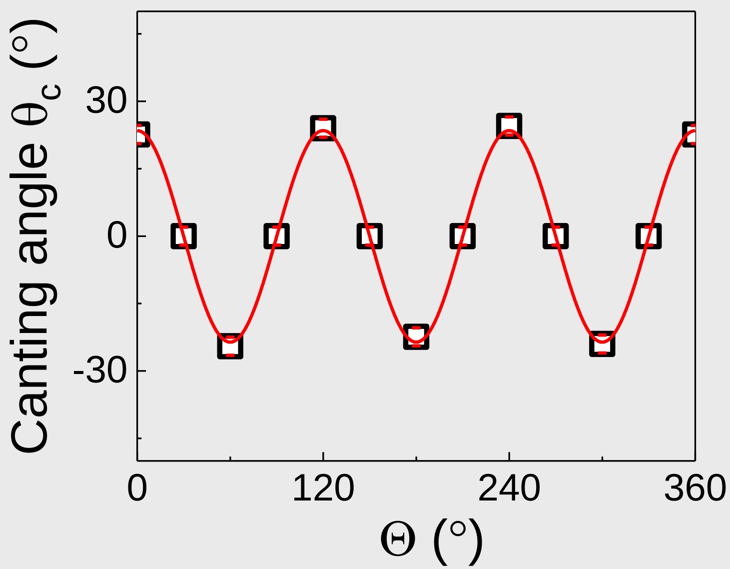

Calculation from S. McKeown Walker and F. Baumberger

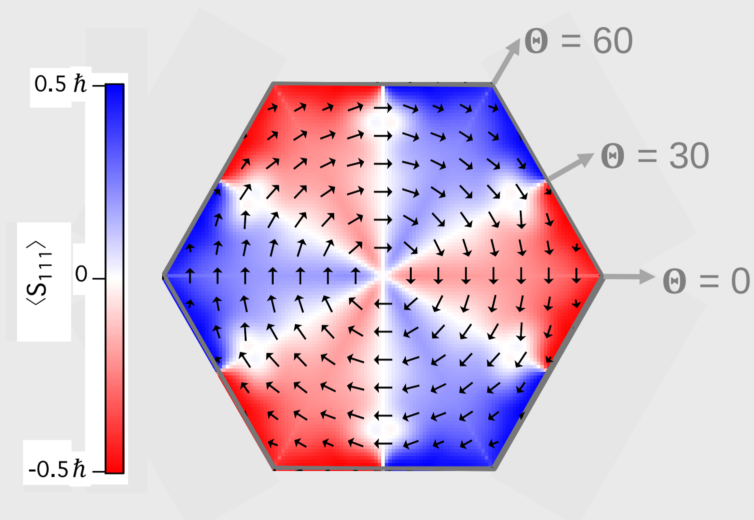

Strong crystal field effects induces out-of-plane spin texture

Question the validity of single relaxation time approximation in STO(111)

PRL **120**, 266802 (2018)

Spin orbit torque efficiency vs. Power consumption

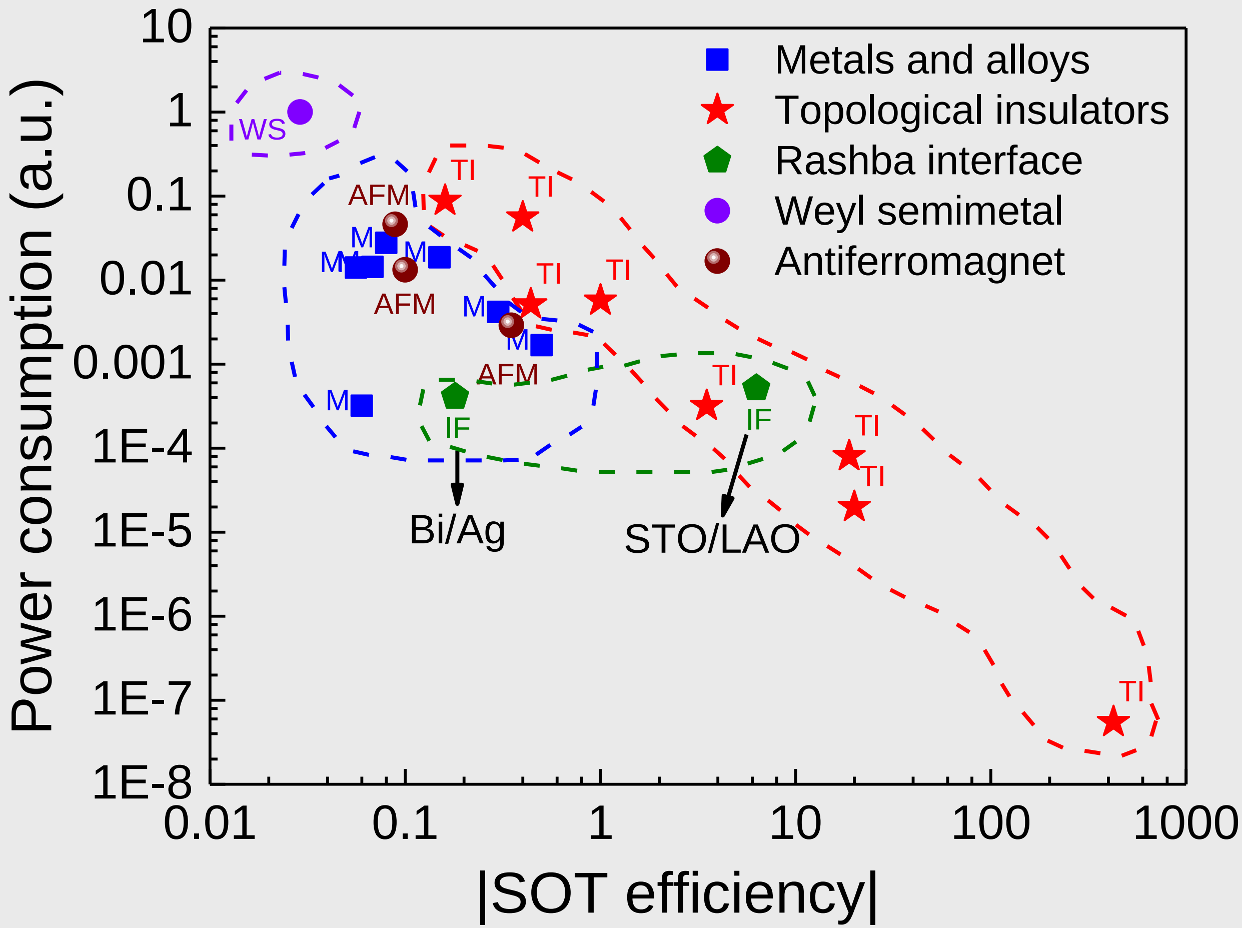

$$P \sim 1/(\sigma \times (\theta_{sh})^2) \sim 1/\theta_{sh}$$

Review: J. Phys. D: Appl. Phys. **51**, 273002 (2018)

Field-free SOT switching by symmetry breaking

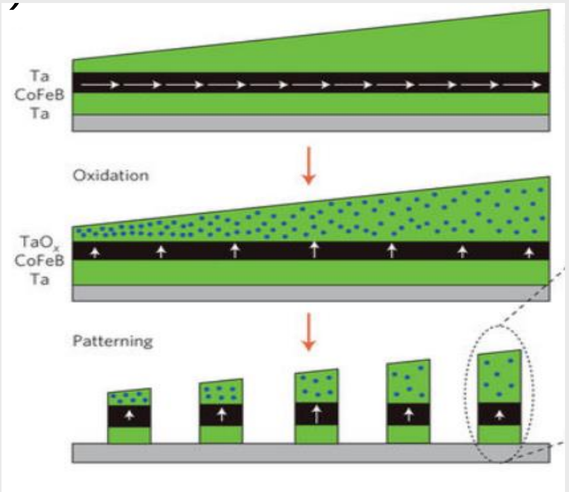

Nat. Nano. **9**, 548 (2014)

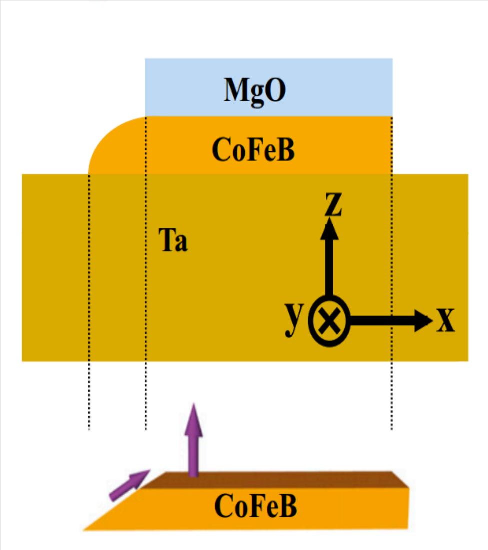

PNAS **112**, 10310 (2015)

Oblique deposition

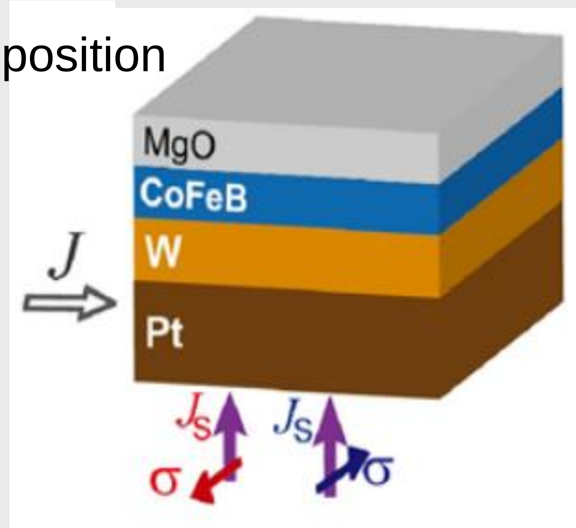

PRL **120**, 117703 (2018)

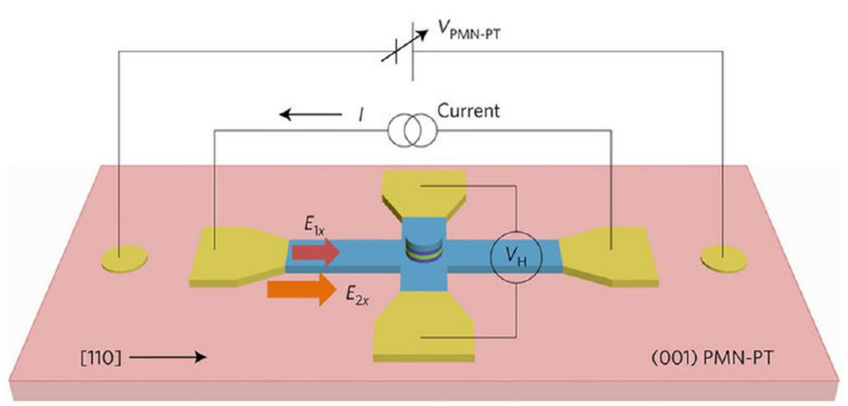

Nat. Mater. 11, 712 (2017)

NUS National University of Singapore

Break the symmetry, but not friendly for applications

Field-free SOT-exchange bias or interlayer coupling

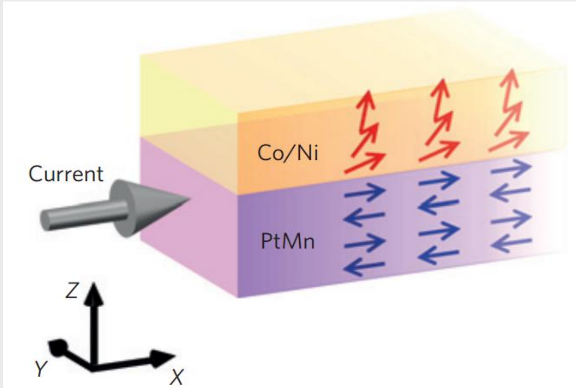

Nature Materials **15**, 535 (2016)

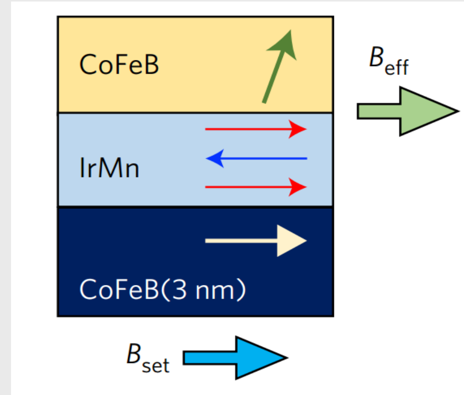

Nature Nanotechnology **11**, 878 (2016)

(c)

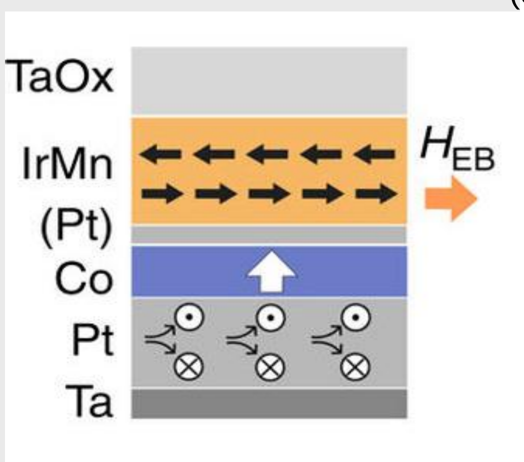

Nat. Commun. **7**, 10854 (2016)

(d)

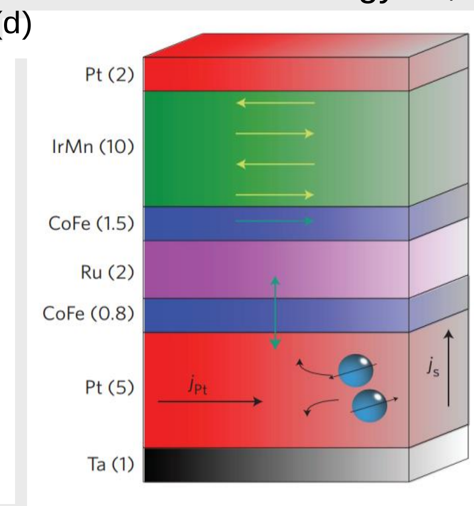

Nature Nanotechnology **11**, 758 (2016)

Integration issue with MTJ

Heat or repeated switching induced decrease of exchange bias

Review: *Appl. Phys. Rev.* **5**, 031107 (2018)

NUS National University of Singapore

One domain wall based field-less SOT switching

Domain wall geometric pinning

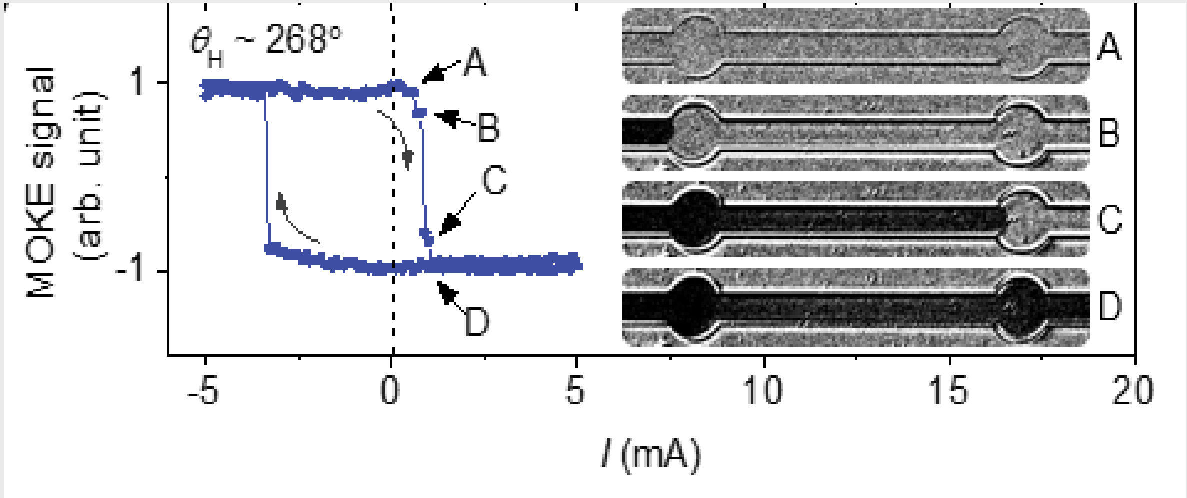

Repeated switching

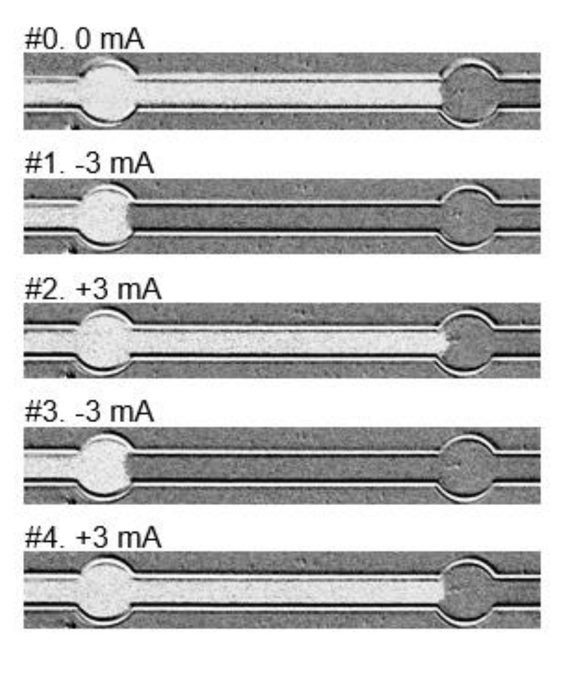

Perpendicular anisotropy system: Ta/CoFeB/MgO

- Single domain wall (DW) can be pinned in anti-notch structure.
- DW stops at the neck part due to lower current density.
- DW surface energy: Phys. Rev. Applied **9**, 024032 (2018)

Nano Lett. **18**, 4669 (2018)

NUS National University of Singapore

Field-free SOT from geometrical domain wall pinning

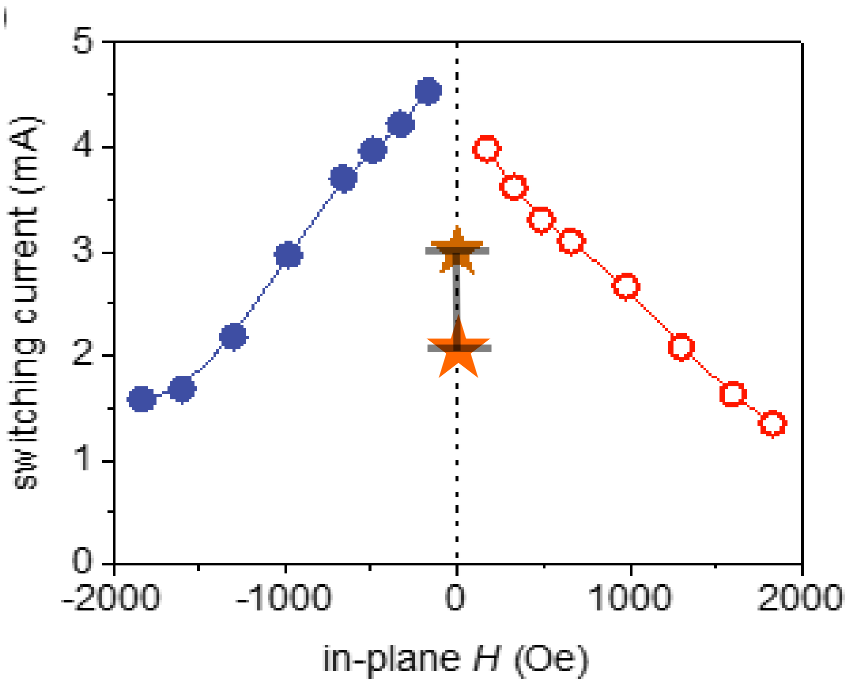

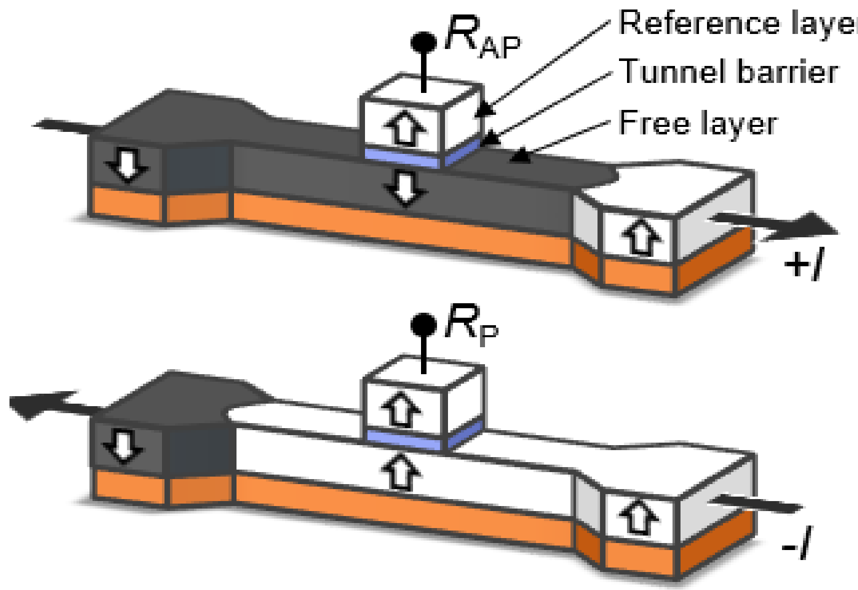

- No additional energy to nucleate DW.
- 2-3x reduction in switching current.
- Easy integration with MTJs.

Nano Lett. **18**, 4669 (2018)

Dzyaloshinskii-Moriya interaction

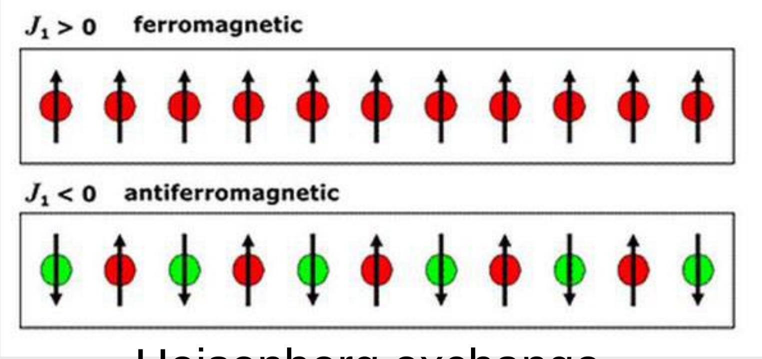

Heisenberg exchange

$$E_{\mathrm{H}} = -\sum_{i,j} J_{ij} S_i \cdot S_j$$

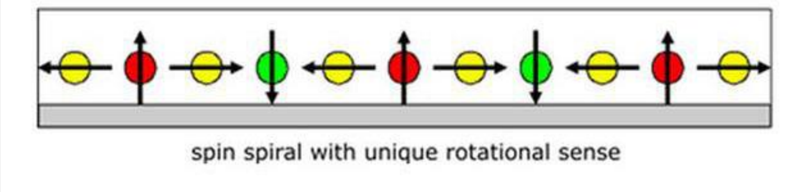

Dzyaloshinskii-Moriya interaction due to spin-orbit coupling

$$E_{\mathrm{DM}} = -\sum_{i,j} D_{ij} \cdot \left(S_i \times S_j\right)$$

Preference of spin alignment → Minimize the system energy

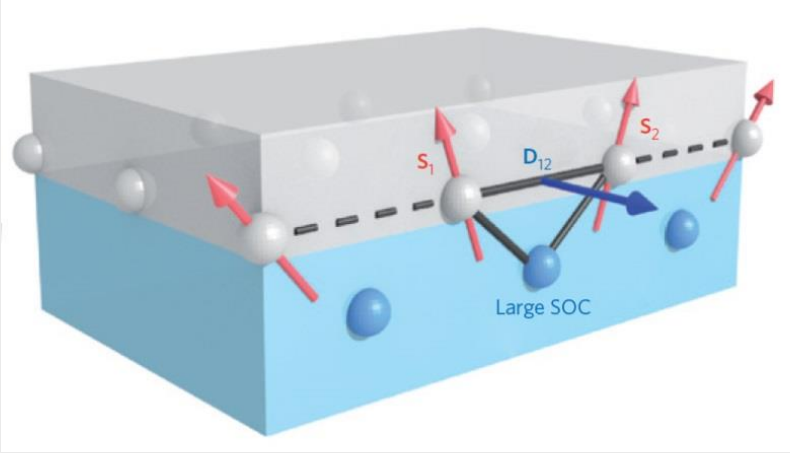

Nat. Nanotechnol . **8**, 152 (2013)

http://www.nanoscience.de/nanojoom/index.php/en/research/current-topics/noncollinear-spins/94-noncollinear-spins.html

Measurement methods of DMI

Current induced DW motion

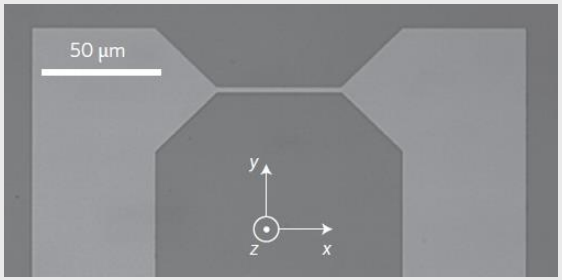

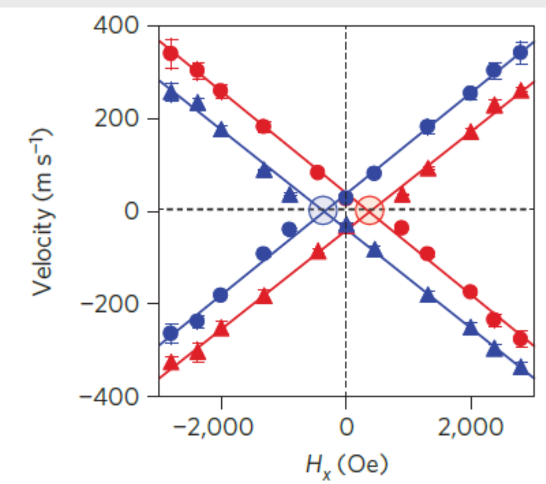

Ryu, K.-S., *et al. Nat. Nanotechnol.* **8**, 527 (2013).

Asymmetric DW creep

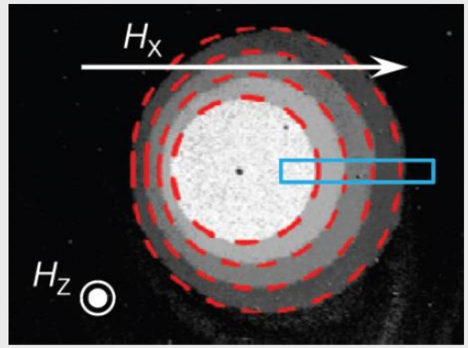

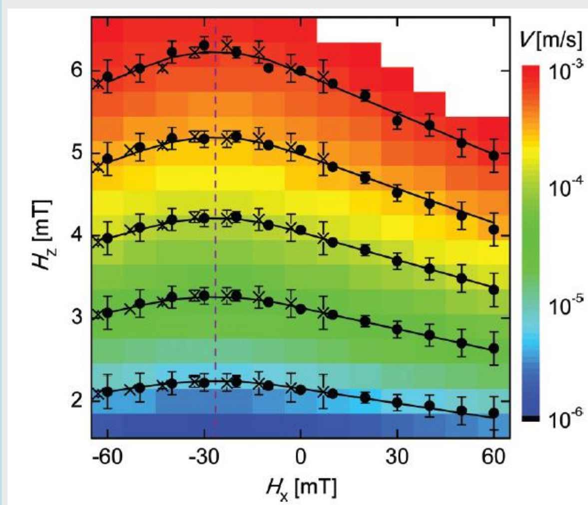

S-G. Je, *et al. Phys. Rev. B* **88**, 214401 (2013).

DW depinning efficiency

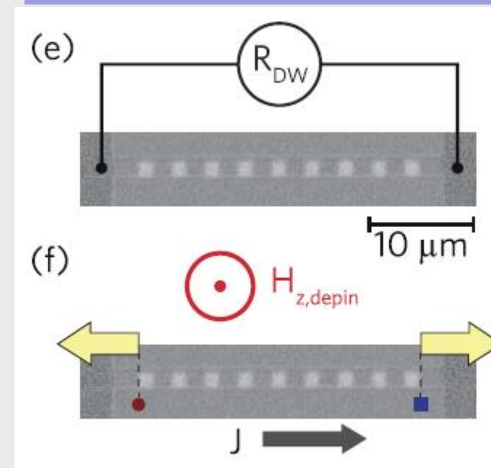

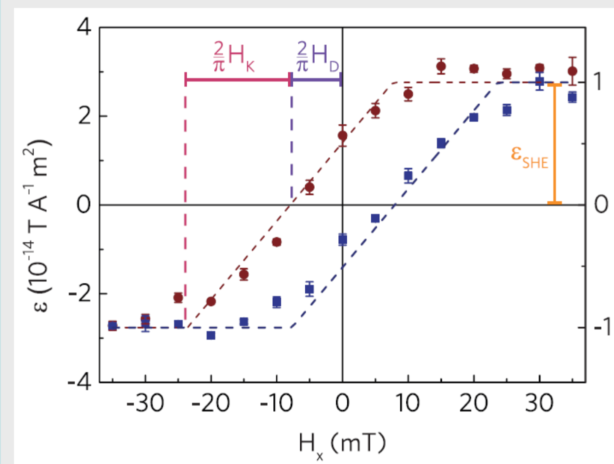

Franken, J.H. *et al. Sci. Rep.* **4**, 5248 (2014).

DMI induced frequency shift in spin waves

Brillouin light scattering (BLS)

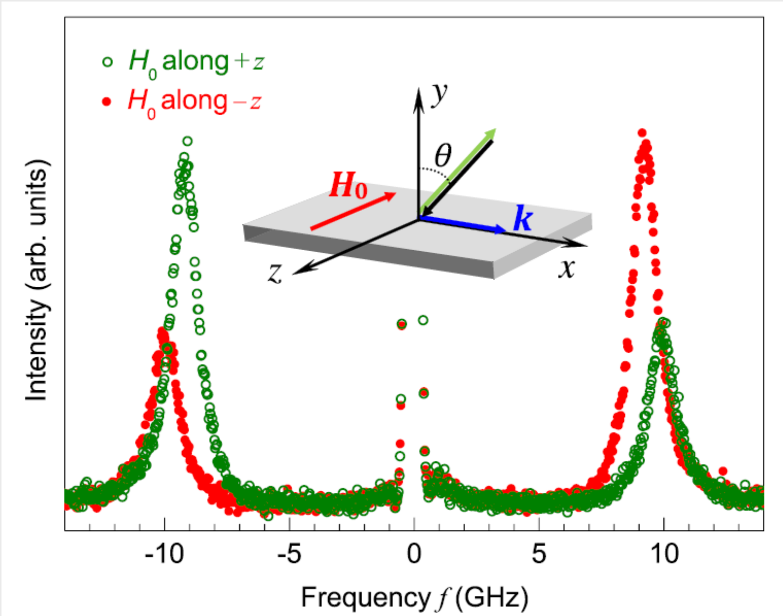

$$\Delta f(k) = [\omega(-k) - \omega(k)]/2\pi = \frac{2\gamma}{\pi M_S} Dk$$

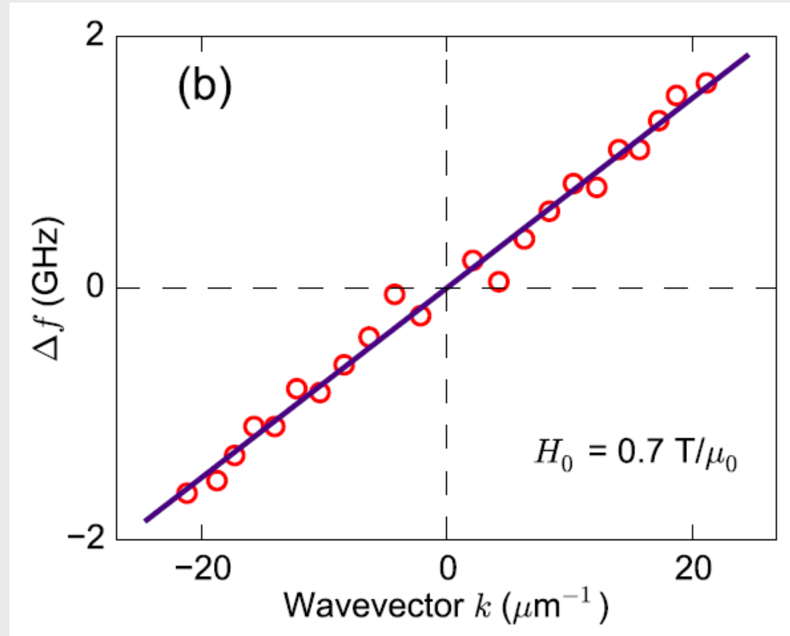

Pt (4 nm)/Co (1.6)/Ni (1.6)/MgO (2)/SiO_2 (3) → D=0.44 mJ/m^2

Pt (2 nm)/CoFeB (0.8)/MgO (2)/SiO_2 (3) → D=1.0 mJ/m^2

Also see Cho *et al*., Nat. Commun. **6**, 7635 (2015)

NUS National University of Singapore

PRL **114**, 047201 (2015)

Skyrmion background

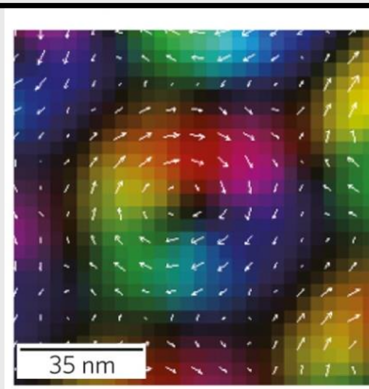

Bloch skyrmion in single crystal FeGe

Nat. Mat. **10**, 106–109 (2011)

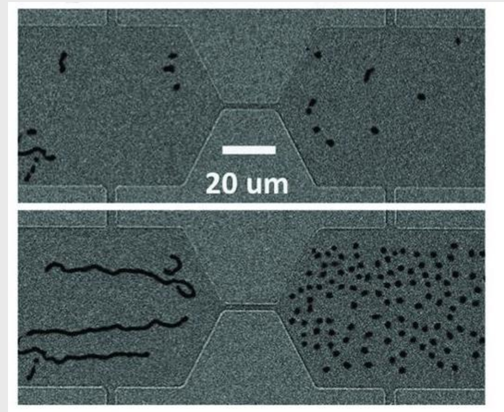

Néel skyrmions in Ta/CoFeB/TaOx ultrathin films

Science **349**, 283-286 (2015)

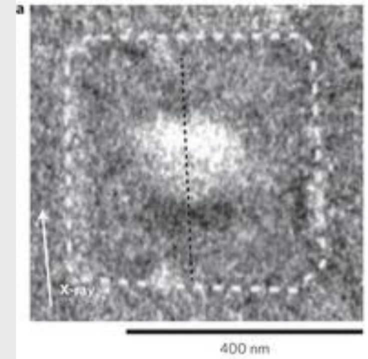

Néel skyrmions in Pt/Co/MgO patterned films

Nat. Nano. **11**, 449–454 (2016)

w = 1
$D > 0$

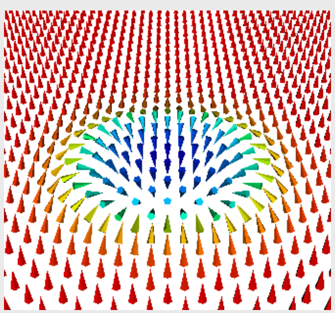

w = -1
$D < 0$

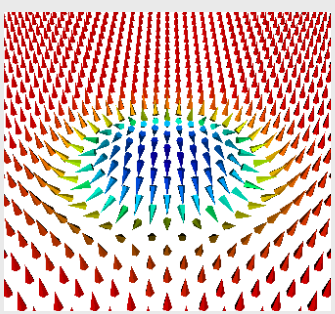

Néel skyrmion structure

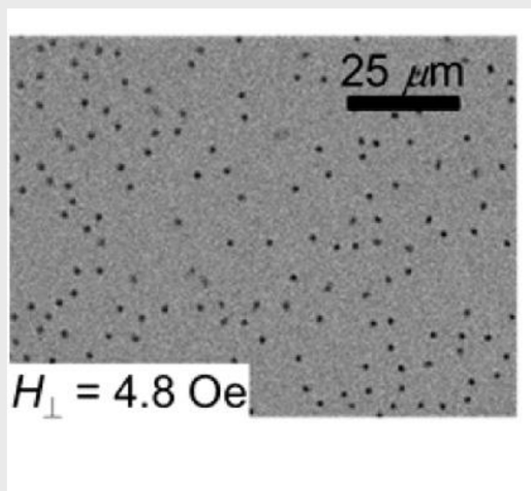

Néel skyrmion in Ta/CoFeB/TaOx ultrathin films

Nano Lett., **2016**, *16* (3), 1981–1988 (2016)

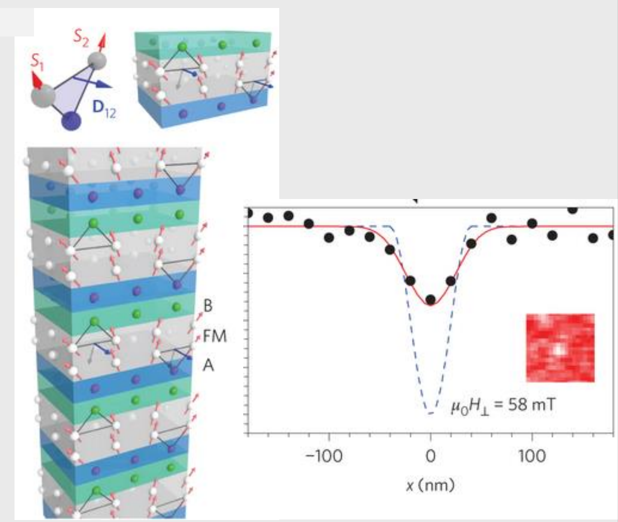

Néel skyrmion in Ir/Co/Pt multilayers

Nat. Nano. **11**, 444–448 (2016)

Chiral magnet & magnetic skyrmion

What will happen if DMI is large in ferromagnetic materials?

Chirality or handness

Chiral domain wall (Bloch → Néel)

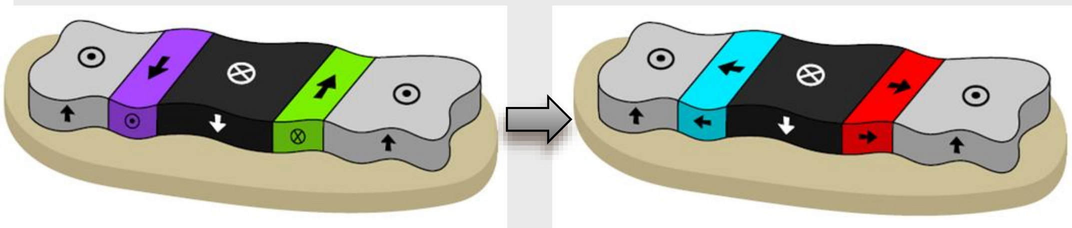

Chen, *et al. Nat. Commun.* **6**, 6598 (2015).

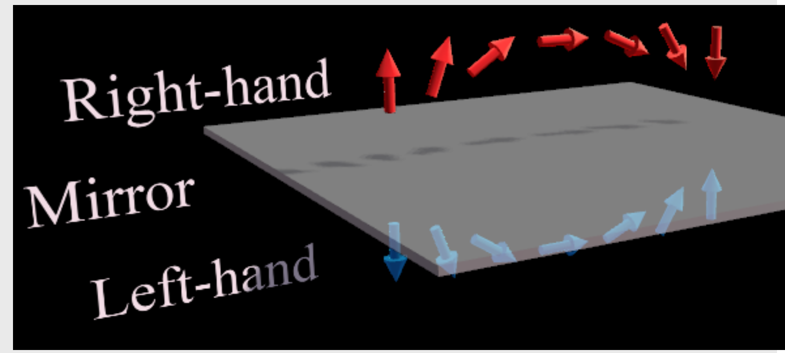

Magnetic skyrmion

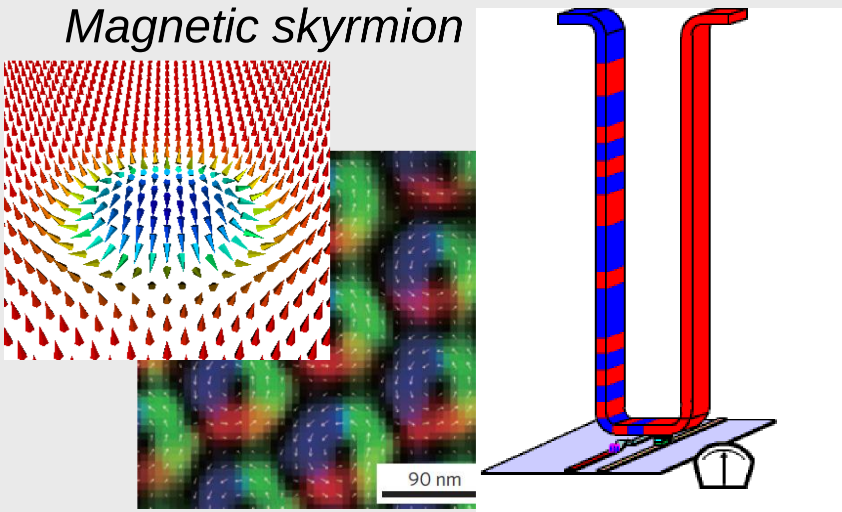

Domain wall

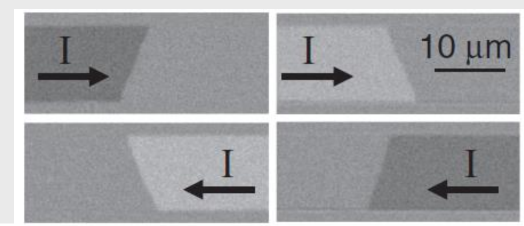

Skyrmion

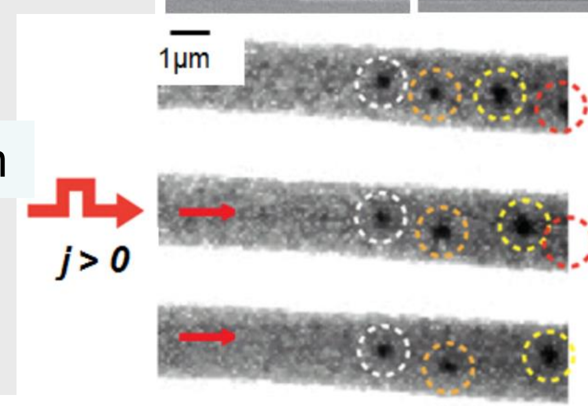

Ryu K-S. *et al. Appl. Phys. Express* **5** 093006 (2012);
Fert, A. *et. al. Nat. Nanotechnol .* **8**, 152 (2013);
Woo S. *et al. arXiv:1502.07376.*

Film geometry and bulk magnetic properties

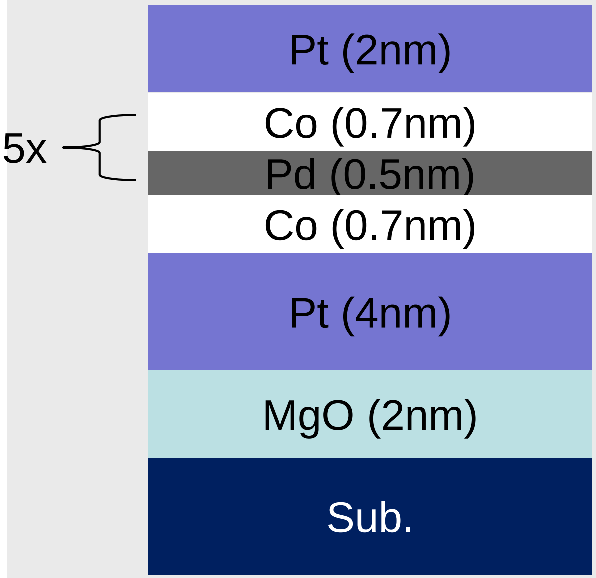

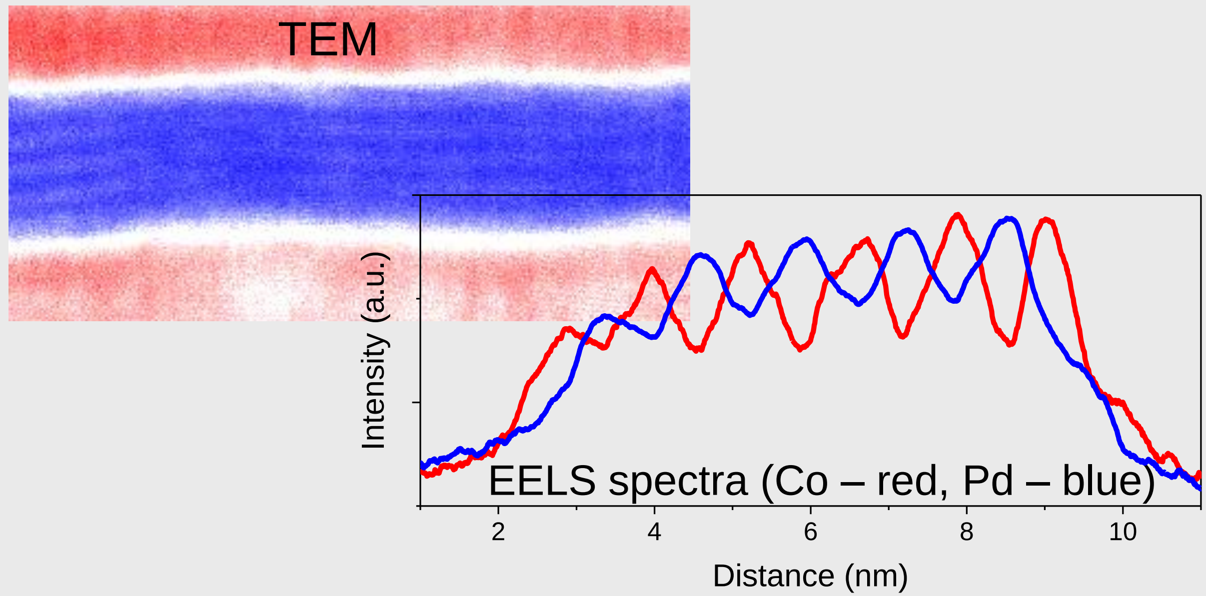

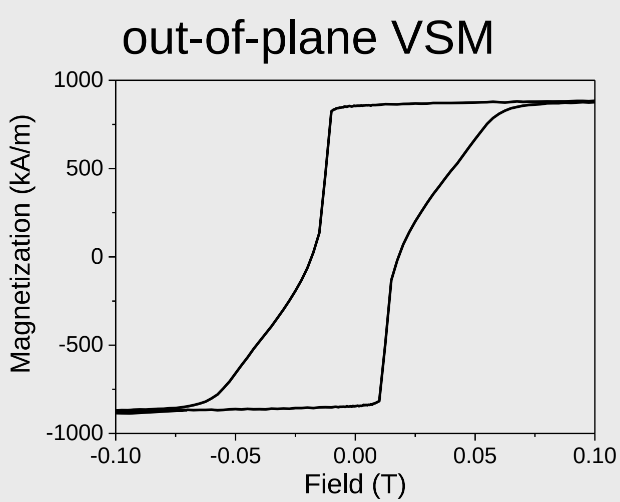

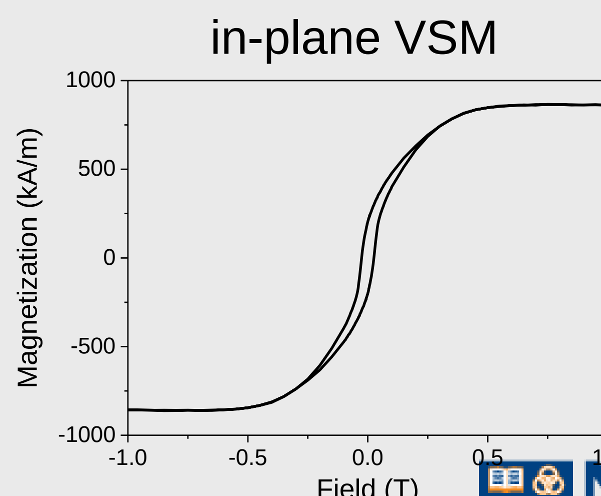

M_s = 880kA/m

$K_{u,eff}$ = 0.24 MJ/m^3

Nat. Commun. **8**, 14761 (2017)

Co/Pd for Dzyaloshinskii-Moriya interaction (DMI) engineering

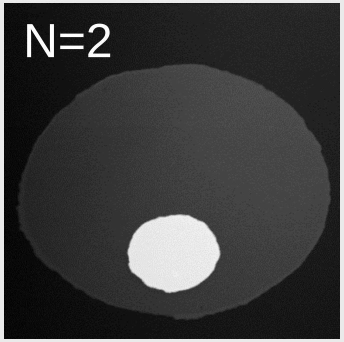

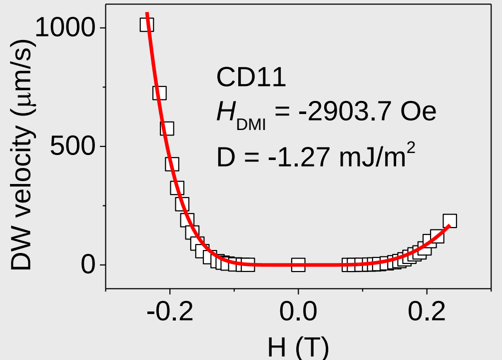

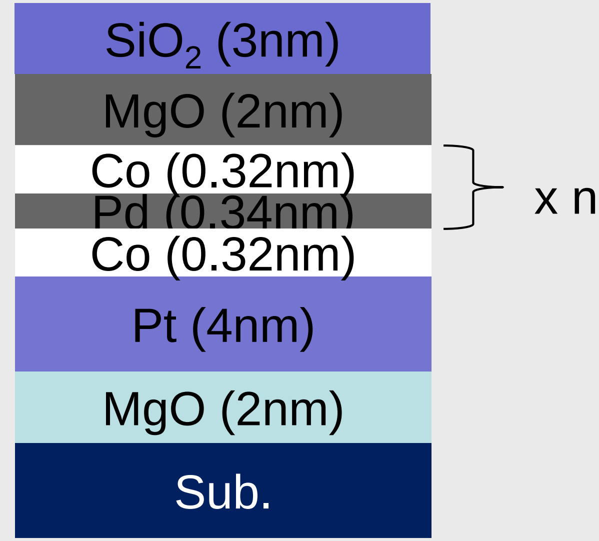

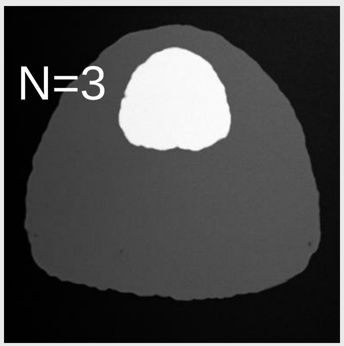

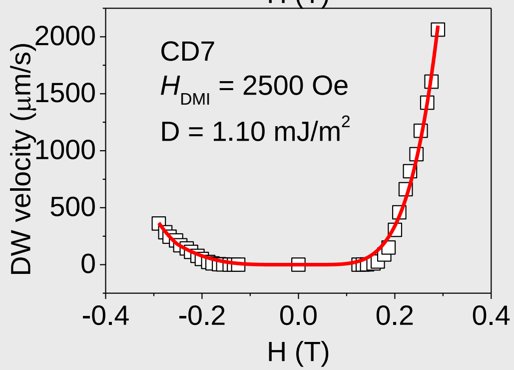

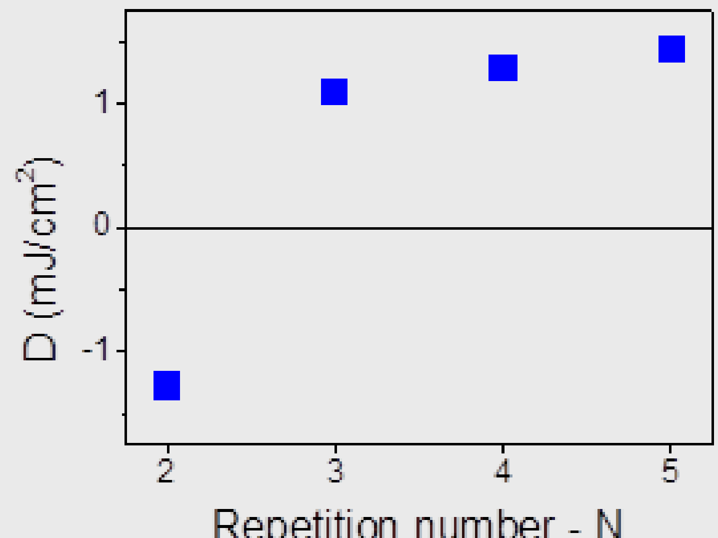

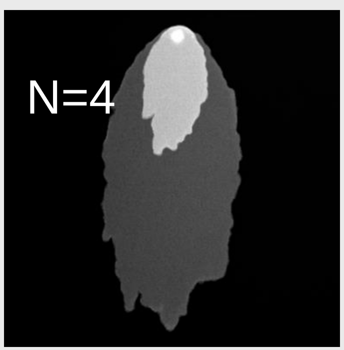

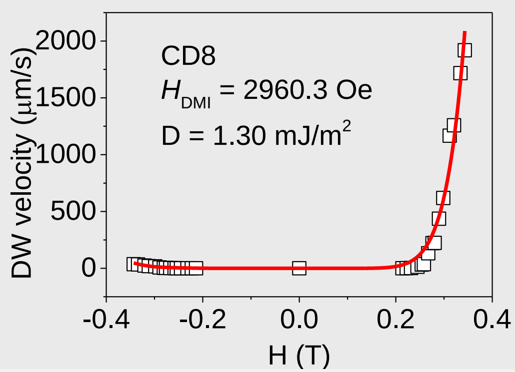

Co/Pd exhibits large DMI despite identical materials at top and bottom interface, a result of the large lattice mismatch. Enforces a single chirality of domain wall.

Nat. Commun. **8**, 14761 (2017)

Simulated and experimental skyrmion images

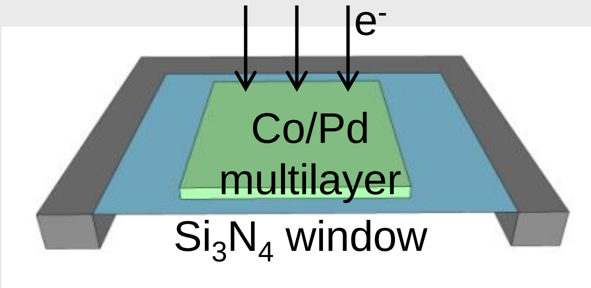

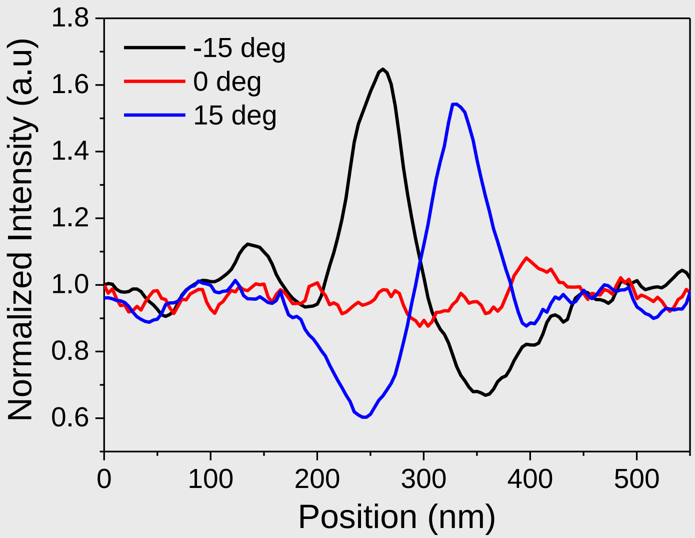

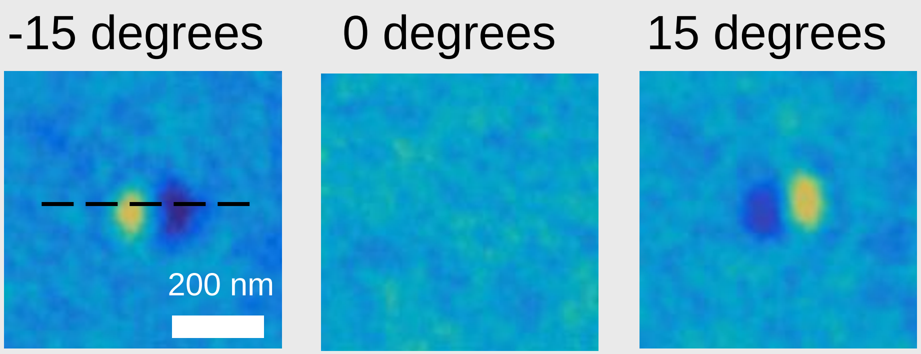

Experimental L-TEM skyrmion contrast

Simulated skyrmion contrast

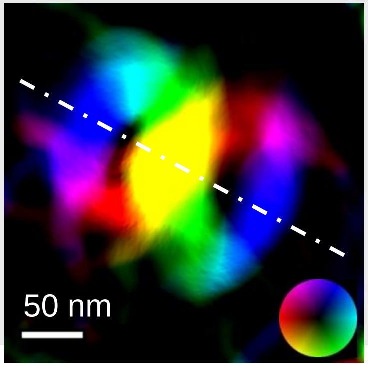

-Only visible when sample is tilted away from normal.
-90 nm Skyrmions are stable at room temperature and no external field

Nat. Commun. **8**, 14761 (2017)

Terahertz waves

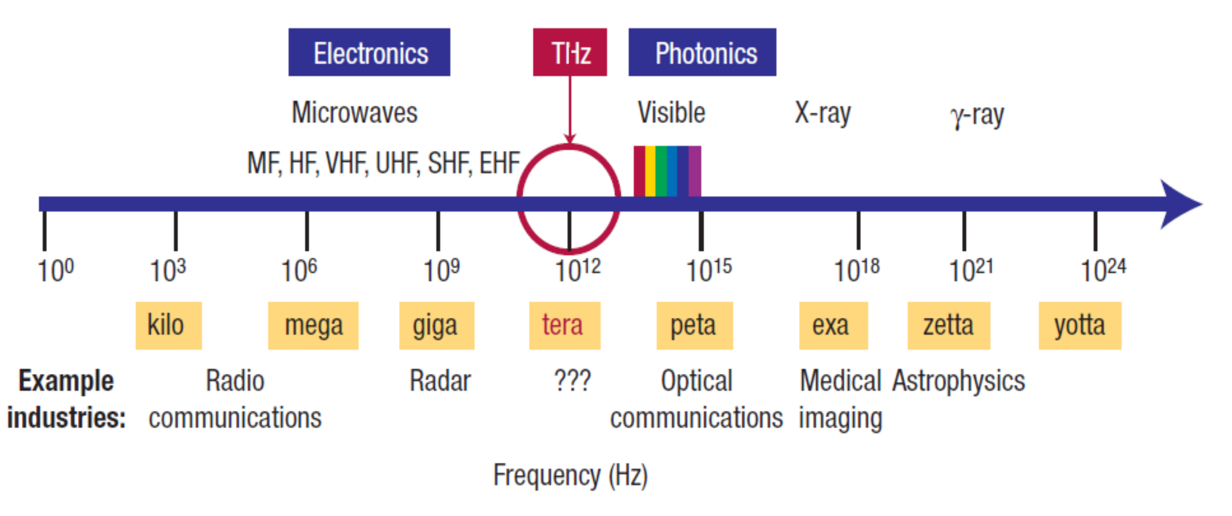

Nature Mater. **1**, 26 (2002)

Frequency 0.1 - 10 THz

Wavelength 0.03 - 3 mm

Photon energy 0.4 - 40 meV

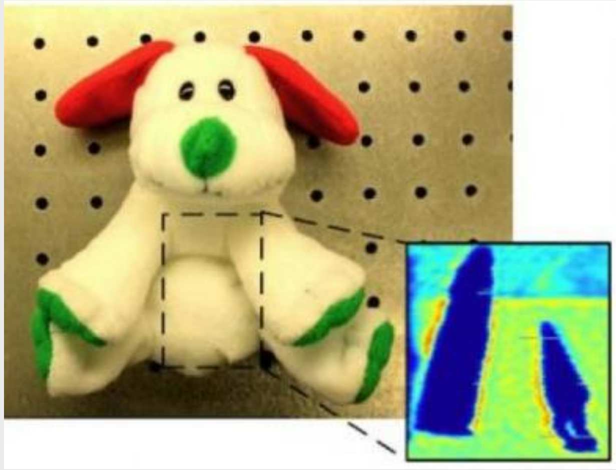

Safety surveillance

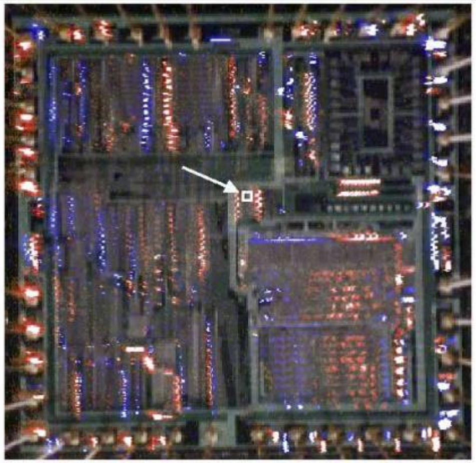

IC chip quality control

Opt. Express 13, 115-120 (2005)

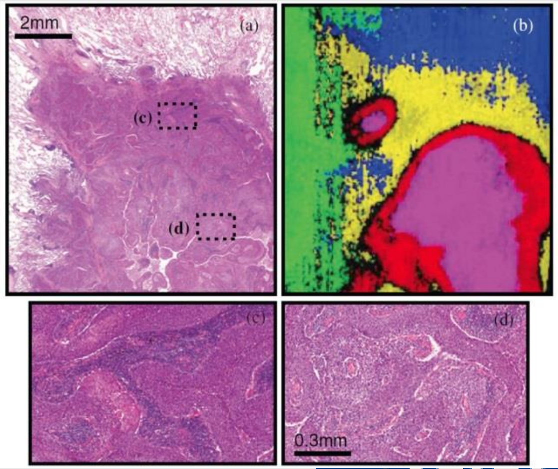

Disease diagnosis

Phys. Med. Biol. 55, 4615 (2010)

THz generation from magnetic multilayers

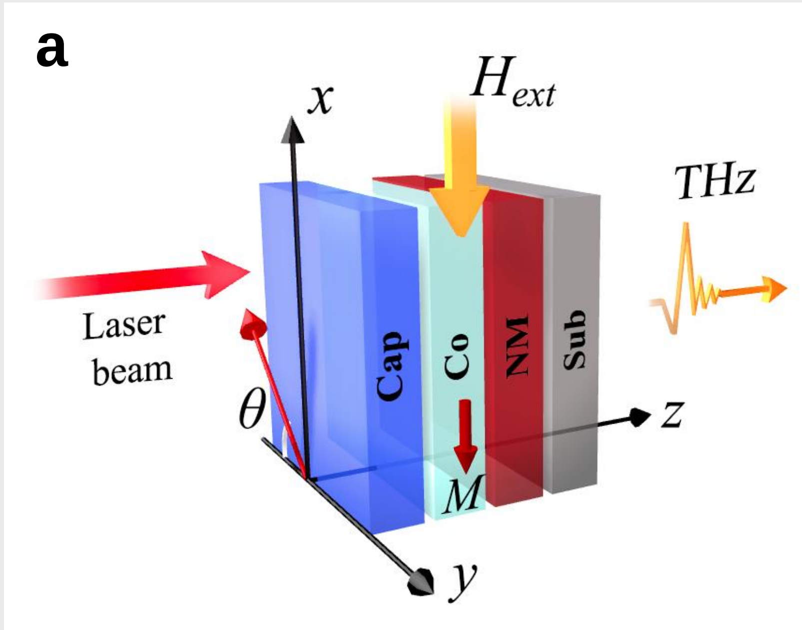

fs laser beam → spin currents → Inverse spin Hall effect (ISHE) → transient charge currents → THz emission

$$J_c = \theta_{SH} \cdot \vec{J_s} \times \vec{M} / |\vec{M}|$$

Nature Nano, **8**, 256 (2013)

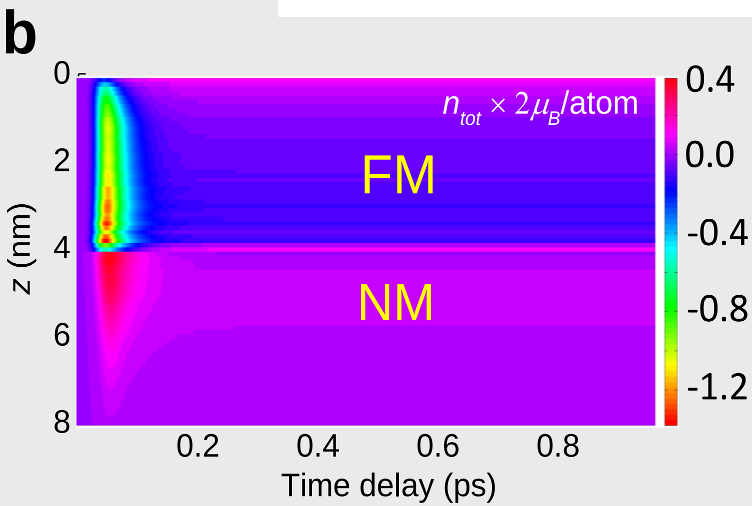

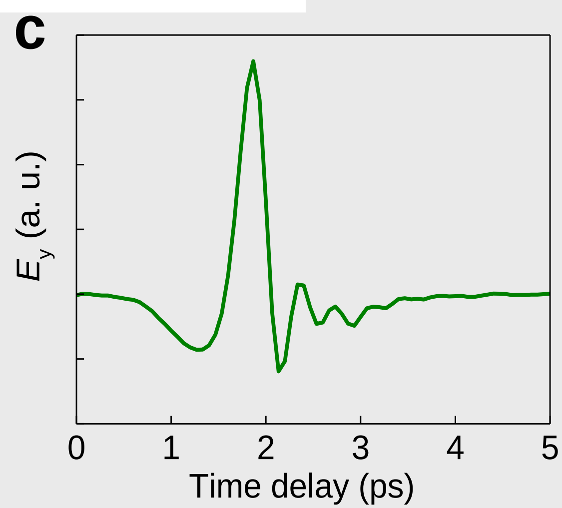

Adv. Mat **29**, 1603031 (2017)

THz signal probes inverse spin Hall effect

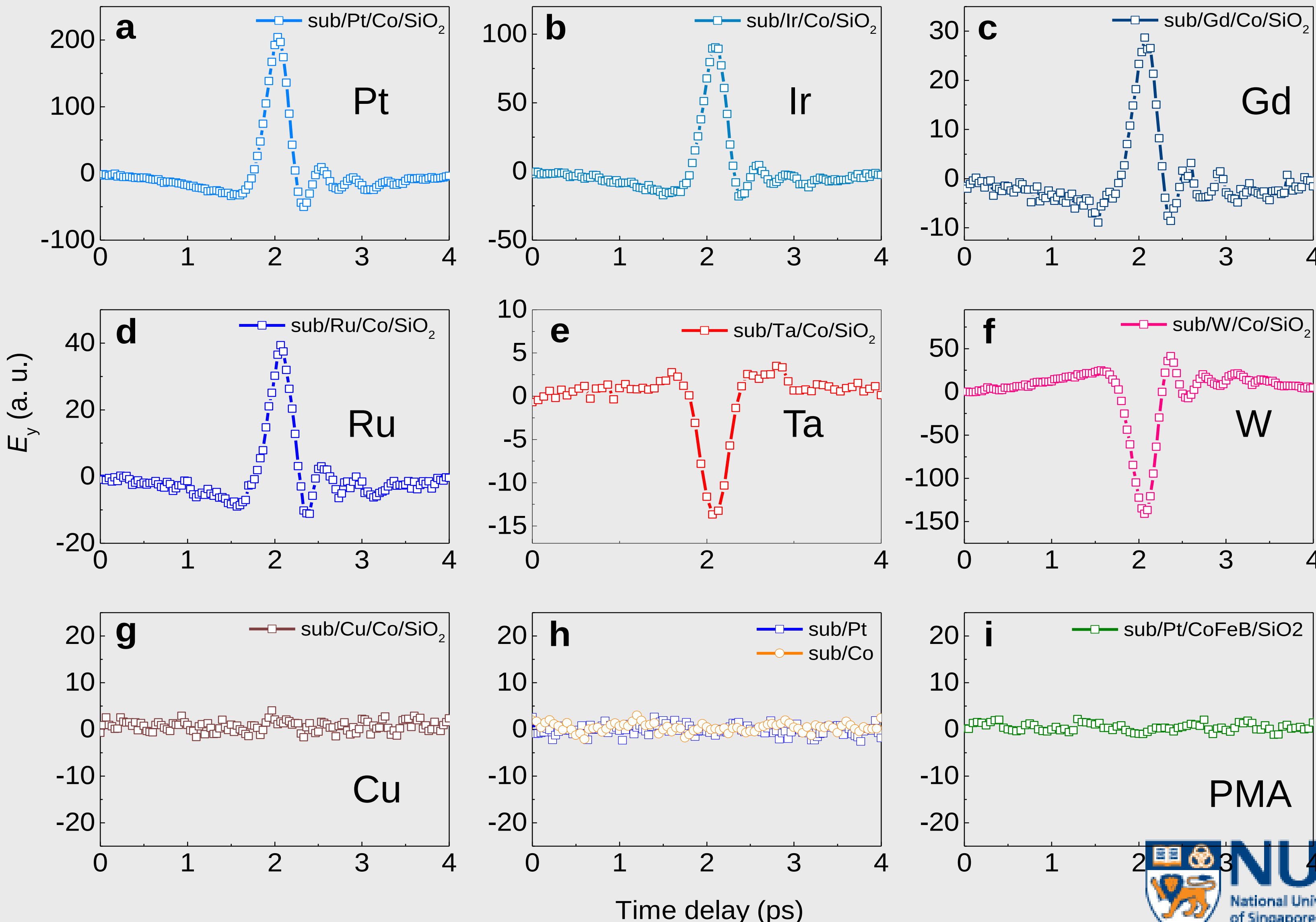

Adv. Mat **29**, 1603031 (2017); Adv. Opt. Mat. **6**, 1800430 (2018)

THz emitter optimization

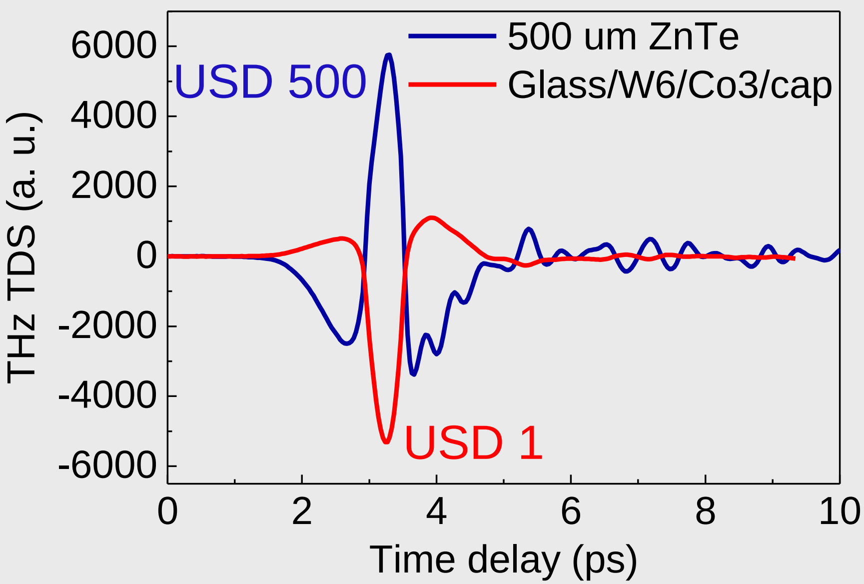

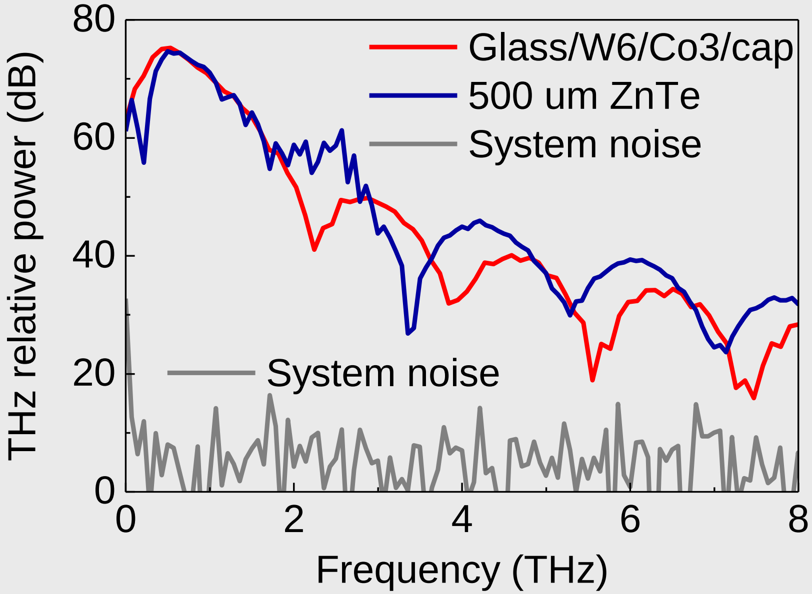

THz signal is optimized by choosing:

- NM material with large spin Hall angle
- Suitable FM & NM film thickness
- Proper substrates

Emitted THz wave:

- High signal to noise ratio (comparable with 500 μm ZnTe crystal)
- Broadband

Adv. Mat **29**, 1603031 (2017)

Flexible THz emitters

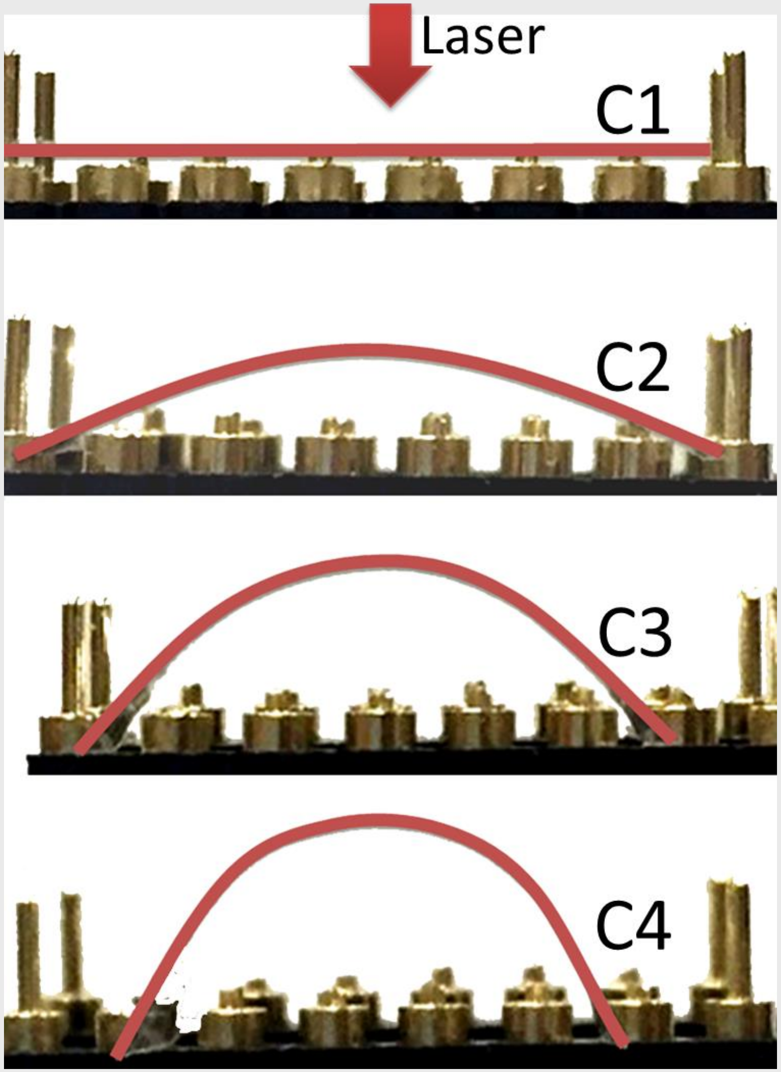

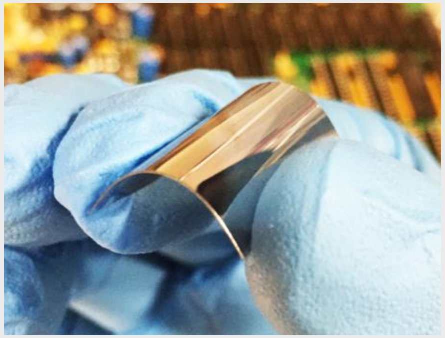

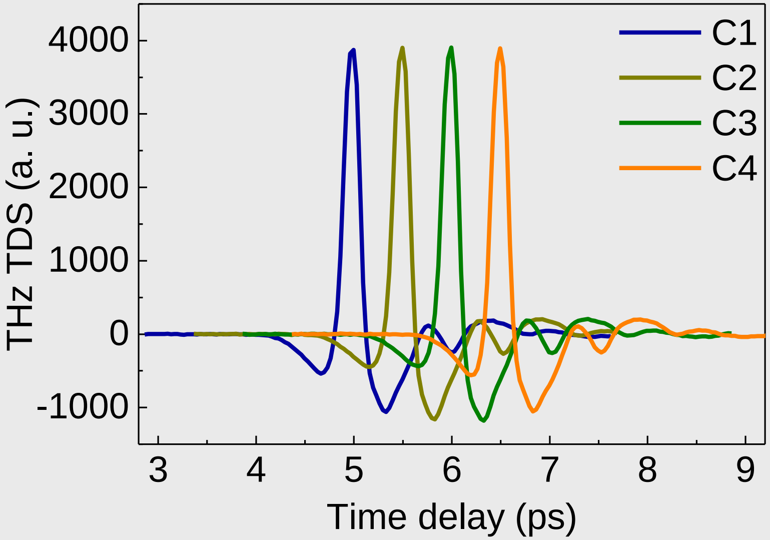

Samples (on PET) are curved
→ no clear degradation of the THz emission efficiency
→ great flexibility of the new emitters.

Adv. Mat **29**, 1603031 (2017)

Summary

- Spin orbit technologies
  - Spin wave based devices
  - Oxygen engineering in FM layer, resistivity of HM and FM
  - Structural asymmetry (lattice mismatch, etc.) – multilayers (skyrmions)
  - Strain engineering, spin relaxation at the capping layer
  - Ferrimagnetic spintronics
  - 2DEG (LAO/STO), topological insulators, Weyl semimetals
  - Magnetic heterostructures → THz emitter